

AD No. 34117  
ASTIA FILE COPY

HIGH ALTITUDE OBSERVATORY  
OF  
HARVARD UNIVERSITY AND UNIVERSITY OF COLORADO

TECHNICAL REPORT

Thermodynamic Structure of the Outer Solar Atmosphere

by  
Satoshi Matsushima

8 May 1954

ONR Contract Nonr - 393(01)  
Project NRL Req. 173/6443/53

THERMODYNAMIC STRUCTURE OF THE  
OUTER SOLAR ATMOSPHERE

by

Satoshi Matsushima

A Thesis Submitted to the  
Graduate Faculty of the University of Utah  
and the Research Staff of the High Altitude Observatory  
in Partial Fulfillment of the Requirements  
for the Degree of  
DOCTOR OF PHILOSOPHY

Major Subject: Astrophysics

Approved:

\_\_\_\_\_  
Chairman, Supervisory Committee

\_\_\_\_\_  
Head, Major Department

\_\_\_\_\_  
Co-chairman, Supervisory Committee

\_\_\_\_\_  
Dean, Graduate School

\_\_\_\_\_  
Reader, Supervisory Committee

\_\_\_\_\_  
Reader, Supervisory Committee

\_\_\_\_\_  
Reader, Supervisory Committee  
Department of Physics  
University of Utah  
May 1954

## FOREWORD

A part of the research work on Contract Nonr 393(01) has been carried out by Mr. Satoshi Matsushima, a graduate student participating in a co-operative research program in solar physics between High Altitude Observatory and the University of Utah. The following document is the Ph.D. thesis summarizing his work. It is issued herewith as a contract technical report. The thesis was jointly supervised by the astrophysics group of the University of Utah, the research staff of High Altitude Observatory, and Dr. Richard N. Thomas of Harvard College Observatory.

The thesis reports results on the thermodynamic structure of the solar atmosphere derived principally from the observations of the total solar eclipse at Khartoum, Sudan, on 25 February 1952. The observational materials used for this study were reported in an earlier thesis prepared under this contract by Dr. Russell Grant Athay.

The entire program of this contract, including both the eclipse observations and the post-eclipse analysis, has been carried out in close cooperation with the Naval Research Laboratory. This work on the thermodynamic structure of the sun from optical observations has great relevance to the work of the Naval Research Laboratory on the same problem, using solar radio noise observations. We wish to express our deep appreciation to the Naval Research Laboratory group and in particular to Dr. John P. Hagen and Dr. E. O. Hulbert, for their invaluable consultation and assistance.

The principal scientific results in this thesis will later be made the subject of published articles in the scientific literature, and reprints will be available as additional technical reports under this contract.

Walter Orr Roberts, Director  
High Altitude Observatory

8 May 1954

## ACKNOWLEDGMENT

The first two years of my graduate work in the United States were pursued at the University of Utah and the following two years at Harvard College Observatory, where the major part of this thesis research was undertaken. I also had opportunities to spend all three summer terms between these years at High Altitude Observatory. My sincere thanks go to a host of professors, staff members, and friends at these institutions who are too numerous to mention individually. However, in the following, I would like to name only a few without whose assistance this thesis would never have been completed in the present form.

Among these, I am especially indebted to Professor Richard N. Thomas during all this period. Not only has he been my academic advisor, but he has been responsible for my study, both in scientific and general fields, and has supervised the work reported in this thesis. I also wish to express my hearty appreciation to Dr. Walter Orr Roberts for his thoughtful advice and assistance during my studies at High Altitude Observatory.

My sincere thanks are due to Professor Donald H. Menzel at Harvard College Observatory and Professor Eugene N. Parker at the University of Utah for their encouragement and invaluable advice. I am indebted to Dr. Max Krook at Harvard College Observatory for his assistance in some of the mathematical treatment in this thesis.

Finally, all of the staff at High Altitude Observatory helped and encouraged me to complete the final draft of this thesis. Among these, I wish especially to state that Drs. Donald E. Billings, Russell G. Athay, and Jean-Claude Pecker have kindly and carefully read through the manuscript and have given me invaluable comments concerning it. Mrs. Jennifer W. Harris and Miss Kathryn M. Virnelson undertook the painstaking work of typing the manuscript, and Mr. Robert H. Cooper made the drawings. It is my pleasure herewith to acknowledge their assistance with my cordial thanks.

My earlier graduate work in astronomy was started at the University of Kyoto, where, through the stimulation of Professor Shotaro Miyamoto, I became interested in solar problems. His continuous encouragement through correspondence is appreciated deeply by the author.

The first year of my study in the United States was supported financially by a University of Utah Research Fellowship, and the second year by Air Research and Development Contract AF 33-038-20067 under the supervision of Professor R. N. Thomas. During the third and fourth years, I was supported by Eclipse Contract Nonr-393 Task Order No. 1, supervised by Dr. W. O. Roberts. It is with sincere appreciation that I express my thanks for the opportunity to participate in this research.

## ABSTRACT

Recent observations have shown that the classical theory of the stellar atmospheres is not at all adequate for explaining the thermodynamic structure of the solar chromosphere. In this thesis a special effort was made to develop the theory of the structure of an atmosphere in which departures from thermodynamic equilibrium are predominant. A theory of the phenomenon of self-absorption was also treated. These theoretical developments were carried out with the aim of solving various discrepancies encountered in the interpretation of the flash spectrum by classical theory. The resulting theoretical relationships were then applied to the analysis of the hydrogen spectra observed at the 1932 and 1952 eclipses.

In general, if the kinetic temperature and the radiation temperature in an atmosphere are not identical, the distribution of the atomic energy states can not be described by the equations of thermodynamic equilibrium. The departure from thermodynamic equilibrium may be measured by a dimensionless quantity,  $b_n$ , which is a ratio of atomic density in the  $n$ th energy level to that given by the Boltzmann-Saha formula. The principle of the theoretical calculation of  $b_n$ , developed by Menzel and Thomas, was employed in devising a method of taking collisional transitions into consideration. Numerical calculations were carried out for a pure hydrogen atmosphere, characterized by a kinetic temperature,  $T_k = 35,000^\circ$  and illuminated by a radiation field at a temperature,  $T_r = 6,000^\circ$ . It appeared that the largest differences between our  $b_n$ -values and those that Thomas obtained were in  $b_1$  and  $b_2$ . Thomas neglected collisional excitation from levels other than the first level. We then applied our numerical values of  $b_n$  to explain some inconsistencies that appeared in laboratory measurements of hydrogen arc spectra.

New theoretical expressions for the total Balmer line intensities observable in the eclipse spectra were then developed, so as to include the effect of self-absorption. The resulting formula, for total line emission,  $E_{n2}$ , integrated over a volume above the moon's limb is:

$$E_{n2} = \frac{h\nu_{n2}}{4\pi} A_{n2} \frac{N_n(h)}{\beta} \sum_{n=0}^{\infty} \left\{ (-1)^n \frac{N_2(h) \alpha_{2n,0}}{(n+1)! (n+1)^{3/2}} \right\}$$

where  $N_n(h)$  denotes the total number of hydrogen atoms in the  $n$ th level within a unit column along the line-of-sight at a chromospheric height,  $h$ , and  $\alpha_{2n,0}$  is the atomic absorption coefficient at the line center.  $\beta$  represents the exponential height gradient of hydrogen atom. Some approximate formulae were also derived empirically that agreed with the above expression for the range of physical parameters involved in the present problem.

The following assumptions were made to perform the integration:

1. The density of hydrogen atoms decreases exponentially outwards along a solar radius.
2. The logarithmic gradient,  $\beta$ , is assumed to be the same for all energy states of hydrogen.
3. The kinetic temperature,  $T_e$ , is constant throughout the atmosphere.
4. The central intensity of the lines is solely determined by the Doppler profile.

The formula for self-absorption thus obtained was applied to the analysis of Balmer line intensities of the 1932 and 1952 eclipse spectra to determine the distribution of hydrogen atoms in the 2nd level,  $N_2$ , and the chromospheric electron temperature. It was found that assumptions 1 and 3 are sufficiently consistent in the lower region of the chromosphere where our present investigations are concerned. Assumptions 2 and 4 appeared to be most questionable. At the present stage of this research it seems difficult to examine quantitatively the possible errors due to these simplifications. More precise calculations, including  $\beta_n$  on  $n$  and fine structures of line profiles, would be possible only by numerical integration.

Essentially three methods were developed in analyzing the 1932 and 1952 eclipse spectra: (a) determination of the population of the Balmer ground state from the relative amount of self-absorption in the Balmer lines. (The basic principle of this method was first considered by Thomas.) (b) determination of the amount of self-absorption and the departure from thermodynamic equilibrium,  $b_n$ , simultaneously from the line intensities only; (c) obtaining the amount of self-absorption and  $b_n$  by combining the line intensities and the emission in the continuum; then, determining  $b_n$  by using the results from the first and second methods to examine the internal consistencies. All of the above results showed good agreement within the estimated errors of the observations.

From the 1932 data it was found that  $N_2$ , the total number of atoms in the Balmer ground state within a unit column along the line-of-sight at a chromospheric height,  $h$ , and the exponential height gradient,  $\beta$ , could be well represented by the following formulae:

$$\log N_2 = 16.13 + \frac{1}{2} \log \left( \frac{T_e}{5040} \right) - 0.36 \times 10^{-8} h^{\text{cm}}; \beta = 0.82 \times 10^{-8} h^{\text{cm}^{-1}}$$

Similarly from the 1952 data, it was found that:

$$\begin{aligned} \log N_2 &= 16.37 (\pm 0.023) + \frac{1}{2} \log \left( \frac{T_e}{5040} \right) - 0.578 (\pm 0.018) \times 10^{-8} h^{\text{cm}} \\ \beta &= 1.33 \times 10^{-8} h^{\text{cm}^{-1}} \end{aligned}$$

The most probable value of  $N_2$  at each height was given by using the

$T_e$  distribution determined from the continuum analysis. It was concluded that the physical conditions in the chromospheric regions observed at the 1932 and 1952 eclipses were considerably different. Departure from thermodynamic equilibrium were not predominant in the 1932 data and only the effect of self-absorption may be important for the interpretation of the Balmer decrement. On the other hand, both effects appeared equally important in the 1952 data.

From the 1952 data the observed values of  $b_n$  for  $n$  higher than 10 were found to be almost constant in the region lower than 30,000 km. Detailed calculations showed that the values from  $b_{10}$  to  $b_{30}$  could be expressed by

$$\log b_n = -0.13 (\pm 0.022) + 6.7 (\pm 0.28) \frac{1}{n}$$

or

$$\log b_n = 0.73 (\pm 0.049) - 0.024 (\pm 0.0011) n$$

The value of  $b_2$  at each height was also determined by two independent methods. The results agreed sufficiently to prove the accuracy of the methods.

These values of  $b_n$  provide a measure of the chromospheric electron temperature,  $T_e$ , and electron density,  $N_e$ .  $T_e$  was found to increase upwards but not to reach 30,000° below the height  $h = 3,000$  km. More exact values of  $T_e$  could not be obtained, because of the lack of theoretical values of  $b_n$ . It was therefore suggested that the theoretical calculations of  $b_n$  should be carried out for small intervals of the values of  $T_e$  and  $N_e$ .

## TABLE OF CONTENTS

ACKNOWLEDGMENT	
ABSTRACT	
I. INTRODUCTION	1
II. THE DEPARTURE FROM THERMODYNAMIC EQUILIBRIUM IN THE CHROMOSPHERE	
§1. Introduction	10
§2. Formulation of the equation of analysis	11
§3. Numerical results of the values, $b_n$ , and discussion	17
§4. Reduction of $b_n$ from the laboratory experiments	20
III. THEORETICAL CONSIDERATION OF THE SELF-ABSORPTION IN THE STELLAR ATMOSPHERE	
§1. Introduction and assumptions	23
§2. Formulation of the self-absorption formula for monochromatic light	24
§3. Consideration of total line emission and self-absorption	31
§4. Numerical results and the approximate formula for self-absorption	33
IIIA. APPENDIX	37
IV. APPLICATION TO THE FLASH SPECTRUM OF 1932 ECLIPSE	
§1. Introduction	39
§2. Comment on Thomas' determination of $N_2$ from self-absorption	39
§3. Consideration of the effect of self-absorption, including departure from thermodynamic equilibrium	44
§4. Numerical results and discussion	47
§5. Determination of $N_2$ and $N_2$ -gradient	50
§6. Discussion	54

V. APPLICATION TO THE FLASH SPECTRUM OF 1952 ECLIPSE	
§1. Introduction	56
§2. Method of simultaneous determination of N <sub>2</sub> and b <sub>2</sub>	56
§3. Observed amount of $b_n \cdot e^{X_n} \{Abs_n\}$	67
§4. Determination of the observed b <sub>n</sub>	72
§5. Comparison to the model obtained from the Balmer continuum, and determination of b <sub>2</sub>	77
§6. Discussion of the comparison of the density-height gradient with the emission gradient	82
§7. Concluding remarks	83
REFERENCES	86

## I. INTRODUCTION

It has long been known, even before quantitative measurements were possible, that the flash spectrum of the solar chromosphere has various anomalous features that could not be explained by a simple analogy to the classical theory of stellar atmospheres. One might expect, from Kirchhoff's law, that the flash spectrum should be a reversal of the Fraunhofer spectrum. That is, the relative intensities of the chromospheric emission lines would be the same as photospheric. In a more concrete definition, one may say that the "classical theory" of the chromosphere is a model according to which hydrostatic equilibrium holds, and in which the excitation and ionization of atoms are fully described by the Boltzmann-Saha formula based on the assumption of thermodynamic equilibrium at the photospheric radiation temperature. Thus, once the boundary conditions are set, the classical model completely determines the distribution of physical parameters from which one can predict the quantitative character of the chromospheric spectrum.

A number of eclipse observations for determining the relative intensities of lines and the continuum only confirmed the above mentioned discrepancies with the classical model. The first quantitative measurements were made at the 1932 eclipse by Cillie and Menzel (1935). From the energy distribution in the Balmer continuum they obtained a value for the electron temperature  $T_e = 5000^\circ \text{ K}$ , and, using this temperature, they computed an electron density  $N_e = 2.3 \times 10^{11} \text{ cm}^{-3}$  from the Balmer free-bound emission.

The most conspicuous features of the eclipse spectrum may be the anomalous excitation of hydrogen lines and the presence of lines of He I and He II that are not observed in the photospheric spectrum. Despite the evidence of such superexcitation of H and He, Wildt (1947) obtained a value of  $N_e$  similar to that of Cillie and Menzel by an application of the Inglis-Teller formula (1939) for the resolution of hydrogen lines. Further, Goldberg's (1939) determination of the excitation temperature from the relative population of excited helium levels indicated similar results, except for the upward increase of temperature. For thermodynamic equilibrium, the relative population of atoms in excited levels is given by the Boltzmann-Saha relation for a given  $T_e$  and  $N_e$ . Hence, unless we assume an unreasonably low electron density, the above value of  $T_e$  is much too low to produce the lines of such high excitations.

The appearance of most of the ionized metallic lines as more enhanced than those in the Fraunhofer spectrum was also considered as indicating anomalous excitation. Woolley and Stibbs (1953), for example, insist that the ionization of metals in the chromosphere does not require a temperature higher than that of the photosphere, and that enhanced lines can be adequately accounted for by a decrease in pressure. But, they state that this cannot be extended to the hydrogen and helium excitations.

Thus, the first inconsistency with the classical model appears in the large difference of intensities between the higher excitation lines and the metallic lines. Miyamoto (1947), and the author and Miyamoto (1947) considered the possibility that the ultraviolet radiation emitted inwards from the highly heated corona causes these chromospheric excitations, so that it is not necessary to have a radiation temperature higher than the photospheric temperature. They computed the amount of free-free emission due to the free electrons of velocities corresponding to  $T_e = 1,000,000^\circ \text{ K}$ . The energy values thus obtained at the frequencies corresponding to the ionization potentials of He I and He II were, respectively, equal to energies at these same frequencies in  $8000^\circ$  and  $16,500^\circ$  black body radiation. The computed values were, however, inadequate for explaining the ionization of hydrogen.

The next direct observational contradiction to the classical model is associated with the assumption of hydrostatic equilibrium. The observed limb darkening shows evidence that the photosphere is in hydrostatic equilibrium, under the assumption that the negative hydrogen ion is responsible for the opacity in the continuum. If we assume a layer in hydrostatic equilibrium as an extension of the photosphere and calculate the logarithmic density gradient,  $\beta = \frac{\alpha M}{kT}$ , we get  $\beta = 6.7 \cdot 10^{-8} \text{ cm}^{-1}$  for  $T = 5000^\circ \text{ K}$  and the mean molecular weight,  $\bar{M} = 1$ . Contrary to this theoretical prediction, the observed intensity decrement along the geometrical height appears much too low for the theoretical value. (For thermodynamic equilibrium and no self-absorption, the emission gradient is equal to the density gradient.) According to Cillie and Menzel (1935), for example,  $\beta$  for neutral hydrogen at a height of about 1000 km above the limb is  $1.54 \cdot 10^{-8} \text{ cm}^{-1}$ , which agrees well with the value  $1.62 \cdot 10^{-8} \text{ cm}^{-1}$  obtained by Pannekoek and Minnaert (1928) from the 1927 eclipse data. Again under the assumption of hydrostatic equilibrium, these height gradients require a temperature of the order  $20,000^\circ \text{ K}$ . Wildt (1947), using an ingenuous method covering a number of previous observations, gets  $\beta = 0.9 \cdot 10^{-8} \text{ cm}^{-1}$  which leads to the temperature as high as  $35,000^\circ \text{ K}$ . The disagreement of Wildt's value with those previously obtained is discussed by Thomas (1950b). He argues that the omission of the departure from thermodynamic equilibrium would lower the value of  $\beta$  in Wildt's method. Since Wildt's determination is based on the comparison of lines of different quantum number, the positive quantity due to the departure from thermodynamic equilibrium should enter directly into the density gradient. Further, the eclipse observations show that the emission gradients of hydrogen lines increase systematically towards higher members of the Balmer series. As we shall discuss in the later chapters of this paper, this seems to be one of the pieces of evidence indicating that the chromosphere is not in a state of thermodynamic equilibrium. Thus, the important fact of these eclipse observations is that there exists a sharp line of demarcation between the chromosphere and the photosphere, where the assumption of hydrostatic equilibrium must break down unless we assume a temperature as high as  $20,000 - 30,000^\circ$ .

In addition to the above lower emission gradient, the observed low decrement of Balmer line intensities towards the series limit has been

well known as one of the anomalous features of the flash spectrum. As we shall discuss in detail in Chapter IV, Thomas (1950a) has studied this discrepancy and shown that it is mostly due to the ignoring of the effect of self-absorption, in earlier considerations of the problem.

In the above we have mentioned various observational evidence suggesting that the actual chromosphere departs considerably from the simplest model in which it is considered as an extension of the photospheric surface, and have pointed out that spectroscopic observations may be better explained by assuming a higher temperature in the chromosphere than in the photosphere.

Since the existence of a coronal electron temperature of the order of a million degrees is well established, it is natural to assume a temperature increase outward. That is, there must exist a layer above the photosphere in which the temperature gradient changes its sign. The only question is whether the minimum temperature is at the base or above the chromosphere.

The determination of kinetic temperature by Redman (1942a, 1942b) appeared most likely to give a definite solution for this question. Redman measured the line-profiles of several intense lines of the 1940 eclipse spectrum. From the relative broadening of hydrogen lines and the lines of heavier elements, he concluded that the line width is mainly due to Doppler broadening by thermal motion of atoms corresponding to a kinetic temperature of  $30,000^{\circ}$  K, rather than turbulent motion. These observations apply to chromospheric heights as low as 1500 km. On the other hand, temperatures in the photospheric layers as obtained from limb darkening in the continuum, excitation of molecular or metallic lines, Balmer line profiles, etc. indicated (following recent reviews by Minnaert (1953) and Unsöld (1952)) a temperature of  $3,800$  to  $4,500^{\circ}$  in the external photospheric layers. Similar results were obtained by Pecker (1951) and others from the theory of radiative equilibrium and the blanketing effect. However, contrary to earlier interpretations of the broadening of Fraunhofer lines as due to turbulent motion, Bell (1951) insists that it is caused by thermal motion at a kinetic temperature of at least  $10,000^{\circ}$  K. She has examined the half-widths of line profiles made by elements of various atomic weight and found that the Doppler width varies with atomic weight in such a way as to indicate a thermal motion corresponding to  $T_e = 10,000^{\circ}$  for high excitation,  $17,000^{\circ}$  for low excitation neutral lines and  $20,000^{\circ}$  for ionized lines. The value of  $17,000^{\circ}$  is also confirmed by her curve-of-growth results. Further, Bell considered that the systematic change of  $T_e$  with excitation potential shows that the kinetic temperature increasing upwards, since other evidence, such as the heights to which various lines extend in the chromosphere, agrees in indicating that the lower excitation lines are formed at a greater elevation in the atmosphere than the higher. Also, ionization increases outward and the ionized lines have the highest kinetic temperature of all. She states that the value of  $17,000^{\circ}$  K agrees well with the previous measures by Allen (1937, 1949), Menzel and Bell (1948), Pierce and Goldberg (1948), Shane (1941), van de Hulst (1946), etc., except that in the past the interpretation has been

in terms of turbulent velocities. Bell, however, finds no evidence for velocities independent of atomic weight. Bell's assumption that she may ignore the detailed distribution of atoms and the ambiguity of her method of measuring the half-widths are criticized by J. Houtgast (1952) and others.

While Bell's result is thus open to question, it may be considered evidence to support Redman's hypothesis, indicating that the reversal of temperature may lie even as low as the reversing layer. Since the temperatures discussed above are all kinetic temperatures determined from the lines individually, they are not necessarily contradictory with the radiation temperature which characterizes the continuum and the relative intensities of Fraunhofer lines. Ultimately we must distinguish between radiation temperature, kinetic (electron) temperature, excitation temperature, ionization temperature, etc. These temperatures should be identical only when the atmosphere is in a state of strict thermodynamic equilibrium. If we postulate that the physical state of the chromosphere departs from thermodynamic equilibrium, we must specify the physical conditions in order to relate the temperatures defined in different ways.

The question of how the energy necessary to raise the kinetic temperature above the photospheric temperature is supplied now arises. This problem has been studied by several authors including Bierman (1948), Schwarzschild (1948), Thomas (1948a), Alfven (1947, 1950), Hoyle (1949), Miyamoto (1949), etc. We discuss only a theory by Thomas which starts more directly from observed facts than is the case with other more speculative considerations. Thomas interprets the observation of chromospheric spicules as a system of superthermic jets. These jets supply the energy needed to give the observed high kinetic temperature in the chromosphere. His quantitative calculation based on hydrodynamics predicts theoretically a configuration of the spicules which agrees with the essential features observed by W. O. Roberts (1945) and shows that the energy transferred from the system to the chromosphere appears adequate to maintain a  $35,000^{\circ}$  kinetic temperature.

Further, Thomas (1948b, 1949a, b, c, 1950b, 1952) has developed the hypothesis of a  $35,000^{\circ}$  kinetic temperature to treat the radiation field of the hydrogen chromosphere and has explained the anomalous excitation of the Balmer lines mentioned earlier. He assumed a pure hydrogen atmosphere with a kinetic temperature of  $35,000^{\circ}$  which is illuminated by a photospheric radiation temperature of  $6000^{\circ}$ . In such a high kinetic temperature, the effect of collisional excitation or ionization becomes predominant, causing a severe departure from thermodynamic equilibrium, so that the distribution of populations of each energy state does not obey the Maxwell-Boltzmann distribution. As will be discussed in detail in the later chapters of this thesis, Thomas has shown that in general as the kinetic temperature increases a larger number of atoms remain in lower energy states than there would be in the case of thermodynamic equilibrium. After solving the cyclic (steady state) equations for each transition of hydrogen including the photoelectric and collisional transitions, the numerical results by Thomas show a large excess of atoms in the Balmer ground state for the possible range of chromospheric electron densities assumed.

The same problems were treated independently by Giovanelli (1948a, b, c, d) by a slightly different method. He computed the population of the Balmer ground state directly, while Thomas accounted for its excess over the Boltzmann distribution by a parameter,  $b_n$ . Numerical comparison of the two methods shows comparable results.

Thus while Redman's hypothesis had been supported, the recent development of radio observation provided another means of measuring the electron temperature of the solar atmosphere. The electron temperature may be determined from the total amount of energy emitted at a certain wave length from above a certain height in the sun's atmosphere, provided the distribution of electron densities in the corresponding region is known. Hagen (1951) observed the quiet sun's intensity at a wavelength of 8.5 mm and obtained the equivalent temperature due to the thermal radiation throughout the chromospheric and coronal region. He made an analysis of these measurements in conjunction with many other measurements at longer wave lengths to determine the electron temperature gradient. Since the observed equivalent temperature is an integrated radiation throughout the atmosphere above a certain height, we have to assume the electron density distribution to reduce the observed temperature to the kinetic temperature at each layer. Hagen adopted the values of  $N_e$  obtained by Baumbach (1937), Allen (1947) and van de Hulst (1947) for the corona and Wildt's (1947) values for the chromosphere. According to Hagen, Wildt's  $N_e$  distribution in the chromosphere is somewhat hypothetical, except perhaps for the density (or rather upper limit to the density) of  $1.74 \cdot 10^{11}$  electrons per cubic cm at a height of 500 km. Assuming such a model, Hagen reached the conclusion that the electron temperature is fairly uniform at a value less than  $10,000^\circ$  K to a height of 10,000 km and then rises steeply to a temperature of  $1,000,000^\circ$  K at a height of 25,000 km. To make radio noise data agree with Redman's temperature value at 1500 km, it is necessary to decrease the absorption coefficients so that the principal absorption for the shorter wavelengths will occur at much lower heights. Since the absorption coefficient varies directly with  $N_e^2$  and inversely with  $T_e^{3/2}$ , either an increase in the assigned temperature of the chromosphere, a decrease in the electron density, or some combination of these two is indicated. Hagen's calculations show that, in order to satisfy simultaneously an existence of a kinetic temperature of  $30,000^\circ$  K at a height of 1500 km and the observed equivalent temperature at the various radio wave lengths, the electron density in the lower chromosphere must be reduced to a value about one-tenth of the one he first assumed. This would change the position of maximum temperature gradient from the top of the chromosphere to a point in the chromospheric region.

Although the uncertainty in the  $N_e$  distribution made the interpretation of the radio measurements somewhat indeterminate, Hagen's results at one time appeared to offer an important contradiction to Redman's. Many authors used this radio result as an argument for temperatures as low as  $5000 - 6000^\circ$  K for the chromosphere. Since the temperature determined by Redman is the kinetic temperature, and that determined by radio noise is the electron temperature, we inquire whether or not we should expect the two to agree. We may define the electron temperature as a measure of the

thermal motion of electrons and the kinetic temperature as the same function of the motion of the atoms. If we assume a Maxwellian distribution of velocities and equipartition of energy, then these two temperatures must be identical. Thomas, Krook, Menzel and Bhatnager (1953) have concluded from theoretical considerations that  $T_e$  cannot differ significantly from  $T_k$  for  $T_e < 10^8 \text{ K}$ .

A number of objections have been raised by those who criticize the hypothesis of the higher kinetic temperature in the chromosphere. The most direct objection to Redman's interpretation was made by S. Miyamoto (1951b). He pointed out that the omission of self-absorption in Redman's measurement may cause an erroneous interpretation of the line-profiles. Since self-absorption is more effective in the central portion of a line, it would tend to increase the half-widths of the observed line-profiles. Miyamoto calculated the half-width of  $H_\alpha$ ,  $H_\beta$ , and  $H_\gamma$  including self-absorption and has shown that Redman's measurements agree with his results, if  $T$  is set as  $5,700^\circ$ . This suggestion has been widely accepted by several authors (van de Hulst 1954) including Redman (1952) himself.

It seems that most of the criticisms of Redman's hypothesis are based on the study of the excitations and ionizations of metallic lines. While the high intensity of ionized metallic lines compared to the neutral had been considered at one time as one of the anomalies of the flash spectrum, Menzel (1931) and Woolley and Stibbs (1953) have shown that it can be attributed to the decrease of electron pressure in the chromosphere and does not require a higher temperature. Their detailed calculations, using the ionization formula, have explained the observed relative intensities of ionized metallic lines to those of neutral lines. Miyamoto and Kawaguchi (1950) compared the metallic line intensities in the flash spectra with those predicted by theories of metallic ionization and the emission curve of growth for the Ca II K line. They have shown that for  $T_e = 35,000^\circ$  the metallic ionization by electron collision would be far too great and it would resemble that of the atmospheres of the earliest type stars. It is concluded that the observed emission curve of growth obtained from the 1930 eclipse for the Ca K line is best represented by the theoretical curve for  $T_e = 6000^\circ$ . Further, Miyamoto (1951b) has calculated the ultraviolet emission from the chromosphere of  $T_e = 35,000^\circ$ , in which he argues that for such a high temperature, hydrogen must be so completely ionized that the abundance ratio of hydrogen to metals does not coincide with the observed value,  $10^4 : 1$ .

Wurm (1948a, b) has considered the presence or absence of the nebular forbidden lines of oxygen and nitrogen to be a criterion of chromospheric electron temperature. He has computed, as a function of the electron temperature, the theoretical intensity ratio of forbidden transitions by collision for the ground states of OI, OII, OIII, and NII to the photospheric light scattered by electrons. He shows that these ratios are less than unity for  $T_e = 5000^\circ$ , but are the order of  $10^2$  for  $T_e$  higher than  $20,000^\circ$ . Thus Wurm argues that none of these forbidden lines should be seen if the chromospheric temperature is of the order of  $5000^\circ$ , but, instead, all the lines should be present if the temperature is as high as

35,000°. Since, in spite of the non-appearance of these lines, there must be some layer in the chromosphere where  $T_e$  reaches to 35,000°, Wurm concludes that the layers at such high temperature are exceedingly thin; that is, the temperature rises very steeply in the upper region of the chromosphere as is indicated by radio noise observations.

This conclusion of Wurm has been supported by Woolley and Allen (1950). They considered a theoretical model of the corona and the chromosphere, trying to make a best fit with observed data. Woolley and Allen compute the amount of the ultraviolet (Lyman continuum) radiation emitted from their model as a function of the electron temperature and conclude that the Lyman continuum emission from the low temperature chromosphere just satisfies the observed excitation of the ionosphere, but for temperature as high as 35,000° K the theoretical level of ionization would be much higher than is observed. As a model, they assumed Baumbach's electron density distributions, setting the temperature at 5000° K up to a height of 5000 km, then rising to the order of 1,000,000° within a layer of a few hundred kilometers. This gives a best fit with the radio results.

As an explanation of the appearance of He I and He II lines that would be consistent with Redman's observations, Woolley suggests that the actual chromosphere is not homogeneous but is so irregular that any particular line-of-sight in the flash observation samples a variety of hot and cold spots. That may be the reason why the high excitation lines like He I and He II appear at the same height as the lowest excitation metallic lines. On the other hand, Miyamoto (1951a) has examined the excitation of helium under the assumption of  $T_e = 35,000^\circ$  and hydrogen helium ratio 5:1. He computed the intensities of the resonance lines of He I and He II, using the optical depth in the chromosphere, and showed that the populations of the excited levels of He I and He II should become so large that the strong absorption lines of these elements would be present in the Fraunhofer spectrum. By such arguments he concludes that the study of the helium lines by L. Goldberg (1934) indicates a kinetic temperature not exceeding 10,000°. His result appeared favorable for the lower temperature at lower heights of the chromosphere, although the temperature appears to increase upwards already in the lower layers.

Finally we note the temperature determination from the Balmer discontinuity. Zanstra (1950a, b) has attempted to separate the free-bound emission and the scattered radiation by free electrons at the Balmer and Paschen series limit. Since the capture component of Paschen continuum is sensitive to the temperature and decreases rapidly toward shorter wave lengths for  $T_e = 5000^\circ$ , the intensity jump at the Balmer limit is larger for lower than for higher temperatures. After examining the 1926 eclipse observation by Davidson and Stratton (1927), Zanstra finds the discontinuity is considerably larger than the theoretical upper limit for  $T_e = 30,000^\circ$ . More precise measurements were made by Koelbloed and Veliman (1951), who obtained the upper limit of  $T_e$  as  $15,000^\circ - 20,000^\circ$ . A similar problem has been also discussed by S. Ueno (1950) based on the low chromospheric temperature.

We have summarized above the important studies related to the chromospheric temperature made before the 1952 eclipse. We have seen that there exist many difficulties and inconsistent observations in the path of a self-consistent theory of the chromosphere. A large number of expeditions went to Khartoum, Sudan, for the eclipse, February 25, 1952, aiming to resolve these discrepancies. While the numerical results of these observations have not yet been published at the time this thesis was written, we may discuss the preliminary results for two important observations. Hagen (1953) made solar radio noise observations at 8 mm wave length and examined the intensity change with the moon's motion. He concluded that his results implied a non-homogeneous model of the chromosphere. He suggests that the radio observations may not be fully explained by a uniform chromosphere with a monotonic variation of temperature upwards. According to his explanation, the chromospheric model may be best described as a mixture of spicule-like radial columns of different physical conditions, namely, a mixture of columns with high temperature and low density and columns with low temperature and high density. The integrated emission observed at radio wave length gives a sort of averaged temperature. Redman's spectra obtained at the 1940 eclipse may have been representative of a high temperature region.

At the 1952 eclipse, Redman (1952) repeated his 1940 observations. He obtained eight exposures for each of the wave length regions, 5550A - 6040 A and 3430A - 4110 A. Thus the Balmer lines up to H<sub>32</sub> are covered by his spectrum. Admitting the suggestion by Miyamoto (1951b) Redman states that the strong self-absorption for the early members of the Balmer series may cause an erroneous interpretation of the width as due to thermal motion only, although the shape of the line may not reveal self-reversal like in metallic lines. He proposed that this trouble can be reduced by going to higher members of the series. This may lead to difficulty from the broadening by Stark effect, although Redman observed that the lines do not grow broader and broader towards the series limit, as has been suggested. Allowing for the effects of both self-absorption and Stark effect, Redman's preliminary results show some modification of his former value. That is, he declares that the kinetic temperature estimated from the higher members of Balmer series and the weak metallic lines cannot exceed 17,000° K. A higher value similar to earlier measurements is shown for the lowest Balmer lines. This seems to imply the effect of self-absorption.

After this thesis research had been completed, we received a preliminary summary of the attempt by Woltjer (1954) to construct a spicule-like model for the chromosphere, as has been suggested by Hagen (1953). Woltjer measured intensities of spicules and the parts between spicules on a H<sub>α</sub> monochromatic plate taken by Lyot. He found the quotient of the two intensities to be 1.9 at 5000 km. He deduced a model in which the larger part of the chromosphere has a temperature of some 5000°, whereas for spicule regions it increases from 8000° at a height of 1000 km to 20,000° at 4000 km, then remains constant up to 7000 km. He concludes that the spicules cover 2% of the solar surface and the entire Balmer emission is coming from these spicules. For the spicule temperature value at 2000 km Woltjer proposes T = 10,000°. This is still far too low compared to Redman's determination.

Locally intensified regions have been already noted by Cillié and Menzel (1935) in the flash spectrum of 1932. Athay, Evans and Roberts (1953) suggest that a similar hot region appears on the third contact spectra from the 1952 eclipse. The irregularity of solar surface evidenced by such phenomena as granulation, sunspots, spicules, prominences, flares, radio noise observations, etc. may cause many of the contradictions in the interpretation of chromospheric observations. Thus, the future theoretical model of the chromosphere may have to be based on a non-uniform structure.

More recent theoretical studies are attacking these problems by considering the energy transport by a magneto hydrodynamic wave or the destruction of the state of equilibrium by a shock wave. All these theories consider such localized phenomena on the sun's surface as the magnetic field, turbulent motions, etc. As has been pointed out by Woolley, however, there is wide freedom in the assumptions if we choose an irregular model. Unless more direct observations like Hagen's are accumulated in the future, and a more confirmable choice of the distribution of irregularities becomes possible, it is very difficult to reach an appropriate model.

Along with the expeditions by Hagen and Redman to the 1952 eclipse, that by High Altitude Observatory under the supervision of Robertis, Evans and Thomas, was especially aimed at the determination of the chromospheric temperature distribution as well as the electron density distribution. Highly improved jumping film technique made it possible to obtain the flash spectrum with much greater height resolution. The spectra thus obtained covered the wave length region from 3,800 Å to 3,400 Å, with a dispersion of  $7\frac{1}{2}$  Å mm<sup>-1</sup> in the ultraviolet and 11 Å mm<sup>-1</sup> in the visible and infrared. The intensities of the Balmer lines and the Balmer continuum were obtained approximately every 100 km from the height 500 km above the base of the chromosphere. The major part of the present thesis is aimed at the theoretical reduction of Balmer line intensities from these data together with those of the 1932 eclipse by Cillié and Menzel. We are specifically interested in determining the electron temperature and the population of the hydrogen ground state, and the variation of these quantities with geometrical height. The methods developed in this thesis are related particularly to the problem of departures from thermodynamic equilibrium and the effects of self-absorption in the chromosphere. These effects have been ignored in the earlier reductions, as is discussed above. In the following chapter, the theoretical calculations of departures from thermodynamic equilibrium are treated. Chapter III consists of the development of theoretical formulae for self-absorption in an optically thin atmosphere, and the numerical results are quoted. Chapters IV and V are devoted to the reduction of the 1932 and 1952 eclipse data, respectively.

## II. THE DEPARTURE FROM THERMODYNAMIC EQUILIBRIUM IN THE CHROMOSPHERE.

### §1. Introduction.

In the study of the radiation field of the chromosphere, it has been shown by Menzel and Cillie (1937) that the departures of the populations of the atomic energy levels from the thermodynamic equilibrium values can be expressed by a non-dimensional quantity  $b_n$ .  $b_n$  is the ratio of population,  $N_n$ , in atomic state  $n$ , to the population under conditions of thermodynamic equilibrium at the same electron density and temperature. Hence it is defined by a modification of the Boltzmann-Saha formula:

$$N_n = b_n N_i N_e \left\{ \frac{\pi^2}{2 \pi m k T_e} \right\}^{3/2} \frac{B_n}{2} e^{-\frac{X_n}{k T_e}} \quad (1.1)$$

where  $N_h$ ,  $N_i$ , and  $N_e$  denote the density respectively of hydrogen atoms in the  $n$ th quantum level, of ions, and of electrons.  $X_n$  is the ionization potential from the level  $n$ . The other notation is standard.

Under the assumption that within a small region of the atmosphere there exists a unique kinetic temperature,  $T_e$ , defined by a Maxwellian distribution of velocities of free electrons, we can note immediately that  $b_n$  approaches unity when  $n$  tends to infinity.

An extensive study of the departure from thermodynamic equilibrium in the solar chromosphere in terms of  $b_n$ , has been carried out and published in a series of papers by Thomas (1943b, 1949a, b, c, 1950b, 1952). As we shall discuss later in detail, Thomas obtained the result that for the case in which  $T_e$  exceeds the radiation temperature,  $b_n$  is greater than unity and monotonically decreases to unity as  $n$  increases. Recently, however, a few theoretical computations have been in disagreement with this conclusion. For example, Chamberlain (1953) computed the values of  $b_n$  from the same equations of statistical equilibrium, but at very much lower values of  $N_e$ . For  $T_e = 10,000^\circ K$ , he obtained  $b_n$  slightly less than unity for optically thick models and considerably less for an optically thin medium. It is not certain that these contradictory results have physical significance. Since the methods of deriving  $b_n$ -expressions were practically the same for both cases, the disagreement seems due to the uncertainty of the factors employed for the computation, such as the cross-section for collisional excitation. Thus it is important to determine the  $b_n$ 's observationally. We return to this point later, in Chapters IV and V.

In the following section, we formulate the method of computing  $b_n$  and discuss the collisional cross-sections employed in the equations. The numerical results are discussed in section 3. In section 4, we shall consider a method of determining the departure from thermodynamic equilibrium empirically from laboratory measurements of the hydrogen arc spectrum. The present theoretical results are compared to the results of this experiment.

## §2. Formulation of the equations of analysis.

The relative distribution of the atoms over  $n$  energy levels is defined by the equation (1.1) which includes  $b_n$  as a parameter. Hence, the expressions for  $b_n$  as a function of  $T_r$ ,  $T_e$ , and  $N_e$  can be obtained from a set of cyclic equations representing the statistically steady state. The cyclic equations for a very dilute radiation field and negligible collisional excitation have been discussed by Menzel and his associates (1937-1945). Thomas has later extended this method to the case of a pure hydrogen atmosphere illuminated by a radiation field of intensity  $I(\nu)$  and characterized by a kinetic temperature  $T_e > T_r$ , where  $T_r$  is the temperature representing the continuum of the radiation field. Computations were carried out for the cases  $T_e = 35,000^\circ$  and  $T_r = 6000^\circ$ . He included the collisional ionization from the discrete levels and collisional excitation from the ground level, but ignored the excitations by collision from and between the other levels. Here we follow the same procedure to compute  $b_n$  for the case including the collisional excitations from all the levels.

In general, we employ the same notations adopted by Menzel and Thomas, except for a few cases, mentioned specifically. In particular  $F_{AB}$  denotes the number of optical transitions from state A to B per cubic centimeter per second, whereas  $C_{AB}$  refers to collisional excitations, or ionizations. The condition for a statistically steady-state is then expressed as:

$$\begin{aligned} & \sum_{n=1}^{\infty} (F_{nn} + C_{nn}) + \int_{\nu_x}^{\infty} F_{nn} d\nu + \sum_{n=1}^{n-1} (F_{nn} + C_{nn}) \\ &= \sum_{n=1}^{\infty} (F_{nn'} + C_{nn'}) + \int_{\nu_x}^{\infty} (F_{nn'} + C_{nn'}) \\ & \quad + \sum_{n=1}^{n-1} (F_{nn'} + C_{nn'}) \end{aligned} \quad (2.1)$$

where we use the convention for principal quantum numbers  $n' > n > n'$ .  $\chi$  denotes a certain state in the continuum for which we can set  $\chi = -\infty$  to extend the formal expressions for discrete transitions to the continuum. Then  $\nu_x = (RZ)^{1/3} / n^2$ , and for hydrogen  $Z = 1$ .  $C_{nn'}$  and  $C_{nn'}$  represent the collisional de-excitations. We neglect the three-body collisional recombination, and omit the fine-structure of the energy levels.

For writing the explicit expressions for the terms in equation (2.1), we use the following symbols:

$$K = \frac{\hbar^3}{(2\pi m k)^{3/2}} \frac{8\pi^2 e^2 k^2}{mc^3} \frac{2^4}{3\sqrt{3}\pi} = 3.2 \times 10^{-6}$$

$$X_n = \frac{h\nu_n}{kT_e} ; \quad X_{nn'} = X_n - X_{n'}.$$

$$Y_n = \frac{h\nu_n}{kT_e} ; \quad Y_{nn'} = Y_n - Y_{n'}.$$

$$-E_i(-X) = \int_x^{\infty} \frac{e^{-x}}{x} dx.$$

$$C_0 = \frac{a_s^2 k^3}{\lambda \pi m^2 k} = 1.16 \times 10^{-26}.$$

The formulae for optical transitions are given by Menzel and his associates (1937-1945). For the spontaneous transitions from the discrete level,  $n''$ , or the continuum,  $\infty$ , to the level  $n$ , we have

$$F_{n''n} = K \frac{N_i N_e}{T_e^{3/2}} b_{n''} \frac{g_{n''}}{n^3} \frac{2}{n'^3} \frac{e^{X_{n''}}}{\frac{1}{n^2} - \frac{1}{n'^2}}, \quad (2.2)$$

$$\int_{\nu_0}^{\infty} F_{n''n} d\nu = K \frac{N_i N_e}{T_e^{3/2}} \frac{1}{n^3} e^{X_{n''}} \bar{g}_{n''} [E_i(-X_n)], \quad (2.3)$$

For the radiation induced transitions, we have

$$F_{n''n} = K \frac{N_i N_e}{T_e^{3/2}} S_y \left[ \frac{b_n e^{X_{n''}} - b_n}{e^{Y_{n''}} - 1} \right] \frac{g_{n''}}{n^3} \frac{2}{n^3} \frac{e^{X_n}}{\frac{1}{n^2} - \frac{1}{n^2}}, \quad (2.4)$$

$$\begin{aligned} \int_{\nu_0}^{\infty} F_{n''n} d\nu = & K \frac{N_i N_e}{T_e^{3/2}} \frac{e^{X_n}}{n^3} \bar{S} \bar{g}_{n''} \left\{ b_n \sum_{a=1}^{\infty} [-E_i(-aY_n)] \right. \\ & \left. - \sum_{a=1}^{\infty} \left[ -E_i(-Y_n \left\{ a + \frac{T_r}{T_e} \right\}) \right] \right\}, \end{aligned} \quad (2.5)$$

where  $\bar{g}_{n''}$  denotes the Gaunt factor, which is tabulated by Menzel (1937-1945). The quantity  $S_y$  is a factor intended to account for the presence of absorption lines or any other effects, such as dilution, which cause

the radiation to depart from a true Planck distribution. In order to perform the integration over the range of frequencies higher than  $\nu_n$ , for the transitions from or to the continuum, we use the averaged quantities  $\bar{g}_{nk}, \bar{S}$ . In the actual computation, we set  $\bar{g}_{nk} = 1$ . Further, we note that equations (2.4) and (2.5) include the radiation induced emissions.

Now we proceed to consider the collisional term,  $C_{nn'}$ . As discussed in detail by Thomas (1948b), we may generally neglect collisional excitation by atoms relative to that by electrons. Then we can write the number of collisions per second per  $\text{cm}^3$  in which the atom is raised from level  $n$  to  $n'$ :

$$C_{nn'} = \pi a_0^2 N_n N_e 4\pi \left[ \frac{m}{2\pi k T_e} \right]^{\frac{3}{2}} \left( 1 - \frac{b_{n'}}{b_n} \right) \int_{v_0}^{\infty} v^3 Q_{nn'}(v, n) e^{-\frac{mv^2}{2kT_e}} dv, \quad (2.6)$$

where  $v$  is the electron velocity which is assumed to follow a Maxwellian distribution at the temperature  $T_e$ .  $Q_{nn'}$  denotes the cross-section to excite the atom from level  $n$  to  $n'$ .  $v_0$  corresponds to the lowest energy at which  $Q$  is not zero. Recalling the definition of the  $b_n$ , we see that the factor  $b_{n'}/b_n$  in the bracket enters because of collisional de-excitations. After completely eliminating  $N_n$  and representing  $\frac{mv^2}{2}$  by  $E$ , we have:

$$C_{nn'} = \pi a_0^2 \frac{4\pi}{m^2} N_n N_e \left[ \frac{e}{2\pi k T_e} \right]^{\frac{3}{2}} b_n \left( 1 - \frac{b_{n'}}{b_n} \right) \tilde{Q}_{nn'} \int_{E_n}^{\infty} E Q_{nn'} e^{-\frac{E}{kT_e}} dE. \quad (2.7)$$

We proceed to consider the value of  $Q_{nn'}$ .

At the present stage, the theoretical calculations of  $Q_{nn'}$  are rather obscure. The Born first-order approximation for excitation from the ground state holds only for the collision by electrons of energies higher than 100 eV. Thomas has tried to estimate a more reliable cross-section for low energy excitation from the ground state only. Giovanelli (1948a, b) has suggested that an assumption setting the value of  $Q_{nn'}$  proportional to the corresponding transition probabilities,  $B_{nn'}$ , is valid for collisions by electrons whose energies are slightly above the corresponding excitation potential. He further assumed that, for high-energy electrons, the value of  $Q_{nn'}$  varies as  $E^{-\frac{1}{2}}$  and derived the general expression for

$Q_{nn'}$  as a function of  $E$ . The integration in equation (2.6) was approximated by separating the problem into two cases,  $1 \ll E/kT_e$  and

$1 \gg E/kT_e$ . In the present case the values of  $E/T_e = X_{nn'}$  are very close to unity for the Lyman and Balmer series. Therefore, we assume that  $Q_{nn'}$  is constant, and set it proportional to  $B_{nn'}$  throughout the whole range of possible energies of electrons. Then we write,

$$Q_{nn''} = \mu B_{nn''} = \mu \frac{n''^2}{n^2} \frac{A_{nn''}}{8\pi\hbar R^3 \left(\frac{1}{n^2} - \frac{1}{n''^2}\right)^3}. \quad (2.8)$$

The value of the proportionality constant,  $\mu$ , may be evaluated by introducing the appropriate value for certain definite transitions, say  $Q_{12}$ . Thus

$$\mu = \frac{Q_{12}}{B_{12}} = \frac{Q_{12}}{2.02 \times 10^{19}}. \quad (2.9)$$

As a first approximation we assume that  $Q_{12}$  (measured in units of  $\pi a_0^2$ ) is equal to 1. Substituting the numerical values, equation (2.8) can be expressed as

$$Q_{nn''} = 2.25 \times 10^{-10} \frac{n''^2}{n^2} \frac{A_{nn''}}{\left(\frac{1}{n^2} - \frac{1}{n''^2}\right)^3}, \quad (2.10)$$

where the spontaneous transition probabilities  $A_{nn''}$  are given by Menzel and Pekeris (1935).

Integrating equation (2.7) and arranging the constant factors, we obtain,

$$C_{nn''} = C_0 \frac{N_i N_e}{T_e} b_n \left(1 - \frac{b_{n''}}{b_n}\right) \pi n'' e^{X_{n''}} (X_{nn''} + 1) 2.25 \times 10^{-10} \frac{n''^2}{n^2} \frac{A_{nn''}}{\left(\frac{1}{n^2} - \frac{1}{n''^2}\right)^3}, \quad (2.11)$$

or substituting the constant  $C_0$ , which represents the terms shown on page 12, we write

$$C_{nn''} = 5.23 \times 10^{-36} \frac{N_i N_e}{T_e} b_n \left(1 - \frac{b_{n''}}{b_n}\right) e^{X_{n''}} (X_{nn''} + 1) n''^2 \frac{A_{nn''}}{\left(\frac{1}{n^2} - \frac{1}{n''^2}\right)^3}. \quad (2.12)$$

Now we consider the number of collisional ionizations by electrons,  $C_{ni}$ , where we use the suffix  $i$  instead of  $\kappa$  to denote the integration of  $C_{n\kappa}$  over transitions to the whole range of continuum energies rather than to a certain state,  $\kappa$ , in the continuum. We have an expression of  $C_{ni}$  similar to equation (2.10) as follows:

$$C_{ni} = C_0 \frac{N_i N_e}{T_e} b_n \left(1 - \frac{1}{b_n}\right) \pi (X_n + 1) Q_{ni}. \quad (2.13)$$

For the value of  $Q_{ni}$ , Giovanelli (1948a) has also adopted a theoretical formula. On the other hand, Thomas gives an empirical expression for  $Q_{ni}$  evaluated from laboratory experimental data. We may compare the values from these expressions with experimental data in the following table.

Table I.

	20 eV	25 eV	30 eV	50 eV	100 eV
Giovanelli	1.79	2.03	2.03	1.61	0.96
Thomas	0.18	0.32	0.45	1.00	0.95
Experimental*	0.4	0.6	0.8	1.2	1.2

\* Mott and Massey. Theory of Atomic Collision (2nd Ed: Oxford: Clarendon Press (1949).) p. 244.

Thus we see that for the more important, low energy values, Thomas' empirical formula agrees better with experiments. Therefore, we adopt this empirical cross-section for ionization from the ground level, and for the ionizations from the higher levels we again assume proportionality to the optical transition probabilities,  $B_{ni}$ . Thus,

$$Q_{ni} = \frac{B_{ni}}{B_{1i}} Q_{1i} = 0.096 \frac{B_{ni}}{B_{1i}}, \quad (2.14)$$

after substituting the integrated value of  $Q_{1i}$  of Thomas' formula (1948b).  $B_{nk}$  may be expressed as,

$$B_{nk} = \frac{C^3}{8\pi\hbar\nu_{nk}^3} \frac{\pi\lambda}{\lambda} A_{kn} = \frac{\pi\epsilon^2}{m\hbar\nu_{nk}} f_{kn}, \quad (2.15)$$

where the oscillator strength,  $f_{kn}$ , is given by the formula,

$$f_{ni} = \int df_{kn} = \int_{R/n^2}^{\infty} \frac{mc}{\pi\epsilon^2} \frac{32\pi^2\epsilon^2}{3\sqrt{3}ch^3\nu_{nk}^3} \frac{J_1}{n^5} d\nu_{nk}, \quad (2.16)$$

in which  $J_1$  is the Gaunt factor, tabulated by Menzel and Pekeris (1935). For our present calculations we set  $J_1$  equal to unity.

After integrating equation (2.15) and substituting it in equation (2.14), we have,

$$B_{ni} = \frac{32\pi^2 e^6}{3\sqrt{3} h^3} \frac{n}{3R^3} = 3.67 \times 10^{-11} n. \quad (2.17)$$

Thus, we finally obtain from equation (2.13)

$$Q_{ni} = 0.096 n. \quad (2.18)$$

Substituting the above  $Q_{ni}$  in the equation (2.12), we obtain

$$C_{ni} = C_0 \frac{N_i N_e}{T_e} b_n \left(1 - \frac{1}{b_n}\right) \varpi_n (X_n + 1) Q_{ni}, \quad (2.19)$$

or, after evaluating the constant terms, it becomes

$$C_{ni} = 2.23 \times 10^{-27} \frac{N_i N_e}{T_e} b_n \left(1 - \frac{1}{b_n}\right) n^3 (X_n + 1). \quad (2.20)$$

Now we substitute equations (2.2), (2.3), (2.4), (2.5), (2.12) and (2.20) into the cyclic equations (2.1) and have, finally,

$$\begin{aligned} & \frac{2N_i N_e K}{T_e} \frac{1}{n^3} e^{X_n} \left[ \sum_{n=1}^{\infty} \left\{ \left( b_n - S_v \frac{b_n e^{X_{nn''}} - b_{n''}}{e^{Y_{nn''}} - 1} \right) \frac{g_{nn''}}{n'^3} \frac{e^{-X_{nn''}}}{\frac{1}{n^2} - \frac{1}{n'^2}} \right. \right. \\ & \left. \left. - b_n \left(1 - \frac{b_{n''}}{b_n}\right) J_{nn'} \right\} - \sum_{i=1}^{n-1} \left\{ \left( b_n - S_v \frac{b_n e^{X_{nn''}} - b_n}{e^{Y_{nn''}} - 1} \frac{g_{nn''}}{n'^3} \frac{1}{\frac{1}{n^2} - \frac{1}{n'^2}} \right. \right. \right. \\ & \left. \left. \left. - b_n \left(1 - \frac{b_n}{b_{n'}}\right) J_{nn'} \right\} + \frac{1}{2} \left\{ -E_i(-X_n) \right\} - \frac{S_v}{2} \sum_{a=1}^{\infty} \left\{ b_n \left[ -E_i(-a Y_a) \right] \right. \right. \\ & \left. \left. - \left[ -E_i(-Y_n \left\{ a + \frac{T_i}{T_e} \right\}) \right] \right\} - \left\{ b_n \left(1 - \frac{1}{b_n}\right) J_{ni} \right\} \right] = 0, \end{aligned} \quad (2.21)$$

where

$$J_{nn''} = 8.2 \times 10^{-31} T_e^{\frac{1}{2}} N_e n^3 n'^2 e^{-X_{nn''}} (X_{nn''} + 1) \frac{A_{nn'}}{\left(\frac{1}{n^2} - \frac{1}{n'^2}\right)^3}, \quad (2.22)$$

$$J_{n'n} = 8.2 \times 10^{-31} T_e^{1/2} N_e n^5 (X_{n'n} + 1) \frac{A_{n'n}}{\left(\frac{1}{n'^2} - \frac{1}{n^2}\right)^3}, \quad (2.23)$$

and

$$J_{ni} = 3.5 \times 10^{-22} T_e^{1/2} N_e n^6 e^{-X_n} (X_n + 1). \quad (2.24)$$

For computing purposes, we may rewrite these equations in the following form:

$$\begin{aligned} b_n & \left[ \sum_{n''=n+1}^{\infty} \left\{ \frac{S_v}{e^{Y_{nn''}-1}} \frac{g_{nn''}}{n''^3} \frac{1}{\frac{1}{n^2} - \frac{1}{n''^2}} + J_{nn''} \right\} \right. \\ & + \sum_{n'=1}^{n-1} \left\{ \left( 1 + \frac{S_v}{e^{Y_{nn'-1}}} \right) \frac{g_{nn'}}{n'^3} \frac{1}{\frac{1}{n^2} - \frac{1}{n'^2}} + J_{nn'} \right\} \\ & \left. + \frac{S_v}{2} \sum_{a=1}^{\infty} \left\{ -E_i(-a Y_n) \right\} + J_{n,i} \right] \quad (2.25) \\ & = \sum_{n''=n+1}^{\infty} b_{n''} \left\{ \left( 1 + \frac{S_v}{e^{Y_{nn''}-1}} \right) \frac{g_{nn''}}{n''^3} \frac{e^{-X_{nn''}}}{\frac{1}{n^2} - \frac{1}{n''^2}} + J_{nn''} \right\} \\ & + \sum_{n'=1}^{n-1} b_{n'} \left\{ \frac{S_v}{e^{Y_{nn'-1}}} \frac{g_{nn'}}{n'^3} \frac{e^{-X_{nn'}}}{\frac{1}{n^2} - \frac{1}{n'^2}} + J_{nn'} \right\} \\ & + \frac{1}{2} \left\{ -E_i(-X_n) \right\} \frac{S_v}{2} \sum_{a=1}^{\infty} \left\{ -E_i(-Y_n \left[ a + \frac{T_r}{T_e} \right]) \right\} + J_{n,i}. \end{aligned}$$

We obtain the values of  $b_n$  by solving the above system of equations by successive approximations.

### 3. Numerical results of the values, $b_n$ , and discussion.

We see in the equation (2.25) that the values,  $b_n$ , are given for four parameters,  $T_e$ ,  $T_r$ ,  $N_e$ , and  $S_v$ . Since the factor  $N_i$  drops out in the final equation, the usual assumption  $N_i = N_e$  is not necessary. The computations were carried out under the same assumption as Thomas'. That is, we assume a constant radiation temperature of  $6000^\circ$ , a kinetic

temperature of  $35,000^{\circ}$  and an electron density  $N_e = 2 \times 10^{11}$ . (Thomas put the Boltzmann constant  $k$  equal to  $1.4 \times 10^{-16}$ ; however, we take the more exact value  $1.37 \times 10^{-16}$  for the present computation.)

i). Results neglecting the chromospheric radiation field.

Following Thomas, we consider the cases  $\bar{S}_\nu = 1$  and  $\bar{S}_\nu = 0$ . Our numerical results, along with those obtained by Thomas, are tabulated in Table II.

Table II.

b<sub>n</sub> for No Chromospheric Radiation Field.

$S$	b <sub>1</sub>	b <sub>2</sub>	b <sub>3</sub>	b <sub>4</sub>	b <sub>5</sub>	b <sub>6</sub>	b <sub>7</sub>	b <sub>8</sub>	b <sub>9</sub>	b <sub>10</sub>
(A) 1.	$1.61 \times 10^6$	9.03	3.82	2.80	2.31	2.01	1.75	1.54	1.38	1.20
	$2.1 \times 10^6*$	10.9*	4.67*	3.45*	2.93*	2.62*	2.42*	2.27*	2.17*	1.08*
(B) 0.	$1.85 \times 10^6$	10.3	4.41	3.24	2.72	2.43	2.17	1.90	1.61	1.43
	$2.3 \times 10^6*$	12.3*	5.33*	3.92*	3.31*	2.96*	2.75*	2.60*	2.47*	2.36*

\* Denotes Thomas solution, Paper II.

We see from Table I that there are no great differences in the numerical results of b<sub>n</sub> between the two calculations. The higher-level terms are altered the most, relatively, as is to be expected. Any great differences, if they exist, must arise in the next case where the effect of the chromospheric radiation field is included.

ii). Consideration of the chromospheric radiation field.

If we add the chromospheric absorption and emission to the radiation field from the photosphere,  $\bar{S}_\nu$ , may or may not be greater than unity. For the Lyman lines, whose chromospheric opacity is high, this consideration is particularly important. Thomas has discussed the problem and has shown that the essential perturbation to the radiation field by the chromosphere is in the Lyman region, with a small effect also in the center of the lower order Balmer lines. He obtained in his paper, for  $\bar{S}_\nu$  in the Lyman lines,

$$\bar{S}_\nu = b_n b_i^{-1} (e^{Y_{in}} - 1) e^{-X_{in}}. \quad (3.1)$$

In a private communication, however, Thomas has mentioned that equation (3.1) is in error because of the faulty inclusion of the induced emission. The correct expression, which follows from the fifth

paper of Thomas' series (1949b) under conditions of large values for  $(\frac{n_w \alpha}{\beta})$  where  $\beta$  is the atmospheric logarithmic density gradient, is

$$\bar{S}_v = (e^{Y_{1n}} - 1) \left( \frac{b_1}{b_n} e^{X_{1n}} - 1 \right)^{-1}. \quad (3.2)$$

With this expression for  $\bar{S}_v$ , the bracket in equation (2.25) involving the Lyman line radiative transitions vanishes. In the following solutions we neglect the chromospheric emission outside the Lyman lines. As in the earlier results by Thomas, the significant parameter is  $\alpha S$ , the residual intensity in the Balmer lines. Therefore we have shown the solution for  $b_n$  in Table III for two extreme values of  $\alpha S$ .

Table III.

b<sub>n</sub> including the Chromospheric Emission.

	b <sub>1</sub>	b <sub>2</sub>	b <sub>3</sub>	b <sub>4</sub>	b <sub>5</sub>	b <sub>6</sub>	b <sub>7</sub>	b <sub>8</sub>	b <sub>9</sub>	b <sub>10</sub>
(C) n <sup>S</sup> =1 (1< n). 4.24x10 <sup>4</sup>	1.18x10 <sup>3</sup>	57.4	19.0	11.2	8.14	6.54	5.57	4.87	4.41	
(D) n <sup>S</sup> =0 (n=2). 2.41x10 <sup>5</sup>	2.36x10 <sup>5</sup>	71.9	26.6	15.9	11.34	8.60	6.75	5.53	4.59	n <sup>S</sup> =1 (2< n)

From the results in Table III we see that b<sub>n</sub> has a larger value for high n than in the case without chromospheric emission. The difference of b<sub>2</sub> in the two cases is especially great. b<sub>2</sub> has almost the same value as b<sub>1</sub>. We also find considerable difference between the results for the case n<sup>S</sup>=1, n>1 and the case 2<sup>S</sup>=0, n<sup>S</sup>=1, n>2.

It may be interesting to check these results by comparing the value of b<sub>2</sub> with that which we can compute from the population of the Balmer ground state, N<sub>2</sub>, which Thomas obtained from the Balmer decrement in the 1932 flash spectrum of Menzel. Thomas obtained N<sub>2</sub> = 2.4 x 10<sup>16</sup> at 670 km and N<sub>2</sub> = 0.52 x 10<sup>16</sup> at 1500 km where N<sub>2</sub> is the total number of atoms in the second energy level in a 1 cm<sup>2</sup> column of chromosphere along the line of sight. (These numbers are corrected by a factor of 2 for a reason discussed in the following section.) We may evaluate the values of b<sub>2</sub> from these results, assuming an isothermal chromosphere at T<sub>e</sub> = 35,000° and N<sub>e</sub> = 2 x 10<sup>11</sup>. We obtain:

$$\text{at } h = 670 \text{ km}; \quad b_2 = 1.15 \times 10^5$$

$$\text{at } h = 1500 \text{ km}; \quad b_2 = 2.5 \times 10^4.$$

These results agree well with those in Table III if we note that the most likely value of 2<sup>S</sup> is somewhat less than 1. While we must note that

Thomas' values of  $N_2$  are open to question, as will be discussed in the following chapter, the above agreement seems rather interesting.

#### §4. Reduction of $b_n$ from the laboratory experiments.

The theoretical value of  $b_n$  discussed in the preceding sections may be compared indirectly with laboratory experiments on the hydrogen emission spectra taken under conditions in which thermodynamic equilibrium does not hold. Unfortunately, only a small amount of work has been done for different excitation conditions.

H. Edels and J. D. Craggs (1951) have investigated the hydrogen arc spectrum excited by the electric discharge to determine the excitation temperature from the relative intensities of  $H_\alpha$ ,  $H_\beta$  and  $H_\gamma$  lines. They measured the ratios of the total intensities,  $I_\alpha/I_\beta$  and  $I_\beta/I_\gamma$ , from the line profiles of  $H_\alpha$ ,  $H_\beta$  and  $H_\gamma$ . The experiments were performed under various conditions of gas pressure and electric current. The effects of self-absorption on the line-profiles were removed.

The emission line intensities due to the spontaneous transition,  $n \rightarrow 2$ , can be expressed by,

$$I_{n2} = \hbar \nu_{n2} A_{n2} N_n \quad (4.1)$$

where  $I_{n2}$  is the total intensity corrected for the self-absorption, and  $N_n$  is the total number of atoms in the  $n$ th level along the line-of-sight. If thermodynamic equilibrium is assumed,  $N_n$  may be written in terms of  $N_2$  as,

$$N_n = N_2 \frac{\bar{w}_n}{\bar{w}_2} e^{-\chi_{n2}/k T_{ex}} \quad (4.2)$$

where  $T_{ex}$  represents the excitation temperature. From (4.1) and (4.2), we have

$$\frac{I_{n2}}{I_{n'2}} = \frac{A_{n'2} \nu_{n'2} \bar{w}_{n'}}{A_{n''2} \nu_{n''2} \bar{w}_{n''}} \exp \left\{ \frac{\chi_{n''2} - \chi_{n'2}}{k T_{ex}} \right\}. \quad (4.3)$$

From the above relation, Edels and Craggs determined  $T_{ex}$  using their measurements on Balmer line arcs taken at 1 to 2 atmospheres pressure and carrying currents varying from about 3 to 10 amperes. They found that  $T_{ex}$  determined from  $I_{n2}/I_{n'2}$  differs considerably from, and is greater than, the values obtained from  $I_{n2}/I_{n''2}$ . Apart from the experimental errors, the excitation temperature should be identical for every pair of the lines in the state of thermodynamical equilibrium.

Therefore, it is natural to consider that finding non-identical temperatures may be due to the effect of the departure of the experimental condition from thermodynamical equilibrium.

We will consider this effect in terms of  $b_n$ . From our theory, the alternative expression of equation (4.3) may be given as

$$\frac{I_{\nu_2}}{I_{\nu_2'}} = \frac{b_{n'} A_{n'2} V_{n'2} \omega_{n'}}{b_{n''} A_{n''2} V_{n''2} \omega_{n''}} \exp \left\{ \frac{(X_{n''} - X_{n'})}{K T_e} \right\}. \quad (4.4)$$

Since  $b_n$  is defined by equation (1.1), the temperature appearing in the above equation refers to the electron temperature. (In thermodynamical equilibrium, however, only a unique temperature should exist, and  $T_e = T_{ex}$ .) Taking the logarithm of the above equation we have

$$T(n', n'') = \frac{(X_{n''} - X_{n'}) \frac{h}{K}}{\ln \frac{I_{n'2}}{I_{n''2}} - \ln \frac{A_{n'2} V_{n'2} \omega_{n'}}{A_{n''2} V_{n''2} \omega_{n''}} - \ln \frac{b_{n'}}{b_{n''}}}. \quad (4.5)$$

Substituting the numerical values, we write,

$$T_{\alpha\beta} = \frac{0.762 \cdot 10^4}{\ln \frac{I_\alpha}{I_\beta} - 0.779 - \ln \frac{b_3}{b_4}} \quad (4.6)$$

and

$$T_{\beta\gamma} = \frac{0.353 \cdot 10^4}{\ln \frac{I_\beta}{I_\gamma} - 0.642 - \ln \frac{b_4}{b_5}}. \quad (4.7)$$

$T_{\alpha\beta}$  and  $T_{\beta\gamma}$  are conventional notations for temperatures derived from  $\frac{I_\alpha}{I_\beta}$  and  $\frac{I_\beta}{I_\gamma}$ , respectively. The factors  $b_n$  are absent in the equations for thermodynamic equilibrium, so that  $b_n$  may be considered as the correction factor to give the equality  $T_{\alpha\beta} = T_{\beta\gamma}$ . Thus, equating (4.6) to (4.7), we have the relation

$$\ln \frac{b_3}{b_4} - 2.16 \ln \frac{b_4}{b_5} = \ln \frac{I_\alpha}{I_\beta} - 2.16 \ln \frac{I_\beta}{I_\gamma} + 0.61. \quad (4.8)$$

Table IV shows the results of computation of the right hand side of the above equation, using the values of  $I_x/I_p$  and  $I_p/I_y$  measured by Edels and Craggs. It is interesting to see that there are no great systematic changes in the last column for different conditions of pressure and electric current. The values in the last column of Table IV may be compared with corresponding quantities computed from the theoretical data in Tables II and III. We have the values corresponding to the left hand side of equation (4.8) as;

$$(A) -0.10 \quad (B) -0.08 \quad (C) -0.04 \quad (D) -0.12$$

where (A), (B), (C), and (D) correspond to each row designated by the same letter in Table II and Table III. We see that the value varies slightly for the different conditions assumed for computations. If we consider that the physical situation postulated in the theoretical computation is considerably different from that under which each experiment is performed, the theoretical values may be considered harmonious with the experimental results. We may be able to conclude at least that the orders of the relative values of  $b_n$  are reasonable as a first approximation.

Table IV.

Arc. No.	Current (amp)	$\ln \frac{I_x}{I_p}$	$\ln \frac{I_p}{I_y}$	$\ln \frac{b_2}{b_4} - 2.16 \ln \frac{b_4}{b_5}$
86 cm Hg	1	5.7	1.84	-0.40
	2	6.0	1.76	-0.59
	3	7.3	1.65	-0.48
	4	9.4	1.50	-0.61
	5	9.9	1.52	-0.44
110 cm Hg	6	3.35	9.95	-0.35
	7	3.53	9.92	-0.38
	8	5.2	9.97	+0.06
	9	5.4	5.85	-0.30
	10	8.6	4.22	-0.65
	11	8.68	4.14	-0.65
	12	8.80	---	x
153 cm Hg	13	3.70	5.89	-0.47
	14	4.05	5.33	-0.51
	15	5.1	4.94	-0.60
	16	5.9	4.52	-0.56
	17	6.0	4.51	-0.47
	18	8.3	3.74	-0.75
	19	8.9	3.53	-0.94

Since we are comparing the relative values of  $b_n$  rather than the absolute, the above agreement is significant even though the experimental conditions are very different from those assumed in the computation.

III. THEORETICAL CONSIDERATION  
OF THE SELF-ABSORPTION IN THE STELLAR ATMOSPHERE

§1. Introduction and assumptions.

Despite the importance of the possible effect of self-absorption in the chromosphere, little attempt has been made to consider this effect in the interpretation of eclipse spectra. The chief difficulty for a theoretical study of self-absorption seems to be the lack of information on the distribution of the density of atoms and electrons, as well as on the temperature gradient. Further, for stronger lines where the self-reversal appears predominant, one meets the more fundamental problems related to the details of line-formation.

A quantitative analysis of the effect of self-absorption in the Balmer lines was first carried out by Thomas (1950b) to interpret the Balmer decrement for the higher series members, as will be discussed in more detail in the following chapter. Thomas derived an expression for the total amount of self-absorption in the Balmer line observed with a slitless spectrograph. He assumed an exponential decrease of hydrogen density with height and a constant temperature throughout the atmosphere. In the analysis of the 1932 eclipse, Cillie and Menzel (1935) gave a similar series formula, obtained from the same assumptions; but as they considered the emission from unit cross-section of the chromosphere, the convergence of the series was too slow to perform a numerical computation. Hence this method was not practical for eclipse analysis. The series treated by Thomas converges considerably more rapidly, but he uses a cumbersome calculation involving double integrals.

In this chapter, we shall reconsider the mathematical formulation of the problem, and a considerably simpler expression than Thomas' will be given. Further, Thomas took half of the total population of the Balmer ground state in place of the total number in a unit column along the line-of-sight, and the convergence of his series is much slower than in the series using the total number as shown in the following derivation. (The values of  $N_2$  given by Thomas in Table II are, as he stated, half of the total number instead of the total number.)

As we shall see later, the self-absorption for the Balmer emission depends only on the population of the hydrogen second state,  $N_2$ , and the atomic absorption coefficient,  $\alpha_{2n}$ . The temperature enters in the latter only if we use the absorption coefficient at the line center. Thus, it is important to note that the effect of temperature and density may be treated independently, particularly if we want to repeat the method of numerical integration by successive approximations. Hence in the following discussion, we first assume an exponential decrease in density along the radial direction, then set the absorption coefficient constant. Our results, for the weaker lines, are not too sensitive to the latter assumption because most of the emission and absorption originates at the small central region of the moon's limb so that the

temperature may be essentially constant. Since for the stronger lines, we have to take the failure of these assumptions into account, the direct expansion of the absorption formula may not be applicable for these cases. Further, we note that the parameters,  $N_2$  and  $\alpha_{2n}$  enter as a product, so that we can always adjust the actual value of the temperature in the final computation, as will be shown later.

In the following section, we will develop the formula for the observed intensity and the self-absorption at a certain point within a line, then integrate over a line contour to get the total amount of energy and self-absorption (section 3). The resulting formula is much simpler than the one obtained by Thomas. The numerical values of the self-absorption are discussed in the last section and are shown graphically as a function of  $\log N_2 \alpha_{2n}$ . Then, from this curve, we derive some analytical expressions which agree almost exactly with the numerical computation.

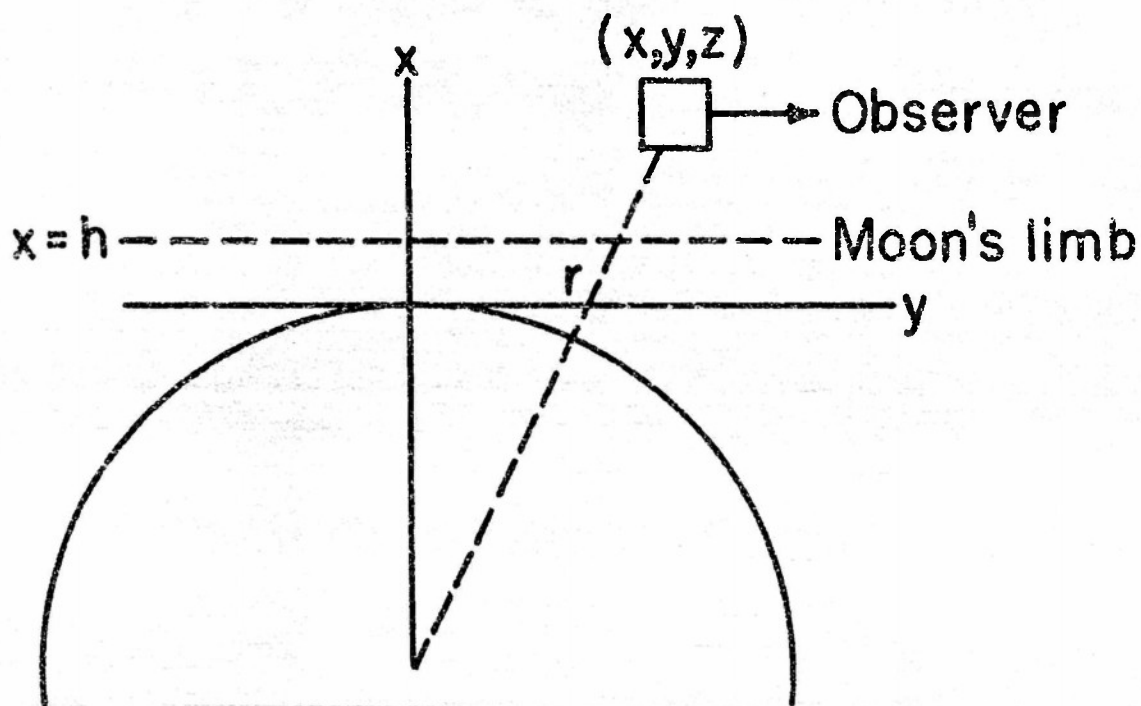


**FIGURE I Geometrical Diagram**

**§2. Formulation of the self-absorption formula for monochromatic light.**

Figure I shows a diagram of the sun's limb, indicating that we take the  $y$ -coordinate along the line-of-sight and the  $x$ - and  $z$ -axis perpendicular

to the y-axis. Let us consider the energy per unit solid angle emitted within a frequency interval  $\nu$  to  $\nu + d\nu$  by transitions from the nth to the second level of the hydrogen atoms in a small volume element at point  $(x, y, z)$ . Thus,

$$d_E_{n_2,\nu} = \frac{\hbar \nu n_2}{4\pi} n_n(x, y, z) A_{n_2} \frac{\alpha_{2n,\nu}}{\int_0^\infty \alpha_{2n,\nu} d\nu} dx dy dz \quad (2.1)$$

where  $n_n$  denotes the number of hydrogen atoms in the nth level within a unit volume, and  $A_{n_2}$  is the Einstein coefficient for the transition probability. (Throughout the remainder of this paper we shall use small letters for the number of particles per unit volume, and capital letters for quantities integrated over a certain volume.)  $\alpha_{2n,\nu}$  refers to the atomic absorption coefficient within the frequency interval  $\nu$  and  $\nu + d\nu$ . We use the suffix  $2n,\nu$  for  $E$  and  $\alpha$  to designate these quantities for a small region at the frequency  $\nu$  within a line and the suffix  $2n$  for the total quantities integrated over the line. Thus we write,

$$\alpha_{2n} = \int_0^\infty \alpha_{2n,\nu} d\nu. \quad (2.2)$$

The other notations are conventional.

It will be easiest if we consider the radiation from a slab of width 1 cm in the z-direction, so that we can eliminate the z-component by operating with  $\int_{z_0+\frac{1}{2}}^{z_0+\frac{1}{2}} dz$  on equation (2.1). Thus, from equation (2.1) and (2.2) we get

$$d_E_{n_2,\nu} = \frac{\hbar \nu n_2}{4\pi} n_n(x, y) A_{n_2} \frac{\alpha_{2n,\nu}}{\alpha_{2n}} dx dy. \quad (2.3)$$

We will now consider the effect of self-absorption on the above radiation. Since all hydrogen atoms in the second state from the point  $(x, y)$  to the observer contribute to the absorption, the amount of energy that finally emerges from the solar atmosphere will be

$$dE_{n_2,\nu} = d_E_{n_2,\nu} e^{-\alpha_{2n} \int_y^\infty n_2(x, y) dy} \quad (2.4)$$

where  $n_2(x, y)$  is the population of hydrogen atoms in the second level at the point  $(x, y)$ . We introduce the notation

$$N_2(x, y) = \int_y^\infty n_2(x, y) dy. \quad (2.5)$$

Then equation (2.4) becomes

$$dE_{n_2,v} = d_0 E_{n_2,v} e^{-\alpha_{2n,v} N_2(x,y)} \quad (2.6)$$

From the photometric measurements of the flash spectrum taken through a slitless spectrograph, we obtain the total energy emitted from the volume of the chromosphere in a 1 cm slab above a certain height,  $h$ . Therefore, we integrate equation (2.6) along the  $x$ - and  $y$ -axis,

$$E_{n_2,v} = \frac{h v_{2n}}{4\pi} A_{n_2} \frac{\alpha_{2n,v}}{\alpha_{2n}} \iint_{h-\infty}^{h+\infty} n_n(x,y) e^{-N_2(x,y) \alpha_{2n,v}} dx dy. \quad (2.7)$$

Here  $n_n(x, y)$  may be expressed as a function of  $b_n$ ,  $T_e$  and  $N_e$  according to the Boltzmann-Saha formula which includes the departure from thermodynamic equilibrium:

$$n_n(x,y) = \left( \frac{h^2}{2\pi m k} \right)^{3/2} \frac{w_n}{2} n_i(x,y) n_e(x,y) e^{\frac{X_n}{kT_e}} b_n(x,y) T_e(x,y). \quad (2.8)$$

Thus, we see that the integration of equation (2.7) is difficult, for it depends on the distributions of the parameters,  $b_n$ ,  $T_e$ ,  $n_i$ , and  $n_e$  throughout the atmosphere. If we know these quantities as functions of  $x$ ,  $y$ , and  $z$ , we may at least perform the integration numerically. Since, however, these parameters enter implicitly in equation (2.7), one method is to assume some analytical form for the distribution of the atoms instead of assuming each parameter. For the present case, we introduce the assumption of spherical symmetry for the distribution of hydrogen atoms, and assume an exponential decrease in density along the radial direction,  $r$ . Thus, we write

$$n_n(x,y) = n_n(0,0) e^{-\beta r} \quad (2.9)$$

where the constant  $n_n(0,0)$  represents the number of atoms in the  $n$ th level at the base of the chromosphere. In general, the density gradient,  $\beta$  also should be considered to vary for different regions in the atmosphere. While we set  $\beta$  constant in the following development, we may have to consider its variation with height in the numerical integration. According to the usual geometric approximation, we set

$$n_n(x,y) = n_n(0,0) e^{-\beta x} e^{-\frac{\beta y^2}{2r}}. \quad (2.10)$$

Substituting equation (2.10) into (2.11), we have

$$E_{n_2, \nu} = \frac{\hbar v_{n_2}}{4\pi} A_{n_2} \frac{\alpha_{2n,\nu}}{\alpha_{2n}} n_n(0,0) \iint_{-\infty}^{\infty} e^{-\beta x} e^{-\frac{\beta y^2}{2r}} e^{-N_2(x,y)} dx dy. \quad (2.11)$$

Or, recalling our notation given in (2.5), we may write (2.11) as

$$E_{n_2, \nu} = \frac{\hbar v_{n_2}}{4\pi} A_{n_2} \frac{\alpha_{2n,\nu}}{\alpha_{2n}} n_n(0,0) \iint_{-\infty}^{\infty} e^{-\beta x} e^{-\frac{\beta y^2}{2r}} \exp\left\{-\alpha_{2n,\nu} n_n e^{-\beta x} \int_0^y e^{\frac{\beta t^2}{2r}} dt\right\} dx dy. \quad (2.12)$$

Let us now consider the double integral

$$\iint_{-\infty}^{\infty} e^{-\beta x} e^{-\frac{\beta y^2}{2r}} e^{-N_2(x,y)} dx dy. \quad (2.13)$$

We will first consider the integration over  $y$ , then over  $x$ . Expanding the last exponential term, we write

$$e^{-N_2(x,y)} \alpha_{2n,\nu} = \sum_{n=0}^{\infty} (-1)^n \frac{\{N_2(x,y) \alpha_{2n,\nu}\}^n}{n!} \quad (2.14)$$

where  $N_2(x, y)$  may be written as

$$\begin{aligned} N_2(x,y) &= n_2(0,0) e^{-\beta x} \int_y^{\infty} e^{-\frac{\beta s^2}{2r}} ds \\ &= n_2(0,0) e^{-\beta x} \sqrt{\frac{2r}{\beta}} \int_y^{\infty} e^{-\frac{p^2}{\beta}} dp, \end{aligned} \quad (2.15)$$

and

$$p^2 = \frac{\beta y^2}{2r}.$$

Hence, for  $y > 0$ , we have

$$N_2(x,y) = n_2(0,0) e^{-\beta x} \sqrt{\frac{2r}{\beta}} \left\{ \frac{\sqrt{\pi}}{2} - \int_0^y e^{-\frac{p^2}{\beta}} dp \right\}. \quad (2.16)$$

Introducing a notation

$$g(p^2) = \frac{2}{\sqrt{\pi}} \int_0^p e^{-p^2} dp \quad (2.17)$$

we may write equation (2.16) as

$$N_2(x, y) = \frac{n_2(0, 0)}{2} e^{-px} \sqrt{\frac{2\pi r}{p}} \left\{ 1 - g(p^2) \right\}. \quad (2.18)$$

Here we see that the quantity,  $n_2(0, 0) e^{-px}$  represents the total number of hydrogen atoms in the second level within a column of unit cross-section along the line-of-sight at a height  $x$  above the base of the chromosphere. We denote this number by  $N_2(x)$  or simply  $N_2$ , so that

$$N_2 = N_2(x) = n_2(0, 0) e^{-px} \sqrt{\frac{2\pi r}{p}}. \quad (2.19)$$

Thus, substituting (2.19) into (2.18), we have

$$\text{for } y > 0, \quad N_2(x, y) = \frac{1}{2} N_2(x) \left\{ 1 - g(p^2) \right\}. \quad (2.20)$$

By a similar method, we readily obtain

$$\text{for } y < 0, \quad N_2(x, y) = \frac{1}{2} N_2(x) \left\{ 1 + g(p^2) \right\}. \quad (2.21)$$

For substitution in the power series (2.14), we calculate,

for  $y > 0$ ,

$$\left\{ N_2(x, y) \alpha_{2n, y} \right\}^n = \left\{ \frac{1}{2} N_2 \alpha_{2n, y} \right\}^n \left\{ \sum_{m=0}^n \frac{(-1)^m n!}{m!(n-m)!} g^m \right\}, \quad (2.22)$$

and, for  $y < 0$ ,

$$\left\{ N_2(x, y) \alpha_{2n, y} \right\}^n = \left\{ \frac{1}{2} N_2 \alpha_{2n, y} \right\}^n \left\{ \sum_{m=0}^n \frac{n!}{m!(n-m)!} g^m \right\}. \quad (2.23)$$

Now returning to the integral (2.13), we first write the  $y$ -dependent part of the integral as follows:

$$\int_{-\infty}^{\infty} e^{-\frac{p y^2}{2r}} e^{-N_2 \alpha_{2n,y}} dy = \int_{-\infty}^0 e^{-\frac{p y^2}{2r}} e^{-N_2 \alpha_{2n,y}} dy + \int_0^{\infty} e^{-\frac{p y^2}{2r}} e^{-N_2 \alpha_{2n,y}} dy. \quad (2.24)$$

From equation (2.14) we may write,

for  $y > 0$ ,

$$e^{-N_2 \alpha_{2n,y}} = \sum_{n=0}^{\infty} (-1)^n \frac{\left(\frac{1}{2} N_2 \alpha_{2n,y}\right)^n}{n!} \left\{ \sum_{m=0}^n (-1)^m \frac{n!}{m!(n-m)!} g^m \right\} \quad (2.25)$$

and, for  $y < 0$ ,

$$e^{-N_2 \alpha_{2n,y}} = \sum_{n=0}^{\infty} (-1)^n \frac{\left(\frac{1}{2} N_2 \alpha_{2n,y}\right)^n}{n!} \left\{ \sum_{m=0}^n \frac{n!}{m!(n-m)!} g^m \right\}. \quad (2.26)$$

Hence, equation (2.24) may be written

$$\int_{-\infty}^{\infty} e^{-\frac{p y^2}{2r}} e^{-N_2 \alpha_{2n,y}} dy = \int_0^{\infty} e^{-\frac{p y^2}{2r}} \left\{ 2 \sum_{n=0}^{\infty} (-1)^n \frac{(N_2 \alpha_{2n,y})^n}{n! 2^n} \cdot \left( 1 + \frac{n!}{2!(n-2)!} g^2 + \dots \right) \right\} dy. \quad (2.27)$$

Again integrating over  $y$ , we have

$$\int_{-\infty}^{\infty} e^{-\frac{p y^2}{2r}} e^{-N_2 \alpha_{2n,y}} dy = \sqrt{\frac{2\pi r}{p}} \left\{ \sum_{n=0}^{\infty} (-1)^n \frac{(N_2 \alpha_{2n,y})^n}{n! 2^n} \cdot \left( 1 + \frac{n!}{2!(n-2)!} I_2 + \frac{n!}{4!(n-4)!} I_4 + \dots \right) \right\} \quad (2.28)$$

where we introduce a notation  $I_m$ :

$$I_m = \frac{2}{\sqrt{\pi}} \int_0^{\infty} e^{-p^2} g^m (p^2) dp. \quad (2.29)$$

Now equation (2.28) involves a series of  $I_m$ , which requires a tedious computation if the convergence of the series is slow. We can, however,

simplify the equation by methods fully developed in Appendix IIIA, (see page 37). Namely, we can write;

$$S_n = 1 + \frac{n!}{2!(n-2)!} I_2 + \frac{n!}{4!(n-4)!} I_4 + \dots = \frac{2^n}{n+1}. \quad (2.30)$$

Substituting the above into equation (2.28), we have

$$\int_{-\infty}^{\infty} e^{-\frac{\beta y^2}{2r}} e^{-N_2 \alpha_{2n,y}} dy = \sqrt{\frac{2\pi r}{\beta}} \sum_{n=0}^{\infty} (-1)^n \frac{(N_2 \alpha_{2n,y})^n}{(n+1)!}. \quad (2.31)$$

Returning to the integral,  $\mathcal{J}$ , given in (2.13), we multiply both sides of equation (2.31) by a factor  $e^{-\beta x}$ , and integrate over  $x$  from  $h$  to infinity. Thus, recalling our definition (2.10),

$$N_2(x) = N_2(0) e^{-\beta x}, \quad (2.32)$$

we finally obtain

$$\begin{aligned} \mathcal{J} &= \int_h^{\infty} e^{-\beta x} \sqrt{\frac{2\pi r}{\beta}} \sum_{n=0}^{\infty} (-1)^n \frac{\{N_2(0) \alpha_{2n,y}\}^n e^{-n\beta x}}{(n+1)!} \\ &= \frac{1}{\beta} e^{-\beta h} \sqrt{\frac{2\pi r}{\beta}} \sum_{n=0}^{\infty} (-1)^n \frac{\{N_2(h) \alpha_{2n,y}\}^n}{(n+1)! (n+1)}. \end{aligned} \quad (2.33)$$

We again note that  $N_2(h)$  is the total number of hydrogen atoms in the second level in a  $1 \text{ cm}^2$  column along the line-of-sight at a height,  $h$ .

Now, from equation (2.10), we finally obtain the equation for the observed Balmer line emission within the frequency interval  $\nu$  and  $\nu + d\nu$  in the slitless flash spectrograms in the form:

$$E_{n_2, \nu} = \frac{\hbar \nu_{n_2}}{4\pi} A_{n_2} \frac{\alpha_{2n,y}}{\alpha_{2n}} n_n(0,0) \frac{1}{\beta} \sqrt{\frac{2\pi r}{\beta}} e^{-\beta h} \sum_{n=0}^{\infty} (-1)^n \frac{\{N_2(h) \alpha_{2n,y}\}^n}{(n+1)! (n+1)}, \quad (2.34)$$

or, using the relation (2.19),

$$E_{n_2, \nu} = \frac{\hbar \nu_{n_2}}{4\pi} A_{n_2} \frac{\alpha_{2n,y}}{\alpha_{2n}} N_n(h) \frac{1}{\beta} \sum_{n=0}^{\infty} (-1)^n \frac{\{N_2(h) \alpha_{2n,y}\}^n}{(n+1)! (n+1)}. \quad (2.35)$$

The series representing the last factor of the above equation corresponds to the fraction of energy absorbed in the atmosphere, which we hereafter denote by a symbol,  $\{\text{Abs}_n\}_v$ . Namely,

$$\{\text{Abs}_n\}_v = 1 - \frac{(N_2 \alpha_{2n,v})}{2! 2} + \frac{(N_2 \alpha_{2n,v})^2}{3! 3} - \dots \quad (2.36)$$

Returning to the integration (2.13), we recognize that  $\alpha_{2n,v}$  has been implicitly assumed to be constant to perform the integration over the atmosphere. According to our definition,  $\alpha_{2n,v}$  refers to the absorption coefficient at a frequency,  $v$ , so that it depends on the atmospheric conditions determining the line-profile. The line-profile may be determined by various effects, and  $\alpha_{2n,v}$  becomes a function of various parameters. Therefore, in a rigorous sense, a numerical integration only may be possible for a given model of atmosphere. In the following section, we shall integrate equation (2.35) over frequency to derive the total emission of the line. As we shall discuss later, we may assume Doppler broadening to be predominant for chromospheric conditions, for which  $\alpha_{2n,v}$  is a function of  $T_e$  only. Hence, only the isothermal atmosphere must be assumed in performing the integration (2.13). We shall return to this point later.

### §3. Consideration of total line emission and self-absorption.

In the previous section, we have considered the monochromatic emission corrected for self-absorption in the solar atmosphere. For the analysis of the eclipse spectrum, it may be desirable to have the corresponding expression for the total amount of energy involved in a line. We, therefore, integrate equation (2.35) over the line. While the line contour may be determined by various effects, we recognize that Doppler broadening is predominant for the chromospheric conditions we assumed, and neglect the terms due to collision damping and Stark-effect. Further, if we consider the formation of the detailed line structure, we have to include the dependence of the emission at the different frequencies on the distributions of various parameters. However, we are considering only the higher members of the Balmer series for which optical depths are small and we may consider that most of the emission comes from a small region of the chromosphere, as we have discussed earlier. For stronger lines, this simplification may not be justified.

Thus, we may approximate the absorption coefficient as follows:

$$\alpha_{2n,v} = \frac{\pi \epsilon^2}{mc} f_{2n} \frac{c}{\sqrt{\pi} v \nu_{n2}} e^{-\lambda^2} \quad (3.1)$$

$$\alpha_{2n} = \int_0^\infty \alpha_{2n,v} dv = \frac{\pi \epsilon^2}{mc} f_{2n} \quad (3.2)$$

where

$$\alpha = \frac{c(v - v_{2n})}{v v_{2n}} . \quad (3.3)$$

Then, from equation (2.35), we have

$$E_{n2} = \int_0^\infty E_{n2,v} dv = \int_0^\infty \frac{\hbar v_{2n}}{4\pi} A_{n2} \frac{c}{\sqrt{\pi} v v_{2n}} e^{-\alpha^2} N_n(r) \frac{1}{\beta} \{Abs_n\}_v dv . \quad (3.4)$$

The integration of the nth term of the series will be

$$\begin{aligned} \int_0^\infty \alpha_{2n,v}^n e^{-\alpha^2} dv &= \left( \frac{\pi c^2}{m c} f_{n2} \right)^n \left[ \frac{c}{\sqrt{\pi} v v_{2n}} \right]^n \int_0^\infty e^{-(n+1)\alpha^2} dv \\ &= (\alpha_{2n,0})^n \frac{v v_{2n}}{c} \frac{\sqrt{\pi}}{\sqrt{n+1}} \end{aligned} \quad (3.5)$$

where

$$\alpha_{2n,0} = \frac{\pi c^2}{m c} f_{n2} \frac{c}{\sqrt{\pi} v v_{2n}}$$

represents the absorption coefficient at the center of the line. Thus, we finally obtain

$$E_{n2} = \frac{\hbar v_{2n}}{4\pi} A_{n2} \frac{N_n(r)}{\beta} \sum_{n=0}^{\infty} (-1)^n \frac{\{N_n(r) \alpha_{2n,0}\}^n}{(n+1)! (n+1)^{\frac{n}{2}}} \quad (3.6)$$

for the total emission in the nth Balmer line in the volume of chromosphere considered. Or we may write

$$\begin{aligned} E_{n2} &= \frac{\hbar v_{2n}}{4\pi} A_{n2} \frac{N_n}{\beta} \{Abs_n\} \\ \{Abs_n\} &= 1 - \frac{(N_n \alpha_{2n,0})}{2! 2^{\frac{n}{2}}} + \frac{(N_n \alpha_{2n,0})^2}{3! 3^{\frac{n}{2}}} - \dots \end{aligned} \quad (3.7)$$

The above series is absolutely convergent, but for  $N_n \alpha_{2n,0}$  larger than 10 the convergence becomes very slow. For example, to obtain three decimal places for  $\{Abs\}$ , we have to carry out six figure computations of 27 terms. The amount of computation increases very rapidly for  $N_n \alpha_{2n,0}$ .

exceeding 10. Comparing (3.8) to Thomas' equation (1950a), however, we see that the form of the series is considerably simplified, and the coefficient of  $(N_2\alpha_{2n,0})^n$  is a factor of  $2^{-n}$  as large. Thus the range of calculations is extended widely.

As we have mentioned, following equation (3.5), the absorption coefficient at the line-center,  $\alpha_{2n,0}$  is proportional to  $v^{-1}$ , hence is a slowly varying function of the kinetic temperature,  $T_e$ ;  $\alpha_{2n,0} \sim (T_e)^{-\frac{1}{2}}$ . Since we have to assume an isothermal chromosphere to perform the integration developed in the preceding section, equation (3.7) may not be adequate for stronger lines (lower members of Balmer series) where the optical depths are so high that the outer layers of the chromosphere contribute considerably to the absorption. For the higher series lines, however, most of the emission originates in the small central region at the lowest layer observed. Hence, we may use this method as a first approximation and a numerical integration must be performed for a detailed analysis.

#### §4. Numerical results and the approximate formula for self-absorption.

In the preceding section we have developed the theoretical expression for self-absorption as a function of  $N_2\alpha_{2n,0}$ . If the observed amount of self-absorption in the Balmer flash spectrum line  $H_n$  is determined, then we can compute the value of  $N_2\alpha_{2n,0}$  from equation (3.8). Hence, the population of hydrogen atoms in the second level,  $N_2$ , may be obtained if we have the value of the chromospheric kinetic temperature for calculating the absorption coefficient,  $\alpha_{2n,0}$ . Equation (3.8) is absolutely convergent, but it requires cumbersome computations for higher values of  $N_2\alpha_{2n,0}$ .

After repeating the computation for a very small interval of  $N_2\alpha_{2n,0}$ , however, the author has found that the logarithms of  $\{\text{Abs}_n\}$  can be represented as a function of  $\log N_2\alpha_{2n,0}$  by a smooth curve, shown in Figure II. The exact calculation of the series has been carried to

$N_2\alpha_{2n,0} = 10$ . As we have discussed in the previous section, we have to compute 27 terms of the series, carrying six figures, to get three decimal places for  $\{\text{Abs}_n\}$ . It is practically impossible to extend the computation beyond  $N_2\alpha_{2n,0} = 10$ . However, we recall that formula (3.8) is derived from certain simplifying assumptions discussed prior to its derivation, so it may not be applicable for stronger lines (higher values of  $N_2\alpha_{2n,0}$ ).  $\log \alpha_{2n,0}$  is found to be -14.59 and -14.97 for  $T_e$  equal to 6,000° and 35,000°, respectively; and  $\log \alpha_{2n,0}$  is -15.16 and -15.54 for the same temperatures. Therefore, we see that Figure II can cover the lines as high as  $H_{10}$ , if  $\log N_2$  is smaller than 16, and to  $H_{15}$  for  $\log N_2$  of the order 16.5. From the results obtained in the following two chapters (cf. equations (6.1), Chapter IV, (2.6), Chapter V, and Figure IV), we estimate the value of  $\log N_2$  to be of the order 16 and 16.5 corresponding to the chromospheric heights of 1400 km and 500 km, respectively. That is, we can obtain  $\{\text{Abs}_n\}$  for the lines of higher order than  $H_{10}$  for the upper levels and  $H_{15}$  for the lower levels in the chromosphere.

While we may thus either use the curve of Figure II to obtain the amount of self-absorption for given  $N_2$  and  $T_e$  or to obtain the value of

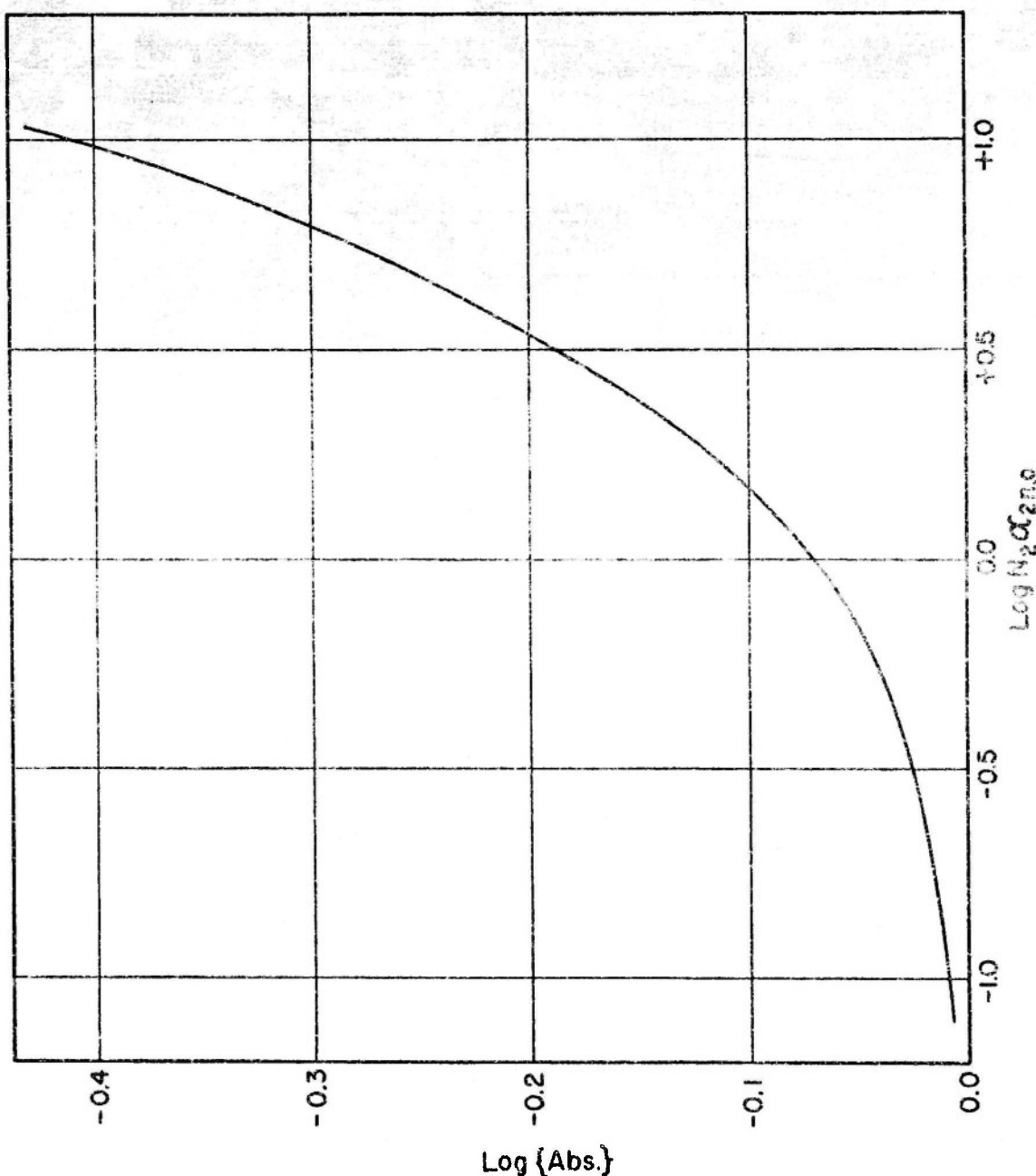


FIGURE II Log {Self Absorption} vs. Log  $N_2\alpha_{2n_0}$

$N_2 \alpha_{2n,0}$  inversely from some otherwise determined self-absorption, it will be very useful if we can find some analytical expression representing it. For example, if we calculate  $N_2$  from the relative amount of self-absorption as will be described in the following chapter, we need to have such a formula. Further, if we rely on our observation that the curve changes its slope very slowly for  $\log N_2 \alpha_{2n,0}$  higher than about 0.3, (that is, the curve appears to be nearly a straight line) the formula thus obtained may be used to extrapolate the function into the region

$$N_2 \alpha_{2n,0} > 10$$

By repeated use of the method of trial and error, we finally found that the expression

$$\log \{ \text{Abs}_n \} = -0.069 e^{2.31 \log (N_2 \alpha_{2n,0}) - 0.58 \{ \log (N_2 \alpha_{2n,0}) \}^2} \quad (4.1)$$

gave the best representation of the curve. Equation (4.1) may also be written

$$\log (-\log \{ \text{Abs}_n \}) = -1.16 + \log (N_2 \alpha_{2n,0}) - 0.25 \{ \log (N_2 \alpha_{2n,0}) \}^2 \quad (4.2)$$

In Table V the values computed from equation (4.2) are compared to those read from various points in Figure II.

Table V.

$\log N_2 \alpha_{2n,0}$	-1.0	-0.7	-0.4	-0.2	0.0	0.2	0.4	0.6	0.8	0.9	1.0
$-\log \{ \text{Abs}_n \}$ (Fig. II)	0.008	0.016	0.030	0.045	0.070	0.106	0.157	0.224	0.303	0.353	0.414
$-\log \{ \text{Abs}_n \}$ Eq. (4.2)	0.004	0.010	0.025	0.043	0.069	0.107	0.158	0.225	0.303	0.345	0.389

Thus, we see that equation (4.1) gives the exact value with an accuracy of three figures except for the first three and the last two columns. Since the last figure is insignificant in the practical analysis of observations, the expression (4.1) may be considered to give the exact solution for  $N_2 \alpha_{2n,0} < 10$ . However, it is obviously incorrect to extrapolate to larger values of  $N_2 \alpha_{2n,0}$  because we see in equation (4.1) that  $\log \{ \text{Abs}_n \}$  tends to zero as  $N_2 \alpha_{2n,0}$  goes to infinity. That is, the gradient of  $\log \{ \text{Abs}_n \}$  evidently changes its sign at some value of  $N_2 \alpha_{2n,0}$  which is obviously without physical significance. We may see the direction of this change appearing in the slight deviation of the values in the later part of the Table IV. It will, therefore, be best to limit the use of equation (4.1) to the analysis of smaller  $N_2 \alpha_{2n,0}$ .

We have also introduced a second approximate formula as follows:

$$\log \{A_{BS_n}\} = -0.076 (N_2 \alpha_{2n,0})^{\frac{3}{4}} \quad (4.3)$$

The comparison of this formula with the exact value is shown in Table VI.

Table VI.

$\log N_2 \alpha_{2n,0}$	-0.8	-0.6	-0.4	-0.2	0.0	0.2	0.4	0.6	0.8	0.9	1.0
$-\log \{A_{BS_n}\}$ Fig. II	10.012	0.019	0.030	0.045	0.070	0.106	0.157	0.227	0.303	0.352	0.414
$-\log \{A_{BS_n}\}$ Equ.(4.3)	10.019	0.029	0.038	0.054	0.076	0.107	0.152	0.214	0.302	0.355	0.427

In the above Table, we see that equation (4.3) gives an even better approximation than equation (4.1) for higher values of  $N_2 \alpha_{2n,0}$ . Further, for the whole range of  $N_2 \alpha_{2n,0}$  the simpler expression (4.3) has two decimal place accuracy. Since the accuracy of the present measurements of the eclipse spectrum could not exceed two decimal places in the logarithm, equation (4.3) may well be taken in the actual analysis.

## III A. APPINDIX

Consider the following series involved in equation (2.28), Chapter III:

$$S_n = 1 + \frac{n!}{2!(n-2)!} I_2 + \frac{n!}{4!(n-4)!} I_4 + \dots \quad (A.1)$$

where  $I_m$  represents the integral

$$I_m = \frac{2}{\sqrt{\pi}} \int_0^\infty e^{-p^2} g^m(p^2) dp, \quad (A.2)$$

in which  $g^m(p^2)$  is defined by

$$g^m(p^2) = \left( \frac{2}{\sqrt{\pi}} \int_0^p e^{-t^2} dt \right)^m. \quad (A.3)$$

From equation (A.3), we can write

$$\frac{dg}{dp} = \frac{2}{\sqrt{\pi}} e^{-p^2}. \quad (A.4)$$

Hence, from equation (A.2), we have

$$\begin{aligned} I_m &= \int_0^\infty \frac{dg}{dp} g^m(p^2) dp \\ &= \int_0^1 g^m(p^2) dg \\ &= \frac{1}{m+1}. \end{aligned} \quad (A.5)$$

Substituting the above equation into (A.1), we get

$$S_n = 1 + \frac{n!}{3!(n-2)!} + \frac{n!}{5!(n-4)!} + \dots \quad (\text{A.6})$$

Now consider the polynomial expansion

$$(1+x)^m = 1 + \frac{m!}{1!(m-1)!}x + \frac{m!}{2!(m-2)!}x^2 + \dots, \quad (\text{A.7})$$

$$(1-x)^m = 1 - \frac{m!}{1!(m-1)!}x + \frac{m!}{2!(m-2)!}x^2 - \dots. \quad (\text{A.8})$$

Comparing the above expansions to series (A.1), we readily see that  $S_n$  may be replaced by an integral

$$S_n = \frac{1}{2} \int_0^1 [(1+x)^n + (1-x)^n] dx. \quad (\text{A.9})$$

Hence, integrating (A.9) directly, we have

$$S_n = \frac{2^n}{n+1}. \quad (\text{A.10})$$

IV. APPLICATION TO THE FLASH SPECTRUM  
OF 1932 ECLIPSE

§1. Introduction.

In Chapter I, it was pointed out that the low decrement of the Balmer series lines is one of the anomalous features of the flash spectrum that cannot be explained by a model of the chromosphere that is a simple extension of the photosphere. Thomas (1950a) has first considered the problem quantitatively, and he suggested that self-absorption is responsible for this characteristic of the spectrum. By comparing the ratio of the observed intensities of a pair of higher order lines of the Balmer series with the theoretical intensity ratio computed from the assumption of thermodynamic equilibrium, Thomas found that the differences of these ratios show a systematic decrease both with order of the lines and height in the chromosphere. Since this systematic difference increases with increasing self-absorption, Thomas assumed that the difference between the observed and the computed Balmer decrement was due to the effect of the self-absorption only. By introducing this difference into his absorption formula (cf. equation (4), Thomas (1950a)), Thomas computed the population of hydrogen atoms in the second state at various heights. In his computation, however, he has taken into account, at each height, only one pair of very high order members of the Balmer series because of the difficulty of computation due to the slow convergence of the absorption formula he derived. Thus, the numerical results for  $N_2$  are open to question if there is evidence of considerable fluctuation in the observations. In fact, the fluctuation of  $N_2$  values computed for different pairs of lines were quite large. We will discuss this point in the next and last sections.

Further, Thomas has explicitly neglected the factor  $b_n$  which should be included under the assumption of high chromospheric temperature. Hence, as he pointed out, the amount of absorption that he estimated is to be considered as a lower limit. In section 2, we will discuss the effect of these simplifications, and point out some additional inconsistencies involved in Thomas' assumptions. Then, in the later sections, we will consider several possible methods for determining a self-consistent model of the chromosphere.

§2. Comment on Thomas' determination of  $N_2$  from self-absorption.

As discussed in the previous section, we will first follow Thomas' method to check his results. We start from the equation for Balmer line intensities, Chapter III, equation (3.7):

$$E_{n_2} = \frac{\hbar \lambda_{n_2}}{4\pi} \frac{1}{\beta} A_{n_2} N_n(\tau) \{ \text{Abs.}(N_2(\tau), \alpha_{2n,0}) \}. \quad (2.1)$$

To make the factor  $b_n$  explicit in the above equation, we replace the spontaneous transition probability,  $A_{n1}$ , by the total atomic absorption coefficient,  $\alpha_{2n}$ , according to the relation

$$\frac{A_{n2}}{\alpha_{2n}} = \frac{8\pi\nu_m^2}{c^2} \frac{W_2}{W_n} \left(1 - \frac{n_n}{n_2} \frac{W_2}{W_n}\right)^{-1},$$

therefore,

$$\frac{A_{n2}}{\alpha_{2n}} = \frac{8\pi\nu_m^2}{c^2} \frac{n_2}{n_n} \left(\frac{n_2}{n_n} \frac{W_n}{W_2} - 1\right)^{-1} \quad (2.2)$$

where

$$\frac{n_2}{n_n} \frac{W_n}{W_2} = \frac{b_2}{b_n} e^{\frac{\hbar\nu_{2n}}{kT_e}} \quad (2.3)$$

from the definition of  $b_n$ , Chapter II, equation (1.1). Hence we can write

$$\frac{A_{n2}}{\alpha_{2n}} = \frac{8\pi\nu_{2n}}{c^2} \frac{n_2}{n_n} \left(\frac{b_2}{b_n} e^{\frac{\hbar\nu_{2n}}{kT_e}} - 1\right)^{-1}. \quad (2.4)$$

From equation (2.2) we note that the second term in the bracket of equation (2.4) gives the contribution due to the radiation induced emission. Substituting equation (2.4) into (2.1), we have

$$E_{n2} = \frac{2\hbar\nu^3}{c^2} \frac{1}{\beta} N_2(\hbar) \alpha_{2n} \left(\frac{b_2}{b_n} e^{\frac{\hbar\nu_{2n}}{kT_e}} - 1\right)^{-1} \{Abs_n\}. \quad (2.5)$$

If we work with the logarithmic gradient of  $E_{n2}$ , we eliminate all the factors that do not depend on the quantum number,  $n$ . Thus we have

$$\begin{aligned} \Delta \log E_{n2} &= 3 \Delta_n \left(\frac{1}{q} - \frac{1}{n^2}\right) + \Delta_n \log \alpha_{2n} \\ &\quad - \Delta_n \log \left(\frac{b_2}{b_n} e^{\frac{\hbar\nu_{2n}}{kT_e}} - 1\right)^{-1} + \Delta_n \log \{Abs_n\} \end{aligned} \quad (2.6)$$

where  $\Delta_n \rightarrow f(n) - f(n+k)$ . The above equation corresponds to equation (3a) in Thomas' paper. Note that Thomas, in equation (1), implicitly omitted the radiation induced emission term by placing outside the integration. This is not generally justified, even though as we shall see, it leads to the same equation.

We first consider the term  $b_2/b_n \exp\left(\frac{\hbar\nu_{2n}}{kT_e}\right)$ . The numerical values of  $\exp\left(\frac{\hbar\nu_{2n}}{kT_e}\right)$  are shown in Table VII.

Table VII.

Value of  $e^{\frac{-h\nu_{n_2}}{kT_e}}$ .

$T_e = .6000$	10,000	20,000	35,000
$\nu_{2,10}$	$8.7 \cdot 10^9$	$2.3 \cdot 10^5$	$8.7 \cdot 10$
$\nu_{2,30}$	$9.1 \cdot 10^9$	$2.5 \cdot 10^5$	$9.1 \cdot 10$

Thus we see that for temperatures lower than  $20,000^\circ$ , we can immediately neglect the induced emission term, since  $b_2 \geq b_n$ . From the results of the theoretical computations in Chapter II, we know that  $b_2/b_n > 10^3$ , at least for  $n$  higher than 10 and  $T_e = 30,000^\circ$ . Therefore, we can state that  $b_2/b_n \exp(h\nu_{n_2}/kT_e) \gg 1$  for the range of conditions in the present study, and we can ignore the radiation induced emissions. Accordingly, we write

$$-\Delta_n \log \left( \frac{b_2}{b_n} e^{\frac{-h\nu_{2n}}{kT_e}} - 1 \right) = \Delta_n \log b_n e^{-\frac{h\nu_{2n}}{kT_e}}. \quad (2.7)$$

Thus, we see that the  $\log b_2$  term subtracts out of equation (2.6), leaving

$$\begin{aligned} \Delta_n \log E_{n_2} = & 3 \Delta_n \log \left( \frac{1}{4} - \frac{1}{n^2} \right) + \Delta_n \log \alpha_{2n} + \Delta_n \log b_m \\ & - \Delta_n \log e^{\frac{-h\nu_{2n}}{kT_e}} + \Delta_n \log \{ \text{Abs.}_n \}. \end{aligned} \quad (2.8)$$

To show the effect of temperature variation, we have tabulated in Table VIII the differences of fourth terms in equation (2.8).

Table VIII.

$\frac{-h\nu_{n,n+k}}{kT_e}$ . mod.

$n - n + k$	$T_e = 6000^\circ$	10,000°	20,000°	35,000°
25 - 30	0.01	0.00	0.00	0.00
20 - 25	0.01	0.01	0.00	0.00
15 - 20	0.02	0.01	0.01	0.00
10 - 15	0.06	0.04	0.02	0.01
10 - 13	0.05	0.03	0.01	0.01

Since the observed data used for the present computation are given to two decimal places only, we can say that, at least for  $n$  higher than

15, logarithmic decrements are not at all sensitive to temperature variations. For  $n$  between 10 and 15, there is also no temperature effect for  $T_e$  higher than  $20,000^\circ$ . Slight differences due to the temperature term may have to be considered for  $n \leq 15$  and  $T_e \leq 10,000^\circ$ .

Thomas has ignored the  $b_n$  factor in equation (2.8). Unfortunately, at the present time, there is no exact computation of  $b_n$  for  $n$  higher than 10. However, we may use the asymptotic values computed by Thomas to estimate the order of magnitude of  $\Delta_n \log b_n$ . (It should be noted that these values are obtained from computations in which collisional excitations are neglected, Cf. Chapter II.). In Table IX we compare these values to the values,  $\Delta_n \log \{Abs_n\}$  at each height for which Thomas computed the values of  $N_2$ . The values inside the brackets are computed using the small corrections in Table VIII for  $T_e = 35,000^\circ$ .

Table IX.

 $\Delta_n \log b_n$  and  $\Delta_n \log \{Abs_n\}$ 

Height	670 km	1500 km	2330 km	3170 km
$n - n + k$	25 - 30	15 - 20	10 - 15	10 - 13
$\Delta_n \log b_n$	0.02	0.07	0.13	0.09
$\Delta_n \log \{Abs_n\}$	0.04	0.05	0.10(0.09)	0.05(0.04)

Thus, from the above table, we see that the factors  $\Delta_n \log b_n$  are even larger than  $\Delta_n \log \{Abs_n\}$ . Even if we consider that the above  $\Delta_n \log b_n$  are upper limits, we may at least say that both factors are about the same order of magnitude, so that the neglect of the  $b_n$  term is by no means justified. On the other hand, if we assume the electron temperature to be as low as  $6,000^\circ$ , where  $b_n$  terms vanish theoretically, the exponential term becomes significant (Table VIII). Therefore, the omission of both these terms leads to much too low a value for  $N_2$ . We will return to this question later. As long as we assume the electron temperature to be of the order of  $35,000^\circ$  the largest factor in determining the temperature as well as its variation seems to be the  $b_n$  factor rather than  $\{Abs_n\}$ , and the contribution of the exponential term is negligible. In the later sections of his paper (1950a), Thomas introduced the logarithmic height gradient of  $N_2$  obtained from his computation into the equation of hydrostatic equilibrium at  $T_e = 35,000^\circ$ , and determined the temperature gradient, ignoring a gradient in  $b_n$ . It should therefore be noted that the computations thus developed are not self-consistent, as Thomas himself has pointed out.

Ignoring for the moment questions involved in the simplified computations of Thomas, we will follow his assumptions and compute  $N_2$  from the other pairs of lines to check the consistency of the results. Since the series for  $\{Abs_n\}$  converges more rapidly in our revised formula discussed in Chapter III, we can now perform the computation for pairs of lower order lines.

Table X.

The population of the Balmer ground state along the line of sight.

$$N_2 \times 10^{-16}$$

$n-n+k \backslash h$	670 km	1500km	2330km	31.70km
25 - 30	2.53			
20 - 25	1.77			
15 - 20	0.82	0.46		
10 - 15	0.68	0.52	0.22	
10 - 13	0.87	0.67	0.33	0.13

The results of computations are shown in Table X. The first entry in each column corresponds to the value Thomas computed at each height. As we have discussed in Chapter III, p.23, Thomas used half the population of the Balmer ground state in place of the total, so that the results shown in Table 2 in his paper should be multiplied by two.

We notice in Table X that the values are considerably scattered for the different combinations of lines. However, the fluctuations are not random. The values decrease rather systematically towards the lower order line combinations for the lowest height, while the effect is in the opposite direction for the next lowest height. Considering this change in the direction of the effect for two different heights, as well as the dependence of the results on a particular choice of combination of two lines, one might simply attribute the effect to the random scattering of the observed data. Before doing so, however, we should consider how the simplifying assumptions made in the computations might affect the results. Let us consider the direction of the contribution of  $\Delta_n \log b_n$  in equation (2.8). Since  $b_n > 1$  and it approaches unity monotonically as  $n$  increases, we see,

$$(\log b_n - \log b_{n+k}) > (\log b_{n'} - \log b_{n'+k}) \text{ for } n < n'. \quad (2.9)$$

That is, the inclusion of  $\Delta_n \log b_n$  adds larger numbers for smaller  $n$  than for larger  $n$  to the left hand side of equation (2.8), which means the relative absorption  $\Delta_n \{A_{\text{bs}_n}\}$  should be larger for the lower lines than the amount we have used in the computation. Hence the contribution due to the  $b_n$  factor would increase the values of  $N_2$  more for combinations of lower than for higher order lines. The direction of the correction expected by the inclusion of the departure from thermodynamic equilibrium

thus seems promising (at the lowest height). If we assume the chromospheric temperature to be as low as  $6000^{\circ}$ , then the effect of the inclusion of the Boltzmann factor  $\Delta_n \log e^{X_n}$  will also be to increase  $N_2$  in the same direction although the amount of this effect is smaller than the inclusion of  $\Delta_n \log b_n$ .

As far as the values shown in Table IX are concerned, the above argument holds only for the lowest height. For the height of 1500 km the first two entries show the opposite effect. The increase in the last row for all three heights is not easily justified without knowing the most probable values of  $b_n$  for  $n$  higher than 10, because the interval of  $n$  is not the same as for the others. We also cannot depend too greatly on the disagreement at 1500 km compared to the lowest, since the calculations are made for only two combinations. We realize that the relative intensity of  $H_{20}$  to  $H_{25}$  at 1500 km implies a negative absorption, which of course is an indication of the observational error.

Thus, we again note the possibility of a considerable dependence of the results on the choice of two lines. We may not be able to draw any conclusions from data at greater heights unless we make computations for a much larger number of line combinations. The importance of the systematic variations of  $N_2$  values for 670 km, therefore, is not affected by the failure of data at greater heights to follow that system. Thus we conclude that it is worth-while to consider methods of including the  $b_n$  factor in the calculation.

### §3. Consideration of the effect of self-absorption, including departure from thermodynamic equilibrium.

There may be two alternative methods to include departures from thermodynamic equilibrium. In order to determine the amount of self-absorption we have essentially two parameters,  $b_n$  and  $N_2$ , both of which are functions of  $T_e$  and  $N_e$ . From the slitless observations of the flash spectra, only the continuum measurements have provided a direct determination of  $T_e$  and  $N_e$  as a function of chromospheric height. That is, from the free-bound emission we can determine  $T_e$  and  $N_e$  and the electron-scattered photospheric continuum gives us  $N_e$  independently. If we thus have the values  $T_e$  and  $N_e$  at each height, we can compute first  $b_n$ , then  $N_n$ , theoretically. Hence one method is to substitute the theoretical values of  $b_n$  thus computed into equation (2.8) to estimate the real amount of self-absorption from the measured line intensities. Then from this amount of self-absorption we can determine the value of  $N_2$  at each height. Since  $N_2$  is a function of  $b_2$ ,  $T_e$  and  $N_e$ , we may recompute the values of  $T_e$  and  $N_e$  from the line intensities. The second method is to assume  $N_2$  at each height, and from it, compute the amount of self-absorption. We then use the self-absorption to make corrections for the observed line intensities, and from the corrected line intensities and equation (2.8) we determine  $b_n$  at each height. Then, from these values of  $b_n$ , we can estimate  $T_e$  and  $N_e$ . Thus, from either one of these methods, we can obtain a preliminary distribution of  $T_e$  and  $N_e$  that we can use to start the second approximation in the analysis. Repeating the same procedure

we may finally determine a self-consistent model of the chromosphere from both line and continuum measurements.

At the present time, unfortunately, we have only Wildt's determination (1947) of the  $N_2$ -gradient, which was obtained by setting the emission gradient equal to the density gradient; but we have no absolute values of  $N_2$  except the one by Thomas discussed in the preceding section. On the other hand, the application of continuum measurements mentioned above involves various uncertainties. Separation of the free-bound emission and the scattered continuum is difficult. Second, since  $T_e$  appears only in the Boltzmann exponential factor of the free-bound emission, we have to depend on small differences in the observed data to determine  $T_e$ , so that small errors in the measurements are of importance.

Further, the theoretical computation of  $b_n$  involves a great amount of computation. We have available only the asymptotic values of  $b_n$  for  $n$  higher than 10, computed for the case  $T_e = 35,000^\circ$ , to which we have referred in section 2. We must also note that the final determination of  $N_2$  in the first method requires another laborious computation, if we follow the same procedure described in section 2 involving every pair of lines in the analysis, because of the difficulty of solving the exponential formula to obtain  $N_2$ .

It is therefore desirable to determine a  $T_e$  and  $N_e$  distribution from the line intensities only, and then to compare these results with the results obtained from the continuum. In general, the temperature determinations discussed in Chapter I that were based on line intensities yielded higher values than those based on continuum intensities. It may be that line emission and continuum radiation originate under different atmospheric conditions.

The following method, based on least square analysis, provides a somewhat independent determination of  $b_n$  and  $N_2$  and minimizes as well the amount of computation necessary to include all the line intensities at a certain height. The least square calculation assumes that all the small fluctuations from the theoretical Balmer decrement may, after including both effects of the departure from thermodynamic equilibrium and the self-absorption, be attributed to observational errors. If we assume some expression for  $b_n$  as an analytical function of  $n$ , we may express the Balmer line intensity as a function of  $n$ . Thus we write equation (2.5) in the following logarithmic form, retaining only terms depending on the quantum number,  $n$ :

$$\log E_{n2} = A + 3 \log \left( \frac{1}{4} - \frac{1}{n^2} \right) + \log \alpha_{1n,0} + \log b_n + B \frac{1}{n^2} + \log \{ \text{Abs}_n \}$$

where

$$A = \log \frac{2\pi R^3}{C^2} \frac{1}{\beta} N_2(r) \frac{1}{b_2} e^{-\frac{\pi R}{kT_e} \frac{1}{2^2}} \quad (3.1)$$

and

$$B = \log e \cdot \frac{kR}{kT_e}.$$

We note that the Boltzmann factor is also included, and we have ignored the radiation induced emission. In the above expression A and B are independent of n but involve  $T_e$  and  $b_2$ .

Now we wish to express  $b_n$  as a function of n. Using Thomas' asymptotic values for  $b_n$  mentioned in section 2, we find the following to be the most simple formula:

$$\log b_n = P + \frac{q}{n} + \frac{\gamma}{n^2}. \quad (3.2)$$

Actually, the first two terms are sufficient to fit Thomas' values. Table XI shows the comparison of the computed values and the values obtained from the formula:

$$\log b_n = 0.3 + \frac{3.75}{n}. \quad (3.3)$$

Table XI.

Theoretical values of  $b_n$ .

n	10	13	15	20	25	30
Thomas	0.68	0.59	0.55	0.48	0.44	0.42
Equation (3.3)	0.68	0.59	0.55	0.49	0.45	0.42

Thus, we assume that the expression (3.2) with the third term introduced is adequate for the whole range of electron temperatures. Substituting (3.2) into equation (3.1), we have

$$\log E_{n2} = 3 \log \left( \frac{1}{4} - \frac{1}{n^2} \right) + \log d_{2n} + C_1 + C_2 n^{-1} + C_3 n^{-2} + \log \{ \text{Abs}_n \} \quad (3.4)$$

where

$$C_1 = A + P, \quad C_2 = q, \quad C_3 = B + \gamma.$$

Since, the coefficients,  $P$  and  $\gamma$  of the  $b_n$  formula are combined with the other constants including  $T_e$ , we cannot determine the absolute value of  $b_n$ . Since, however, as we will show later, the coefficient  $C_3$  is negligibly small, and we can obtain the ratio  $b_n / b_{n'}$ .

The principle of the present method is to assume a certain value for  $N_2$  from which we compute  $\{Abs_n\}$  to substitute into equation (3.4). From this, we compute a correction factor  $\Delta N_2$  and the coefficients for  $b_n$  by assuming that the observed Balmer decrement can be fixed by (3.4) with a small differential correction  $\Delta \{Abs_n\}$ . Thus we obtain both a corrected value  $N_2$  and the ratio  $b_n/b_{n'}$ , which we use in repeating the analysis successively. After adding a differential of  $\log \{Abs_n\}$ , we can arrange equation (3.4) in the following form for convenience of computation:

$$\varphi = C_1 + C_2 n^{-1} + C_3 n^{-2} + \frac{\partial \log \{Abs_n\}}{\partial N_2} \Delta N_2 \quad (3.5)$$

where

$$\begin{aligned} \varphi &= \log E_{\gamma_2} - 3 \log \left( \frac{1}{4} - \frac{1}{n^2} \right) - \log \alpha_{2n} - \log \{Abs_n\} \\ \frac{\partial \log \{Abs_n\}}{\partial N_2} &= \frac{\sum_{m=1}^{\infty} (-1)^m \frac{m (N_2 \alpha_{2n})^{m-1}}{(m+1)! (m+1)^{3/2}} \alpha_{2n,0}}{\sum_{m=0}^{\infty} (-1)^m \frac{(N_2 \alpha_{2n})^m}{(m+1)! (m+1)^{3/2}}} \end{aligned}$$

$\varphi$  represents the observed quantity, and we can determine  $C_1$ ,  $C_2$ ,  $C_3$ , and  $\Delta N_2$ . One advantage of this method is that we do not have to assign a definite value for  $T_e$  and  $N_e$ . Since  $C_1$  is determined by least square calculation, values of electron temperature and electron density above a certain height may be fixed observationally through the coefficient  $C_1$ .

#### §4. Numerical results and discussion.

The calculation was carried out first neglecting, then including, the term  $C/n^2$  in equation (3.5) and comparing the two results. It was concluded that this term was not appreciable at all, which implies that the exponential Boltzmann factor was negligible, and, also, that the last term of equation (3.2) is not significant for a  $b_n$  approximation. In general, we have included every line for which the convergence of the absorption term is sufficient to carry out the computation at each height, excluding the few lines recognized in the literature as blended with other lines. According to Menzel (1931), H<sub>30</sub>, H<sub>28</sub>, H<sub>25</sub>, H<sub>14</sub>, and H<sub>8</sub> are blended with strong lines of Ti<sup>+</sup>, Y<sup>+</sup>, V<sup>+</sup>, Ti<sup>+</sup>, and He, respectively. H<sub>22</sub> is also blended with a weak line of Fe, but is included. For the lowest height, however, we first included all these blended lines and then, for comparison purposes, we repeated the same analysis excluding them. We found that the successive computations did not show a monotonic convergence, probably indicating that the observational data were too inaccurate to determine the numerical figures to the high precision we expected. Therefore, in the following, we will show the number obtained at each step of the successive computations.

##### i). Result for the lowest height, $h = 670$ km.

The lines higher than H<sub>15</sub> were included. We took  $N_2 \alpha_{3s} = 0.86$

and obtained  $\Delta(N_2\alpha_{30}) = 0.13$  and  $C_2 = 3.7$ . To see the effect of small computational fluctuations, we interchanged the order of the  $C_2$  and the  $\Delta N_2\alpha_{30}$  terms in equation (3.5). This gave  $C_2 = 3.6$  and  $\Delta(N_2\alpha_{30}) = 0.12$ . It is interesting to note that  $\Delta(N_2\alpha_{30}) = 0.11$  was also obtained from the analysis covering only the lines from H<sub>25</sub> to H<sub>30</sub>.

All the blended lines were included in the above computation. Repeating the analysis with the same initial value  $N_2\alpha_{30} = 0.86$ , but excluding H<sub>22</sub>, H<sub>25</sub>, H<sub>28</sub> and H<sub>30</sub>, we obtained  $\Delta N_2\alpha_{30} = 0.10$  and  $C_2 = 3.6$ . Then, as the second approximation, we started from the value  $N_2\alpha_{30} = 0.95$ . We obtained  $\Delta N_2\alpha_{30} = 0.04$  and  $C_2 = 3.3$  from both equation (3.5) and the same equation with the order of two terms interchanged. Thus, both approximations give  $N_2\alpha_{30} = 0.99$ , and indicate that this value is reliable. However, the accuracy of the present data is not sufficient to give the value  $\Delta(N_2\alpha_{30})$  to two decimal places for a reason that will be pointed out later.

The final normal equations derived from the analysis, from which the above values were computed, are as follows:

for  $N_2\alpha_{30} = 0.86$ ,  $C_1 + C_2 n^{-1} + \frac{\partial f_{Abs}}{\partial N_2\alpha} \Delta(N_2\alpha) = \phi$

13	6.3438	-4.3590	0.5440
	3.2168	-2.2449	0.2970
	1.6007	-0.2100	
	-0.1210	0.1177	0.0315
		-0.1391	0.0282
		0.0246	0.0024

$\Delta N_2\alpha_{30} = 0.10$ ,

for  $N_2\alpha_{30} = 0.95$ ,

	-4.0868	0.7350
	-2.0902	0.3947
	1.3805	-0.2588
	0.0958	-0.0360
	-0.957	0.0277
	0.0199	0.0008

Since the observed data is given to only two decimal places, only the first two figures after the decimal point are significant in the above calculations. Therefore, for  $N_2\alpha_{30} = 0.95$  the value  $\Delta(N_2\alpha_{30}) = 0.04$  has no meaning and even for  $N_2\alpha_{30} = 0.86$ ,  $\Delta N_2\alpha_{30}$  is not actually determinate within the indicated accuracy. This means that we cannot determine more than one decimal place for  $N_2\alpha_{30}$ . Thus from this analysis, we can only state that at

$$R = 670 \text{ km} \quad (4.1)$$

$$N_2 \alpha_{30} \sim 0.9, \quad N_2 \sim 3 \cdot 10^{16}, \quad B \sim 4$$

It may be interesting to note that the value  $C_2 = 4$  agrees well with Thomas' numerical solution of equation (3.3).

The same computations for this height were repeated, including the term,  $C_3/n^2$  in (3.5). It was found that  $C_3$  was zero for all cases, so we concluded that this term was not appreciable for the present computation. We will discuss in a later section the accuracy of the results shown in equation (4.1).

### ii). Results for $h = 1500 \text{ km}$ .

We will next show the normal equations computed for the height  $h = 1500 \text{ km}$  for various initial values of  $N_2 \alpha_{30}$ . Again, all lines from  $H_{15}$  to  $H_{30}$  except the blended lines were included in the computations. Actual computations were carried to four decimal places, but only three decimals are shown.

$N_2 \alpha_{30} = 0.18$	$C_1 + C_2 n^{-1}$	$\frac{\partial f}{\partial N_2 \alpha}$	$\Delta N_2 \alpha = 0.4$
	13 $6.3438 \times 10$	-7.140	-1.249
	3.2168	-3.844	-0.597
		5.005	0.654
	-0.1210	0.359	-0.013
		-1.084	0.032
		0.017	0.006

$$\Delta N_2 \alpha = 0.4$$

$N_2 \alpha_{30} = 0.49$	$C_1 + C_2 n^{-1}$	$\frac{\partial f}{\partial N_2 \alpha}$	$\Delta N_2 \alpha = -0.4$
	-4.085	-0.391	
	-2.089	-0.139	
	1.380	0.075	
	0.096	-0.052	
	-0.096	0.048	
	0.020	-0.007	

$$\Delta N_2 \alpha = -0.4$$

$N_2 \alpha_{30} = 0.26$	$C_1 + C_2 n^{-1}$	$\frac{\partial f}{\partial N_2 \alpha}$	$\Delta N_2 \alpha = 0.6$
	-6.673	-0.996	
	-3.573	-0.461	
	4.261	0.449	
	0.317	-0.025	
	-0.836	0.062	
	0.007	0.004	

$$N_2 \alpha_{30} = 0.86$$

-4.359	0.394
-2.245	0.274
1.601	-0.218
0.118	-0.082
-0.139	0.086
0.025	-0.007

$$\Delta N_2 \alpha_{30} = -0.3$$

We see that for all four initial values ranging from  $N_2 \alpha_{30} = 0.18$  to 0.86, the final values of  $\varphi$  are less than the last significant value, 0.01. That is, we cannot obtain physically significant values for  $\Delta(N_2 \alpha_{30})$  even to one decimal place. If we calculate

$\Delta(N_2 \alpha_{30})$  using the third figure for  $\varphi$ , we have results that are inconsistent with what we would expect from the method of successive approximations. For  $N_2 \alpha_{30} = 0.26$ , we get a higher positive value of  $\Delta(N_2 \alpha_{30})$  than for  $N_2 \alpha_{30} = 0.18$ . For  $N_2 \alpha_{30}$  as high as 0.86,  $\Delta(N_2 \alpha_{30})$  is less negative than for 0.49. Thus, we cannot obtain even the first decimal place for  $N_2 \alpha_{30}$  at this height. This means that the effect of self-absorption and the departure from thermodynamic equilibrium in the higher members of the Balmer series are not sufficient to lead to self-consistent values of  $N_2$  within the accuracy of the observation.

The same computations were carried out for the height,  $h = 2330\text{km}$  and  $3170\text{ km}$ , covering the lines,  $H_{10} - H_{17}$  and  $H_6 - H_{13}$ , respectively. As we would expect, the results showed that the situation becomes even worse for higher regions, and the conclusion stated above is confirmed.

Now returning to the value shown in (4.1), and comparing the value at this height with those at greater heights, it may not be possible to conclude immediately that at least the first figure of  $N_2 \alpha_{30}$  is determinable even at the lowest height. Unless we repeat the calculations taking various initial values at large intervals, such as  $N_2 \alpha_{30} = 0.5, 1.0, 1.5$ , we cannot prove that the result (4.1) has meaning. However, it seems unwise to repeat such laborious computations; as a matter of fact it is impossible for  $N_2 \alpha_{30}$  greater than 1.0, because of the slow convergence of the  $\{\text{Abs}_n\}$  series. Therefore, in the next section, we consider some simple calculations designed to estimate a rough order of  $N_2$ , following the first method discussed in section 3.

## §5. Determination of $N_2$ and $N_2$ -gradient.

In the preceding section, we found that successive calculations by the least square method did not converge to determine a solution of

sufficient accuracy. The fundamental equation (3.5) was chosen for the analysis under the assumption that the  $b_n$  factor was solely responsible for the systematic errors of the earlier method. That is, we assumed the non-identical values of  $N_2$  shown in Table X were due to the omission of  $b_n$ . It is not very clear whether this basic interpretation was faulty or simply that the accuracy of the observation was not sufficient for obtaining quantitatively consistent results. In the discussion of Table X, we mentioned that the systematic decrease of  $N_2$ -value may not have appeared for a series of different combinations of the lines and suggested that the non-identical results may be attributed to observational errors. The only way to prove this possibility seems to be to repeat the same calculation for a sufficiently large number of different line-combinations and draw a statistical interpretation. Since we have found some approximate formulae for the self-absorption series, the computation described in section 2 is not too difficult. Thus, we made the following calculations using equation (4.3) in Chapter III.

We set

$$\log \{ \text{Abs}_n \} = -0.076 (N_2 \alpha_{2n,0})^{\frac{3}{4}}.$$

Hence, the logarithmic ratio of the self-absorption of two different lines is given by

$$\Delta_n \log \{ \text{Abs}_n \} = \log \{ \text{Abs}_n \} - \log \{ \text{Abs}_{n+k} \} = -0.076 N_2^{\frac{3}{4}} \left\{ \alpha_{2n,0}^{\frac{3}{4}} - \alpha_{2(n+k),0}^{\frac{3}{4}} \right\}. \quad (5.1)$$

Substituting the above into equation (2.8), we have

$$\Delta_n \log E_{n_2}(\text{obs}) - \Delta_n \log E_{n_2}(\text{T.E.}) = \Delta_n \log b_n - 0.076 N_2^{\frac{3}{4}} \left\{ \alpha_{2n,0}^{\frac{3}{4}} \right\}. \quad (5.2)$$

The value,  $N_2$ , can be determined directly from the above equation. The first and second term of the left hand side is the logarithm of the intensities observed to the theoretical intensities in thermodynamic equilibrium neglecting the self-absorption. The Boltzmann factor,  $e^{X_n}$ , is included in the second term, and is not negligible for lower temperatures. Apart from the  $b_n$  term, the temperature factor appears only in the absorption coefficient,  $\alpha_{2n,0}$ , and in the small quantity  $\Delta_n e^{X_n}$ . In the following computation, we consider an isothermal atmosphere at two extreme temperatures,  $T_e = 6000^\circ$  and  $T_e = 35,000^\circ$ . For  $T_e = 6000^\circ$  we can ignore the term  $b_n$  since the assumption of the thermodynamic equilibrium may hold. If we set  $T_e = 35,000^\circ$ , the greatest amount of uncertainty comes in through the term  $\Delta_n \log b_n$ . We have made computations for two cases, one neglecting  $\Delta_n \log b_n$  which corresponds to the computation shown in Table X, and the other including the asymptotic values of  $\Delta_n \log b_n$  discussed in section 3 and computed from equation (3.3). From recent results, as we have discussed in Chapter I, the most probable

Table XII

 $N_2 \times 10^{-16}$ 

Height (km)	$T_e = 6000^\circ$ inc. $e^{xn}$				$T_e = 35000^\circ$ inc. $\frac{b_n}{e^{xn}}$				$T_e = 35000^\circ$ no $b_n$ inc. $e^{xn}$			
	670	1500	2330	3170	670	1500	2330	3170	670	1500	2330	3170
25-30	1.20	*13.70			3.14	*35.7			2.53	*33.1		
24-29	1.04	* 3.48			2.72	* 9.15			2.51	* 8.40		
23-28	0.64	0.37			1.65	0.95			1.49	0.86		
22-27	1.54	#			4.11	#			3.74	#		
21-26	0.47	#			1.23	#			1.03	#		
20-25	0.94	#			2.49	#			1.79	#		
19-24	0.39	#			1.03	#			0.94	#		
18-23	1.50	0.14			3.91	0.36			3.41	0.31		
17-22	0.27	0.15			0.72	0.39			0.63	0.33		
16-21	0.84	0.85			2.26	2.30			1.90	1.93		
15-20	0.31	0.22			0.85	0.62			0.72	0.46		
14-19	0.41	0.29			1.13	0.79			0.88	0.63		
13-18	*0.09	0.23			*0.26	0.67			*0.22	0.51		
12-17	0.33	0.25	*0.46		0.93	0.75	*1.00		0.69	0.54	*0.75	
11-16	0.39	0.26	*0.46		1.12	0.75	*0.98		0.76	0.52	*0.70	
10-15	0.35	0.29	0.18		1.02	0.88	0.37		0.71	0.52	0.25	
27-30	1.18	#			2.91	#			2.83	#		
26-29	# * 1.98				# * 4.60				# * 4.47			
25-28	2.04	* 4.63			5.22	* 11.03			4.92	* 10.40		
24-27	1.75	* 2.56			4.48	* 6.11			4.23	* 5.77		
23-26	0.56	#			1.44	#			1.36	#		
22-25	1.69	#			4.33	#			4.08	#		
21-24	#	#			#	#			#	#		
20-23	1.75	0.90			4.48	2.14			4.23	2.02		
19-22	*5.23	1.04			*13.86	2.56			*12.60	2.33		
18-21	2.11	0.40			5.41	0.97			4.92	0.88		
17-20	0.30	#			0.76	#			0.69	#		
16-19	0.50	0.79			1.28	1.97			1.13	1.74		
15-18	0.24	0.57			0.63	1.38			0.56	1.22		
14-17	*0.20	0.29	0.21		*0.53	0.71	0.53		*0.45	0.61	0.45	
13-16	*0.10	#	0.33		*0.27	#	0.81		*0.23	#	0.69	
12-15	0.24	0.12	0.09		0.65	0.30	0.22		0.54	0.25	0.18	
11-14	0.40	0.38	0.43		1.07	0.94	1.07		0.86	0.76	0.86	
10-13	0.47	0.47	0.19	0.08	1.28	1.20	0.48	0.19	0.97	0.91	0.36	0.14
15-17		*1.33				*3.28				*3.11		
14-16		0.07				0.19				0.17		
13-15		#				#				#		
12-14		*0.45				*1.18				*1.03		
11-13		0.34	0.13			0.79	0.35			0.67	0.29	
10-12		0.14	0.11			0.37	0.30			0.30	0.24	
Mean	0.852	0.422	0.221	0.107	2.223	1.086	0.537	0.280	1.966	0.912	0.437	0.223
$\frac{d \ln N_2}{dh}$	0.85	0.78	0.86		0.86	0.65	0.78		0.92	0.91	0.80	

value of  $T_e$  seems likely to be lower than  $35,000^\circ$ , so that the values,  $\Delta_n \log b_n$  we used may be considered as the maximum values. Further, since we will see later that the final results are not too sensitive to the  $b_n$  factor, we can determine  $N_2$ .

The values of  $N_2 \times 10^{16}$  thus computed are tabulated in Table XII. For each height, we included every line higher than  $H_{10}$  in our computations. For lines lower than  $H_{10}$ , the self-absorption becomes too large for application of our approximate formula. The first column of the table gives the numbers designating the pair of lines taken for the computation of the  $N_2$  values in the corresponding rows. While there is no reason for selection of particular pairs of lines, we computed with every possible combination of line numbers having intervals of five and three. For the two highest regions, we introduced also the combinations of lines having intervals of two in order to have more data. Thus we have repeated the computation a sufficient number of times to obtain for the three lower heights enough results to carry out a statistical analysis. For the highest region, the number of lines observed is not large enough to get a reliable result.

In Table XII, the blank spaces occur where observational data are not available. The entries marked by # indicate that the relative intensities corresponding to these lines show the wrong sign for self-absorption. That is, the basic interpretation for carrying through these computations leads to inconsistencies. As we see in the Table, # appears primarily for the height, 1500 km, and in the table as a whole, the great majority of the results are consistent. We see that the  $N_2$ -values are scattered at random over  $n$  rather than systematically decreasing towards the lower  $n$  as in Table X. That is, the non-identity of  $N_2$  seems more likely to be caused by the observational error. If we compare the results for two cases of  $T_e = 35,000^\circ$ , i.e., the cases with and without the  $b_n$  factor, we see the differences are very small. This implies that the  $b_n$  term is not appreciable and not large enough to correct the decrease of  $N_2$  in Table X. It is also interesting that values of  $N_2$  in Table XII show consistent decrease with height for each combination of lines. Thus we conclude that variation of  $N_2$  at a given height is not systematic but random, and one may take an arithmetic mean to determine a most probable value of  $N_2$  at each height. In averaging all the values shown in Table XI, we exclude the entries designated by \*, because of the unreasonably large variation of these values from the mean.

The mean values thus computed and the logarithmic height gradient of  $N_2$  are shown in the last two rows of Table XI. It may be interesting to note that the height gradient of  $N_2$  is very insensitive to a change in temperature from one to the other extremes, in spite of a difference of more than a factor of 2 in the absolute value of  $N_2$ . This may be a necessary consequence of the assumption of a constant temperature. We note that in equation (5.2) all the temperature dependent terms  $e^{Xn}$ ,  $b_n$ ,  $\alpha_{2n,0}$  were taken as constant throughout the atmosphere. The  $N_2$  height gradient for  $T_e = 6000^\circ$ , where  $b_n$  is equal to unity and the temperature is constant, is subject to less uncertainties than for the higher

temperature. It should be equal to half of the electron density gradient and also to the true emission height gradient (i.e. the observed emission gradient corrected for self-absorption). The results agree very closely with Wildt's (1947) determination of the emission gradient,  $0.92 \cdot 10^8 \text{ cm}^{-1}$  and are smaller than the value of Cillié and Menzel,  $1.54 \cdot 10^8 \text{ cm}^{-1}$ , which is not corrected for self-absorption. Thomas (1950) and Athay et al. (1954) have argued that the density gradient must be higher than the Wildt emission gradient because of the effect of the  $b_n$ 's, which Wildt ignored. Regardless of this point, however, the present results show practically no difference after including  $b_n$ . Further, the small difference between the last two cases in Table XII indicate a direction of increase opposite to their suggestion. It is also important to note that the present  $N_2$ -gradients are almost constant throughout the different heights, whereas Thomas' results showed a large decrease towards the upper region of the chromosphere. Despite the fact that the values obtained for the highest height,  $h = 3170 \text{ km}$ , in Table XII are most uncertain, because only three computations were averaged, the final results of  $N_2$ -gradient seem consistent with the other heights.

Since the  $N_2$ -gradient seems constant through all heights, we computed the most probable  $N_2$ -gradient by the least square analysis. The following results were obtained:

$$\begin{aligned} \text{For } T_e = 6000^\circ, \quad \beta &= 0.83 \cdot 10^{-8} \text{ cm}^{-1}. \\ \text{For } T_e = 35,000^\circ, \text{ including } b_n, \quad \beta &= 0.82 \cdot 10^{-8} \text{ cm}^{-1}. \quad (5.3) \\ \text{For } T_e = 35,000^\circ, \text{ neglecting } b_n, \quad \beta &= 0.87 \cdot 10^{-8} \text{ cm}^{-1}. \end{aligned}$$

Or, we can write the following expression for  $\log N_2$  as a function of the chromospheric height,  $h$ :

$$\begin{aligned} \text{For } T_e = 6000^\circ, \quad \log N_2 &= 16.17 - 0.358 \times 10^{-8} h \text{ cm}. \quad (5.4) \\ \text{For } T_e = 35,000^\circ \text{ including } b_n, \quad \log N_2 &= 16.58 - 0.362 \times 10^{-8} h \text{ cm}. \quad (5.5) \end{aligned}$$

$$\text{For } T_e = 35,000^\circ \text{ neglecting } b_n, \quad \log N_2 = 16.54 - 0.379 \times 10^{-8} h \text{ cm} \quad (5.6)$$

## §6. Discussion.

In the previous section, we derived expressions for  $N_2$  as a function of height for cases of  $T_e = 6000^\circ$  and  $35,000^\circ$ . The effects of departures from thermodynamic equilibrium were examined by including a  $b_n$  factor in the case of  $T_e = 35,000^\circ$ . The important result is that the density-height gradients,  $\beta$ , are practically the same for both temperatures. The difference between the values of  $N_2$  for the two temperature cases, at each height, is due to the temperature dependence of  $\alpha_{2n,0}$ . That is, since we evaluated the absorption coefficient at the line center using the approximation that the line profiles are determined by Doppler broadenings,

$\alpha_{2n,0}$  varies as  $(T_e)^{-\frac{1}{2}}$ . Hence, it is necessary to know the value of  $T_e$  to determine  $N_2$ . However, we should re-emphasize that the empirically determined quantity is the product  $N_2 \alpha_{2n,0}$ , and that the only assumption concerning temperature necessary for its determination is that  $T_e$  is constant throughout the chromosphere. The absolute value assigned to  $T_e$  does not affect this determination. Except for calculating the values of  $e^{X_n}$  and  $b_n$ , we introduced values of  $T_e = 6000^\circ$  and  $35,000^\circ$  only in the final computation to deduce  $N_2$  from  $N_2 \alpha_{2n,0}$ . If we carried out the analysis ignoring  $e^{X_n}$  and  $b_n$ , then  $\beta$  would necessarily be the same for both cases. The insignificant difference we found for  $\beta$  in two cases, implies that the numerical results are not sensitive to departures from thermodynamic equilibrium. This conclusion is confirmed further by the following calculations.

Ignoring the factors  $b_n$  and  $e^{X_n}$ , we consider the variation with temperature of the constant term in equation (5.4) and (5.5) to be due solely to the variation of  $\alpha_{2n,0}$ . Then we express the constant term as a function of  $T_e$ . Since  $N_2$  varies as  $(T_e)^{\frac{1}{2}}$  for  $\alpha_{2n,0}$  varying as  $(T_e)^{\frac{1}{2}}$ , we can write the following expression from equation (5.4);

$$\log N_2 = 16.13 + \frac{1}{2} \log \left( \frac{T_e}{5040} \right)^{-0.36} \times 10^{-8} \text{ cm} \quad (6.1)$$

From the above equation, we get the value of 16.55 as the constant term for  $T_e = 35,000^\circ$ . This differs from that in equation (5.5) by only 0.03. Thus we may conclude that the factor of  $b_n$  does not appreciably affect the present  $N_2$  results. We may therefore consider that equation (6.1) gives the most probable  $N_2$  distribution, at least for a chromospheric region in which  $T_e$  is lower than  $35,000^\circ$ . It should be noted that the  $N_2$ -height gradient in equation (6.1) is determined empirically without any a priori assumption on the value of  $T_e$  or  $\beta$ . Hence, if the electron temperature at each height is given, we can determine  $N_2$  for the corresponding height directly from equation (6.1).

As was discussed in the above, it appears that the 1932 data show very small departures from thermodynamic equilibrium. This implies that the chromospheric electron temperature was much lower than  $35,000^\circ$ . However, the small value we obtained for  $\beta$ , compared to the emission-height gradient determined by Cillie and Menzel (1935) for the higher order lines, gives some evidence that the effects of  $b_2$  may be present and that the temperature increases with height in the lower chromosphere. In this case, the value of  $\beta$  may vary for different lines. We will return to these points in later sections in the following chapter.

## V. APPLICATION TO THE FLASH SPECTRUM OF 1952 ECLIPSE.

### §1. Introduction.

In the preceding chapter, we have considered several methods for determining the absolute value of the population of hydrogen atoms in the second state,  $N_2$ , from the numerical values of self-absorption in the higher order lines of the Balmer series and have applied these methods to the spectra taken at the 1932 eclipse. We discussed critically the uncertainties appearing in the previous analysis by Thomas and computed the most probable values of  $N_2$  at each height within the accuracy of the observations.

In his earlier work, Thomas (1950a) suggested that the above results may be extended to a determination of the chromospheric temperature distribution as well as an electron density distribution, thereby deducing a model of the chromosphere from flash spectra. The 1952 eclipse program of the High Altitude Observatory under the supervision of Roberts, Evans and Thomas, was primarily to obtain data for this purpose. A highly improved jumping film technique made it possible to obtain the flash spectrum with much greater resolution of chromospheric heights. The photometric measurements and a preliminary discussion of the results has been given by Athay, Billings, Evans, and Roberts (1954). The intensities of the higher Balmer lines and the Balmer continuum were obtained at approximately every 100 km, starting from the height of 500 km above the base of the chromosphere. A method has been developed to determine both the electron temperature and the electron density simultaneously by combining the free-bound emission and the electron scattered photospheric continuum. However, the method itself involves various uncertainties as discussed in the above mentioned paper. In fact, the results show a considerable range of values, depending upon the different assumptions made in the calculation. It is therefore desirable to consider the possibility of analyzing the line intensity data independently, especially since the eclipse program was planned primarily for the line analysis following the basic principles described in the preceding chapter.

The photometric measurements of the 1953 spectra were carried out for 2 points on the arc, and the heights for each point were determined independently from moon profile pictures. It turned out that the heights for the 2 points differed by the same amount that occurred between six consecutive exposures, and, as a result, at many of the heights intensities were measured at both points on the limb. In the following computation we took the mean values of the intensities for these heights in all cases. In section 2, we shall reconsider the method of determining  $b_n$  and  $N_2$  simultaneously and in the later sections the general characteristics of the Balmer decrement will be examined.

### §2. Method of simultaneous determination of $N_2$ and $b_n$ .

In sections 3 and 4 of Chapter IV, we developed a method to determine

$b_n$  and  $N_2$  simultaneously from the numerical amount of self-absorption. It was a method of successive trial and error, based on the least square principle. We found that, using the 1932 data, repeated calculations did not give consistent solutions. As we discussed in detail, it was not certain whether the cause of the failure was due to insufficient accuracy of the observations for this detailed calculation, or if the theory itself was not adequate to explain the general character of the phenomena. The method was first developed from the consideration that from the 1932 data the relative absorption at the lowest height decreased with increasing quantum number. This decrease was in such a direction as would be explained by a monotonic decrease of  $b_n$  with quantum number. We have mentioned that the systematic decrease at the lowest height was concluded from only a part of the data, however, it was found that when all lines were considered the systematic change with quantum number was not so evident. The next possible fault in the theory may lie in the assumed form of the  $b_n$ , because the theoretical form for a kinetic temperature of 35,000° was used. We shall therefore examine the general character of the 1952 data, with regard to these two points before going into the calculations. Since the number of heights involved in the 1952 data was much greater than in 1932, we may draw more affirmative conclusions by statistical methods.

We define the quantity  $R_n$  by:

$$R_n = \log E_{n2}(\text{obs.}) - \log E_{n2}(\text{T.E.}) = \log b_n + \log \{\text{Abs}_n\}, \quad (2.1)$$

and, in Figure III, we plot  $R_n$  at each height against the quantum number  $n$ .  $E_{n2}(\text{obs.})$  denotes the observed intensity of line  $n$  and  $E_{n2}(\text{T.E.})$  the theoretical value computed for thermodynamic equilibrium without self-absorption. Hence  $R_n$  represents the combined effects of  $b_n$  and self-absorption. Since  $E_{n2}(\text{T.E.})$  is a function of  $N_2$ , and  $N_2$  depends on  $T_e$ ,  $N_e$  and  $b_2$ , we cannot determine the absolute value of  $R_n$  without knowing these parameters at each height. However, we are interested only in the relative amount of  $R_n$ , which can be determined as a function of  $n$  at each height. (As long as we assume a spherically symmetric distribution,  $T_e$ ,  $N_e$  and  $b_2$  are constant at the same height, so that we can determine the relative values of  $E_{n2}(\text{T.E.})$  by computing  $n$ -dependent terms only.) The shapes of the curves in Figure III demonstrate the general characteristic of  $b_n$  and  $\{\text{Abs}_n\}$ . If the chromosphere is in thermodynamic equilibrium and self-absorption effects are negligible, the curves should be horizontal straight lines. The effect of self-absorption tends to lower the line below the horizontal, and the departure from thermodynamic equilibrium affects it in the opposite direction. The broken lines were drawn horizontally near the maximum point at each height to indicate the combination of these effects. The solid horizontal lines were drawn through the average value of  $R_n$  at each height. The vertical scale, indicated in the top curves, is the same for all heights.

For lower heights, the curves lie lower at lower quantum numbers, but this effect appears to decrease systematically with height. If we ignore

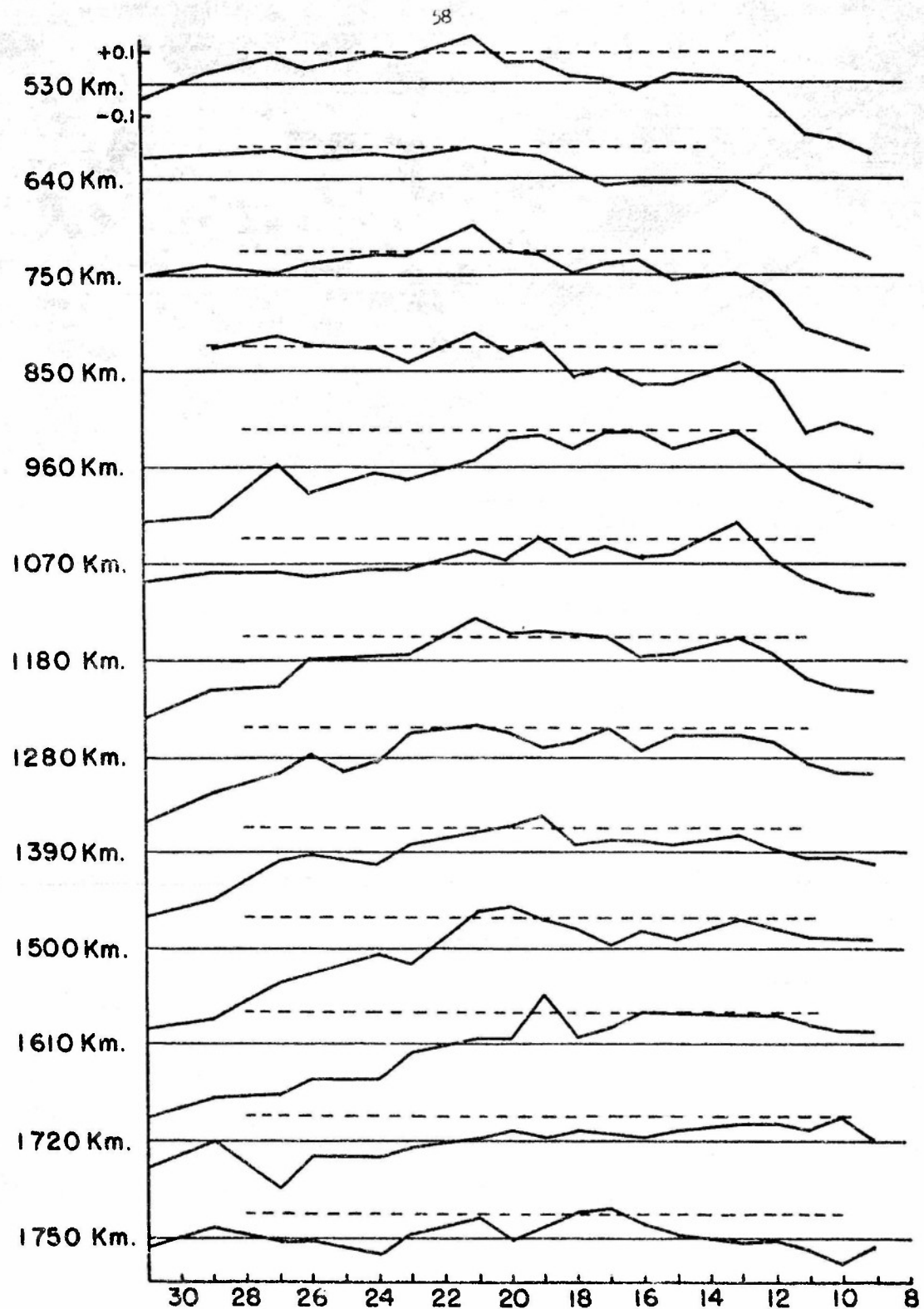


FIGURE IIIa Relative Amount of  $\log b_n \cdot \{\text{Abs.}_n\}$

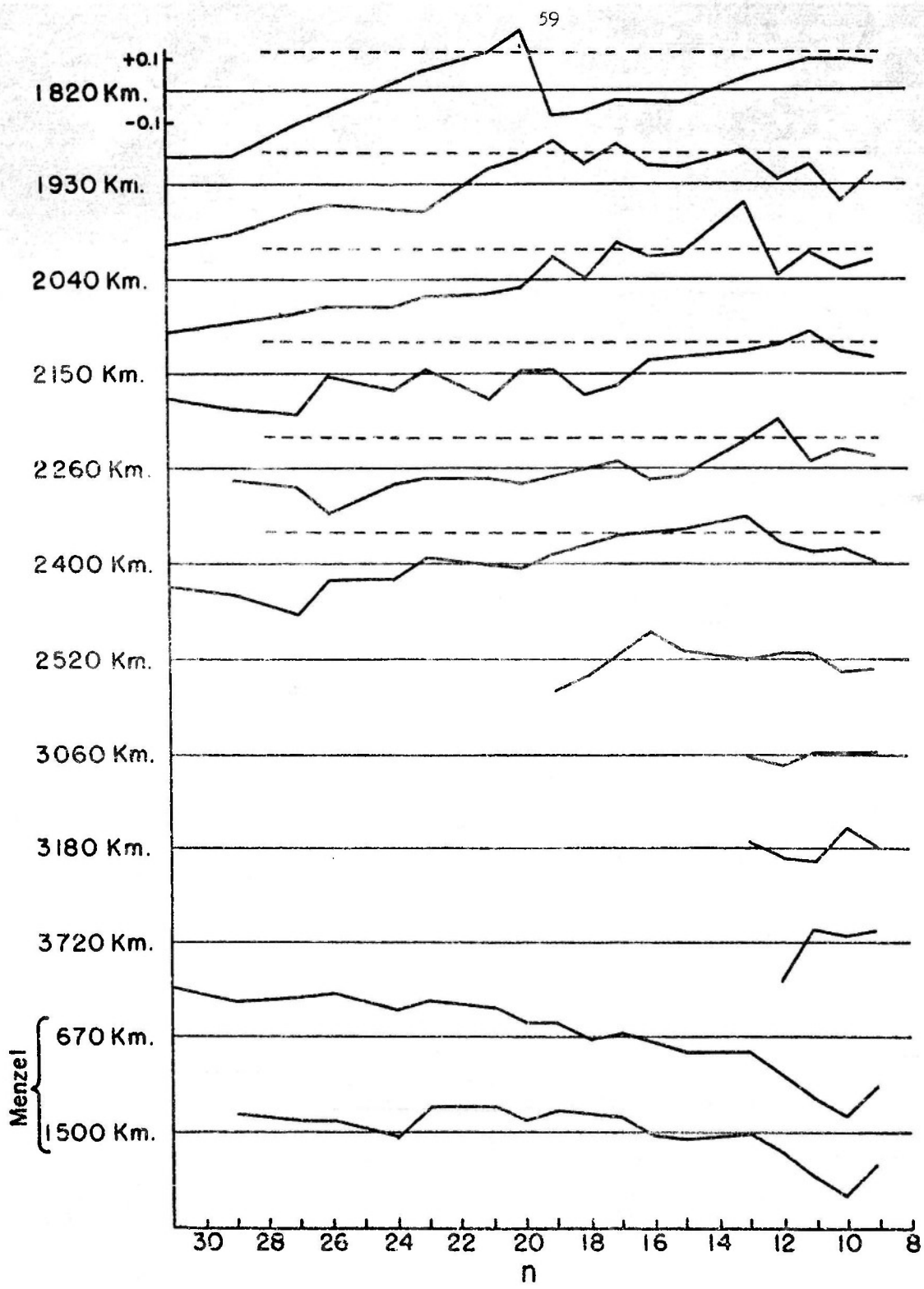


FIGURE III b

$b_n$ , we see that this agrees well with the absorption effect. But for greater heights the effect reverses, i.e.,  $R_n$  decreases for higher lines and the amount of decrease becomes greater for the greater heights. The latter effect may only be explained by a changing  $b_n$ . Since  $b_n$  decreases with  $n$ , we may get a consistent picture for this observed feature, if we assume simply that  $b_n$  increases with height. From the theoretical consideration discussed in Chapter II, this implies that the electron temperature increases upwards in the chromosphere.

The last two curves in Figure III were drawn for the 1932 data for comparison. It is interesting to note that the 1932 data do not show the same tendency for greater heights, an interpretation being that the  $b_n$  effect was smaller in 1932. Thus, our conclusion from the 1932 data discussed in Chapter IV is predicted by this diagram. For the 1952 data, however, in contrast to these 1932 results, we see that the  $b_n$  term should not be excluded if we are to get a consistent picture over the whole region.

Thus we shall repeat the calculations based on the least square principle described in section 3, Chapter IV. In section 3, we used an approximate expression for  $\log b_n$  deduced from the theoretical values computed for  $T_e = 35,000^\circ$ . The equation is hyperbolic in form, with small curvature. Since the continuum data seem to indicate a temperature lower than  $35,000^\circ$ , we assume

$$\log b_n = a + b \cdot n \quad (2.2)$$

for the present case. We also see in Figure III that the above form seems sufficient within the scattering of points plotted. Substituting equation (2.2) into (3.1) of Chapter IV, we have the following formula corresponding to equation (3.5).

$$A + B n + \frac{\partial \{Abs_n\}}{\partial (N_2 \alpha_{2n,0})} \frac{\alpha_{2n,0}}{\alpha_{2,30,0}} \Delta (N_2 \alpha_{30}) = \varphi \quad (2.3)$$

$$\varphi = \log E_{n2} - 3 \log \left( \frac{1}{4} - \frac{1}{n^2} \right) - \log \alpha_{2n} - \log \{Abs_n\}.$$

For convenience of computation, we have written the differentiation by  $(N_2 \alpha_{2n,0})$  instead of  $N_2$ .

The successive computations were repeated until the probable errors of  $\Delta (N_2 \alpha_{30})$  and  $B$  became the same order of magnitude as their solutions. Contrary to the former results, we found that we could determine two decimal places within the observed accuracy at all heights. To illustrate this point both coefficients of the final normal equations from which we obtained the solutions,  $\Delta (N_2 \alpha_{30})$  and  $B$  are shown below. The probable errors are also added.

In the following, the lowest line included in the computation is indicated in the bracket following the height. The first value,  $N_2\alpha_{30}$ , is the initial value of  $N_2\alpha_{2,30,0}$  taken for the computation, and the last  $N_2\alpha_{2,30,0}$  is the final value obtained. For the lowest height,  $h = 530$  km, the last two computations are shown in order to illustrate the convergence of the computation, and for all the other cases we tabulated only the final results. The individual computations were carried out at every other height for the lower region, and for  $h$  higher than 1820 km we found solutions at each height in order to minimize the effects of random errors. The results are as follows:

$$h = 530 \text{ km } (H_{15})$$

$$\begin{aligned} N_2\alpha &= 0.850 & \Delta(N\alpha) &= \frac{0.024}{0.032} = 0.38 \\ N_2\alpha &= 1.15 & \Delta(N\alpha) &= \frac{0.013}{0.301} = 0.04 \pm 0.10 & N_2\alpha_{30} &= 1.19 \\ B &= -\frac{0.299}{14.175} = -0.021 \pm 0.015 \end{aligned}$$

$$h = 750 \text{ km } (H_{13})$$

$$\begin{aligned} N_2\alpha &= 0.826 & \Delta(N\alpha) &= \frac{0.000}{0.024} = 0 \pm 0.470 & N_2\alpha_{30} &= 0.83 \\ B &= -\frac{0.008}{0.427} = 0.024 \pm 0.11 \end{aligned}$$

$$h = 960 \text{ km } (H_{12})$$

$$\begin{aligned} N_2\alpha &= 0.562 & \Delta(N\alpha) &= \frac{0.017}{0.991} = -0.017 \pm 0.042 & N_2\alpha &= 0.54 \\ B &= -\frac{0.479}{16.946} = -0.028 \pm 0.010 \end{aligned}$$

$$h = 1180 \text{ km } (H_{11})$$

$$\begin{aligned} N_2\alpha &= 0.407 & \Delta(N\alpha) &= \frac{0.005}{1.344} = 0.004 \pm 0.046 & N_2\alpha &= 0.41 \\ B &= -\frac{0.341}{14.953} = -0.023 \pm 0.014 \end{aligned}$$

$$h = 1390 \text{ km } (H_{10})$$

$$\begin{aligned} N_2\alpha &= 0.391 & \Delta(N\alpha) &= \frac{0.056}{1.005} = 0.056 \pm 0.035 & N_2\alpha &= 0.45 \\ B &= -\frac{0.300}{10.201} = -0.029 \pm 0.011 \end{aligned}$$

$$h = 1610 \text{ km } (H_9)$$

$$\begin{aligned} N_2\alpha &= 0.245 & \Delta(N\alpha) &= -\frac{0.062}{2.149} = -0.029 \pm 0.023 & N_2\alpha &= 0.22 \\ B &= -\frac{0.291}{12.402} = -0.023 \pm 0.009 \end{aligned}$$

$h = 1820 \text{ km } (H_9)$

$$N_{2\alpha} = 0.196 \quad \Delta(N\alpha) = \frac{0.054}{5.693} = -0.010 \pm 0.040 \quad N_{2\alpha} = 0.19$$

$$B = \frac{-0.639}{5.693} = -0.023 \pm 0.018$$

$h = 1930 \text{ km } (H_9)$

$$N_{2\alpha} = 0.141 \quad \Delta(N\alpha) = \frac{0.263}{12.472} = 0.021 \pm 0.012 \quad N_{2\alpha} = 0.16$$

$$B = \frac{-1.171}{14.150} = -0.027 \pm 0.007$$

$h = 2040 \text{ km } (H_9)$

$$N_{2\alpha} = 0.135 \quad \Delta(N\alpha) = \frac{0.154}{10.001} = -0.015 \pm 0.011 \quad N_{2\alpha} = 0.12$$

$$B = \frac{-0.725}{37.58} = -0.019 \pm 0.006$$

$h = 2150 \text{ km } (H_9)$

$$N_{2\alpha} = 0.080 \quad \Delta(N\alpha) = \frac{0.865}{37.541} = -0.023 \pm 0.007 \quad N_{2\alpha} = 0.057$$

$$B = \frac{-0.984}{37.541} = -0.008 \pm 0.004$$

$h = 2260 \text{ km } (H_9)$

$$N_{2\alpha} = 0.080 \quad \Delta(N\alpha) = \frac{0.77}{31.85} = -0.024 \pm 0.011 \quad N_{2\alpha} = 0.056$$

$$B = \frac{-0.269}{45.275} = -0.006 \pm 0.006$$

$h = 2400 \text{ km } (H_9)$

$$N_{2\alpha} = 0.101 \quad \Delta(N\alpha) = \frac{0.208}{24.019} = -0.009 \pm 0.010 \quad N_{2\alpha} = 0.092$$

$$B = \frac{-0.962}{68.71} = -0.014 \pm 0.006$$

$h = 3060 \text{ km } (H_9)$

$$N_{2\alpha} = 0.047 \quad \Delta(N\alpha) = \frac{0.009}{1.062} = -0.008 \pm 0.012 \quad N_{2\alpha} = 0.039$$

$$B = \frac{0.263}{19.56} = -0.013 \pm 0.007$$

$h = 3180 \text{ km } (H_9)$

$$N_{2\alpha} = 0.041 \quad \Delta(N\alpha) = \frac{-0.035}{1.280} = -0.027 \pm 0.013 \quad N_{2\alpha} = 0.014$$

$$B = \frac{-0.663}{20.570} = -0.032 \pm 0.018$$

Since the observed data, as we have discussed in Chapter IV, give only two decimal places, the last figure in the above results for  $N_2 \alpha_{2,300}$  has not much significance. However, from the probable errors, we may say that at least two figures are reliable. The values of B represent the logarithmic ratios of two successive  $b_n$ 's,  $\log b_n / b_{n+1}$ , and are also reliable to two figures.

The directly determined solution is  $N_2 \alpha_{2,300}$ , instead of  $N_2$  itself. Again we recall that the absorption coefficient introduced here refers to the absorption at the line center so that it is a function of temperature. Since  $\alpha$  varies as  $(T_e)^{-2}$ ,  $N_2$  varies by a factor of 2.6 as  $T_e$  varies from  $5000^\circ$  to  $35,000^\circ$ . The values of  $N_2 \times 10^{-16}$  are shown in Table XIII for various temperatures. If the chromosphere is assumed to be isothermal, then the logarithmic  $N_2$ -gradient,  $\beta$ , is the same for all

Table XIII.

$h \text{ km} \diagup T_e$	$N_2 \times 10^{-16}$			
	5000	10,000	20,000	35,000
530	1.28	1.81	2.56	3.39
750	0.92	1.30	1.84	2.43
960	0.61	0.86	1.22	1.61
1180	0.46	0.65	0.91	1.21
1390	0.50	0.71	1.00	1.32
1610	0.24	0.34	0.48	0.64
1820	0.21	0.30	0.42	0.55
1930	0.19	0.27	0.37	0.49
2040	0.13	0.18	0.26	0.35
2150	0.064	0.090	0.13	0.17
2260	0.060	0.085	0.12	0.16
2400	0.102	0.144	0.20	0.27
3060	0.042	0.059	0.083	0.11
3180	0.015	0.021	0.030	0.040

temperatures. In Figure IV,  $\log N_2$  is plotted against  $h_2$  for  $T_e = 35,000^\circ$ . Four points marked by  $\times$  corresponding to  $h = 1390, 2150, 2260,$

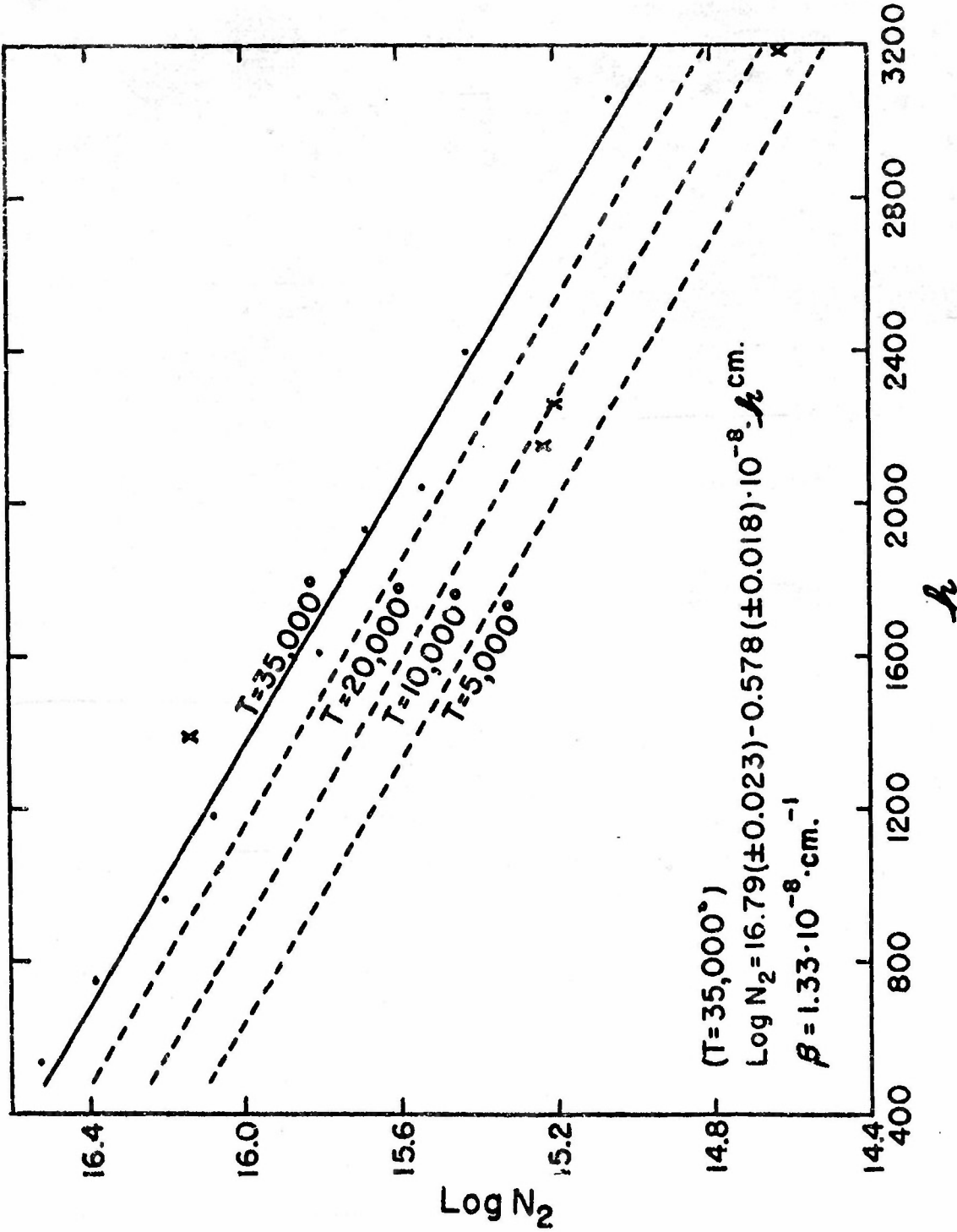


FIGURE IV     $\log N_2$  vs. Height

3180 km, are scattered considerably, but all the rest of the points seem to define a straight line. Hence, we fitted these points to a straight line by the least square method. The point for  $h = 3060$  km is apparently in a good position, but it is 700 km from the next point, and we have to consider the relative error to be greater for the weaker lines. Thus we computed two cases as follows: 1) including every point except four marked by X, and 2) excluding the highest point from 1). We obtained the following formulae:

$$1). \quad \log N_2 = 16.79 (\pm 0.023) - 0.578 (\pm 0.018) \cdot 10^{-8} h \text{cm}. \quad (2.4)$$

$$\beta = 1.33 \cdot 10^{-8} \text{ cm}^{-1}$$

$$2). \quad \log N_2 = 16.81 (\pm 0.025) - 0.597 (\pm 0.021) \cdot 10^{-8} h \text{cm}. \quad (2.5)$$

$$\beta = 1.37 \cdot 10^{-8} \text{ cm}^{-1}$$

The difference between the two cases is not large, and  $\beta$  is considerably higher than the value,  $0.82 \times 10^{-8} \text{ cm}^{-1}$ , previously obtained from 1932 data. (cf. Chapter IV, equation (5.3)). We notice that the emission gradient measured from 1952 data is more than twenty per cent greater than from 1932 data. This implies that either chromospheric or technical conditions for the measurements were considerably different at the two eclipses. If we consider this point together with the various assumptions made in the analysis, the agreement between the two cases is satisfactory. Under the assumption of hydrostatic equilibrium, the observed density gradients for 1952 and 1932 leads to the temperatures of  $25,000^\circ$  and  $40,000^\circ$ , respectively. We will return to this comparison of  $\beta$  in the two eclipses later.

Since the  $N_2$  gradient does not depend on the assumed temperature, we obtain the expressions for  $\log N_2$  for various lower temperatures simply by changing the first term in equation (2.4) or (2.5). In fact, we can write equation (2.4) in either the form

$$\log N_2 = 16.37 (\pm 0.023) + \frac{1}{2} \log \left( \frac{T_e}{5040} \right) - 0.578 (\pm 0.018) \times 10^{-8} h \text{cm} \quad (2.6)$$

or

$$\log N_2 = 14.52 (\pm 0.023) + \frac{1}{2} \log T_e - 0.578 (\pm 0.018) \times 10^{-8} h \text{cm} \quad (2.7)$$

since  $\alpha_{2n,0}$  varies as  $(T_e)^{-\frac{1}{2}}$ . Three broken lines in Figure IV represent  $\log N_2$  given for  $T_e = 20,000^\circ$ ,  $10,000^\circ$ , and  $5000^\circ$ . If we know the temperature at some height and the chromospheric temperature gradient is not large, we can determine the  $N_2$  value at each height from equation (2.6). Later in section 5, we will calculate the value of  $N_2$  at every 500 km in the lower region of the chromosphere, using the temperature distribution obtained from the continuum.

The above argument is especially important when we recall that our final aim is to find the  $T_e$  and  $N_e$  distributions by successive approximations.

If the temperature gradient is small, the form of equation (2.6) will not change significantly in higher order approximations, and we can use it to calculate  $N_2$  immediately. Of course, in a rigorous sense, the empirical value of  $\beta$  may be altered from one model to the next, because the self-absorption will change as  $N_2$  is changed. However, the amount of correction may be negligibly small in the higher regions where  $N_2$  values are small. Thus, the actual amount of work in successive calculations can be considerably reduced.

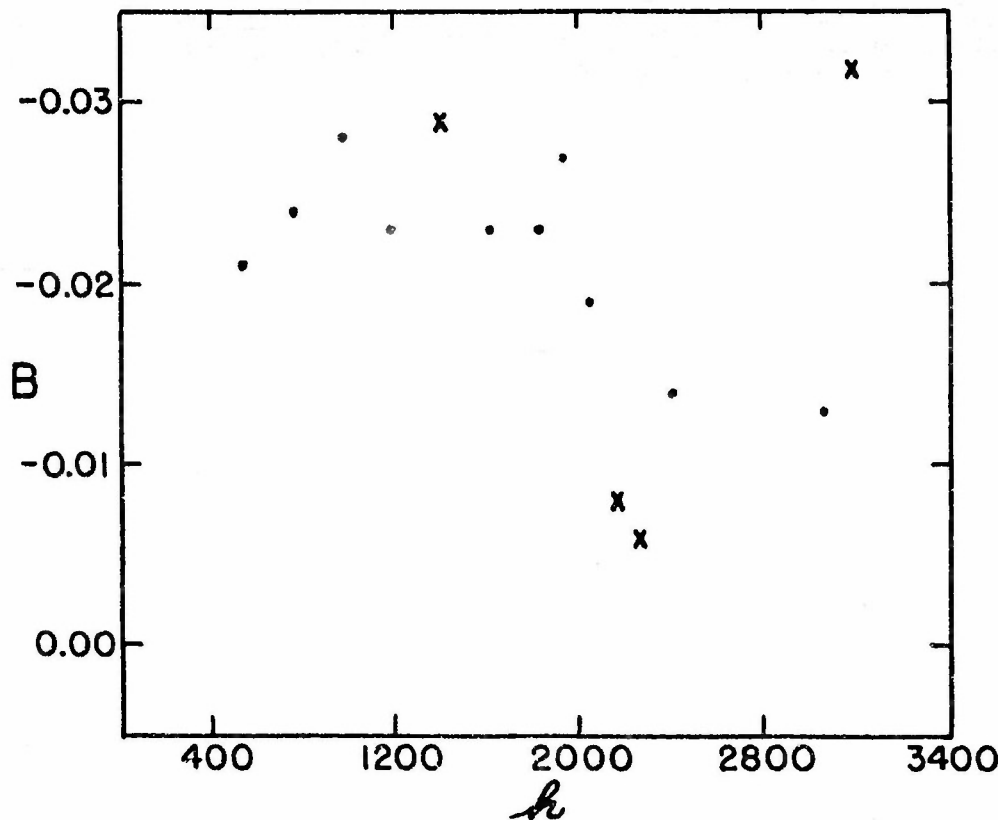


FIGURE V B vs. Height

Now, returning to the results summarized in pages 61 and 62, we plot the coefficient  $B$  against height in Figure V. The points are widely scattered and it seems difficult to presume a correlation with height. However, if we again exclude the four points corresponding to those marked by X in Figure VI, we see that for the region lower than  $h = 2000$  km, the values of  $B$  are almost constant. Therefore, we take an arithmetic mean of these values and write:

$$\log b_n - \log b_n + k = 0.024 k \quad (2.8)$$

for the region lower than  $h = 2000$ , and

$$\log b_n - \log b_n + k = 0.022 k \quad (2.9)$$

for the whole region.

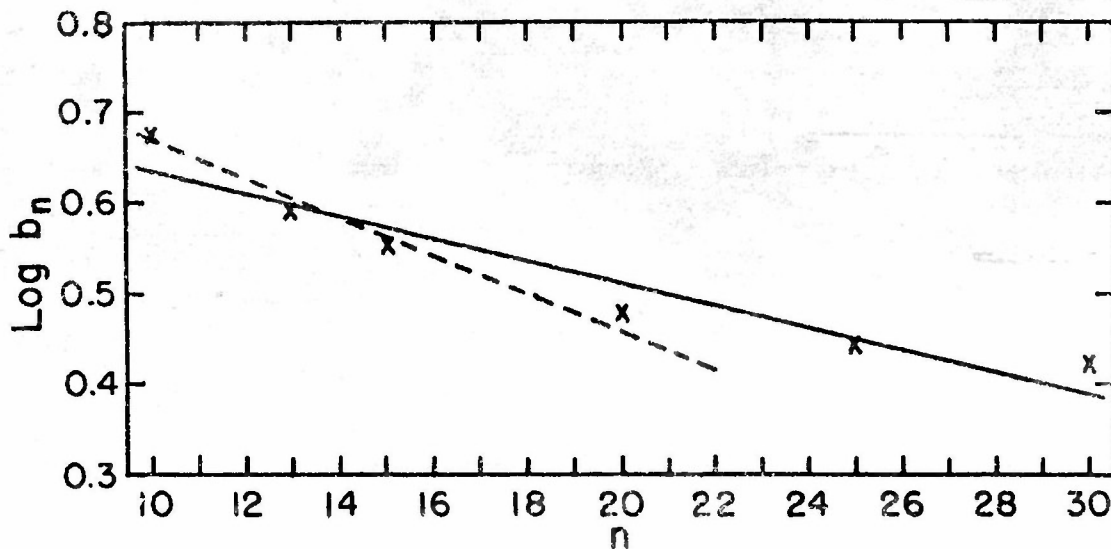


FIGURE VI Theoretical Value of Log  $b_n$  vs.  $n$

As we have discussed in the previous chapter, the only theoretical values of  $b_n$  available for  $n$  higher than 10 are those that Thomas calculated approximately for  $T_e = 35,000^\circ$ . These are plotted in Figure VI. The solid line represents a best fit to these theoretical values. The broken line was drawn from equation (2.9) with the constant adjusted so as to fit the first four points. The gradient of the solid line is 0.012.

### §3. Observed amount of $b_n e^{x_n \{Abs_n\}}$ .

In Figure III of the previous section we plotted the relative effects of departure from thermodynamic equilibrium and self-absorption for each height and observed that the diagrams indicated a systematic change of these relative effects with height. However, the quantity thus plotted is relative and the consistency of the results is examined only qualitatively. In section 3 a method was discussed for determining both the self-absorption and the departure from the equilibrium simultaneously under some simplified assumptions. We now wish to determine the absolute scale of Figure III, so that we can proceed to calculate more rigorously.

$b_n$  must approach unity as  $n$  goes to infinity, since the free electrons can be assumed to obey the Maxwellian distribution at a unique kinetic temperature. Hence, either the continuum (free-bound emission) intensity or the emissions in the lines near the series limit may be regarded as free from the  $b_n$ -effect. At the same time, self-absorption should be negligibly small in these regions. Therefore, using the continuum or the high-order line intensities, we may calculate the absolute amount of  $b_n$  and the self-absorption observationally so that we can fix the zero point of Figure III.

The free-bound emission in the Balmer continuum in a frequency range  $d\nu$  integrated along the line of sight and above the moon's limb may be written as:

$$E_{\nu_2} d\nu = 2.63 \cdot 10^{-33} \frac{1}{\beta} \frac{N_i N_e}{T_e^{3/2}} e^{(X_2 - h\nu)/kT_e} d\nu \quad (3.1)$$

where

$$2.63 \cdot 10^{-33} = \frac{2^9 \pi^5 \epsilon^{10} (Z+1)^4}{(6\pi)^{3/2} m^3 h^2 c^3 2^3 K^{3/2}}$$

and where  $N_i$  and  $N_e$  refer to the integrated quantities of  $n_i$  and  $n_e$  along line-of-sight, as was stated on page 25. A factor  $\beta$  enters through the integration over  $X$ . The integration is carried under the same conditions and assumptions we made in Chapter III.

The total Balmer line intensity is given by equation (2.1) of Chapter III. We replace  $N_n$  in this equation by the Boltzmann-Saha formula to make the terms  $N_i$ ,  $N_e$  and  $T_e$  explicit. Then we have the following expression:

$$E_{n_2} = \text{Const.} \left( \frac{1}{4} - \frac{1}{n^2} \right) \cdot A_{n_2} \cdot \frac{n^2}{\beta} \cdot \frac{N_i N_e}{T_e^{3/2}} \cdot e^{\frac{X_n}{kT_e}} \cdot b_n \cdot \{ \text{Abs}_n \} \quad (3.2)$$

where

$$\text{Const.} = \frac{hR}{4\pi} \left( \frac{h^2}{2\pi mk} \right)^{3/2} = 7.2 \cdot 10^{-28}$$

Taking the logarithmic ratio of (3.2) to (3.1), we write

$$\log E_{n_2} - \log E_{\infty 2} = 5.437 + \log n^2 \left( \frac{1}{4} - \frac{1}{n^2} \right) \\ + \log A_{n_2} + \log e^{\frac{X_n}{kT_e}} \cdot b_n \cdot \{ \text{Abs}_n \} \quad (3.3)$$

where  $E_{\infty 2}$  is the intensity at the series limit. Hence, from equation (3.3), we can obtain the observed amount of  $\exp(X_n) b_n \cdot \{ \text{Abs}_n \}$ . Since the continuum measurements were considerably more scattered than those of the lines, we used the values smoothed by least-square fitting for  $E_{\infty 2}$  and the raw values for lines, although the results were not seriously different.

Figure VII shows  $\log e^{X_n} b_n \cdot \{ \text{Abs}_n \}$  at about every 500 kilometers, plotted against the quantum number. The shape of the line at each height is essentially the same as the corresponding one in Figure III. While, in Figure VII, the value  $\log e^{X_n} b_n \cdot \{ \text{Abs}_n \}$  is plotted for every line, it should be noted that the lines, H<sub>14</sub>, H<sub>22</sub>, H<sub>25</sub>, H<sub>28</sub> and H<sub>30</sub> have been found

to be blended with other lines, as is discussed in Chapter IV. Hence, these lines should be excluded in considering the general characteristics of the diagram that are discussed below.

The essential facts of physical significance in Figure VII are systematic changes of  $\log e^{x_n} b_n \{Abs_n\}$  with chromospheric height as well as with line number. The quantity,  $\log e^{x_n} b_n \{Abs_n\}$ , hereafter denoted by  $R_n$ , increases upwards by a greater amount for the lower members of the series than for the higher members. Towards the series limit it approaches a constant value monotonically, and for  $n$  greater than 26, becomes slightly greater than zero (except for the height, 2400 km). This verifies observationally that both departure from thermodynamic equilibrium and self-absorption are negligible for these higher members. If we draw a horizontal line at the apparent asymptote, we see that  $R_n$  for  $h$  lower than 1000 km comes below this line, and at higher regions it comes above it. Since  $\log \{Abs_n\}$  is a negative quantity, decreasing with height, and  $\log b_n$  is positive, we may say that the self-absorption exceeds  $b_n$  in the lower region, and the latter becomes predominant in the higher chromosphere. We may not, however, conclude immediately that the  $b_n$  increase outwards in the chromosphere until we attempt by estimation to separate  $b_n$  and  $\{Abs_n\}$  independently, as will be done in the following section.

Before proceeding to the  $b_n$  determination, it will be interesting to calculate the  $R_n$ -height relation using the intensity of higher order lines instead of the continuum. As we have discussed, the continuum measurements are considerably scattered and we have used the smoothed values for the present analysis. We have shown that  $b_n$  and  $\{Abs_n\}$  terms become negligible for the highest lines of the series both theoretically and observationally. Hence we can simply calculate the difference between the line intensity of a given line and one of the highest order lines in order to determine  $R_n$ . From equation (3.3), we may write immediately

$$\log e^{x_n} b_n \{Abs_n\} = \log E_{n'2} - \log E_{n'2} - \log \frac{(n^2 - 4)}{(n'^2 - 4)} \frac{A_{n'2}}{A_{n'2}} \quad (3.4)$$

in which  $n'$  refers to the line whose self-absorption and departure from thermodynamic equilibrium are assumed to be negligible. We take the mean value of the intensity of  $H_{31}$ ,  $H_{29}$ , and  $H_{27}$  ( $H_{30}$ ,  $H_{28}$  are blended) as  $E_{n'2}$  and set  $n' = 29$ . Figure VIII shows the result thus obtained for heights corresponding to those taken in Figure VII. The increase of  $R_n$  with the chromospheric height is not as great as when we used the continuum, but the systematic change with height remains.

We have computed  $R_n$  for all heights and obtained a gradual increase with height. For each individual  $n$ , variation of the line intensity by a fraction of the observational error would shift  $R_n$  either positively or negatively. In the latter case where we used high order lines for a reference, most anomalies in  $R_n$  appear for heights higher than 1930 km.  $R_n$  at these higher regions is smaller than for the next lower height,

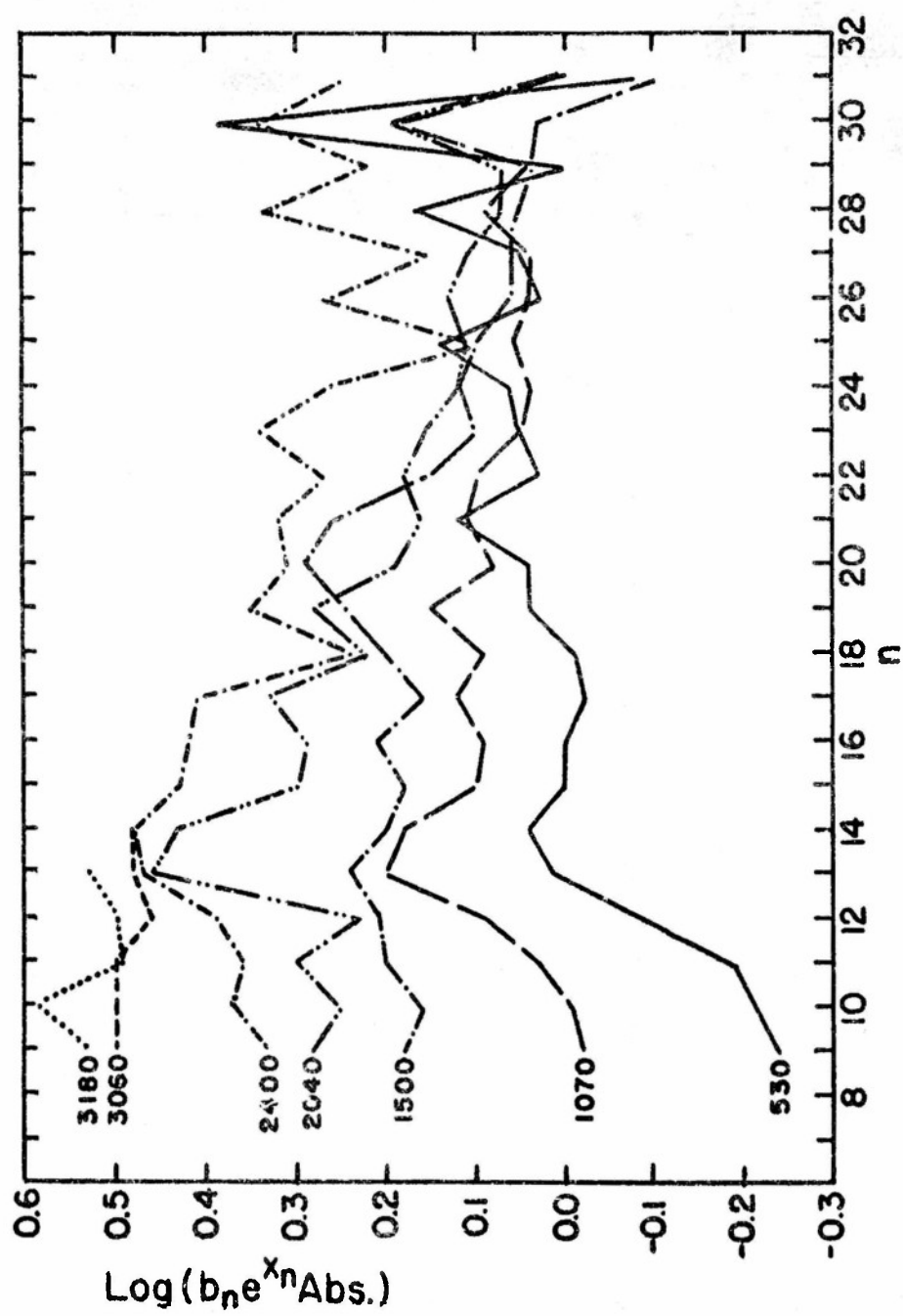
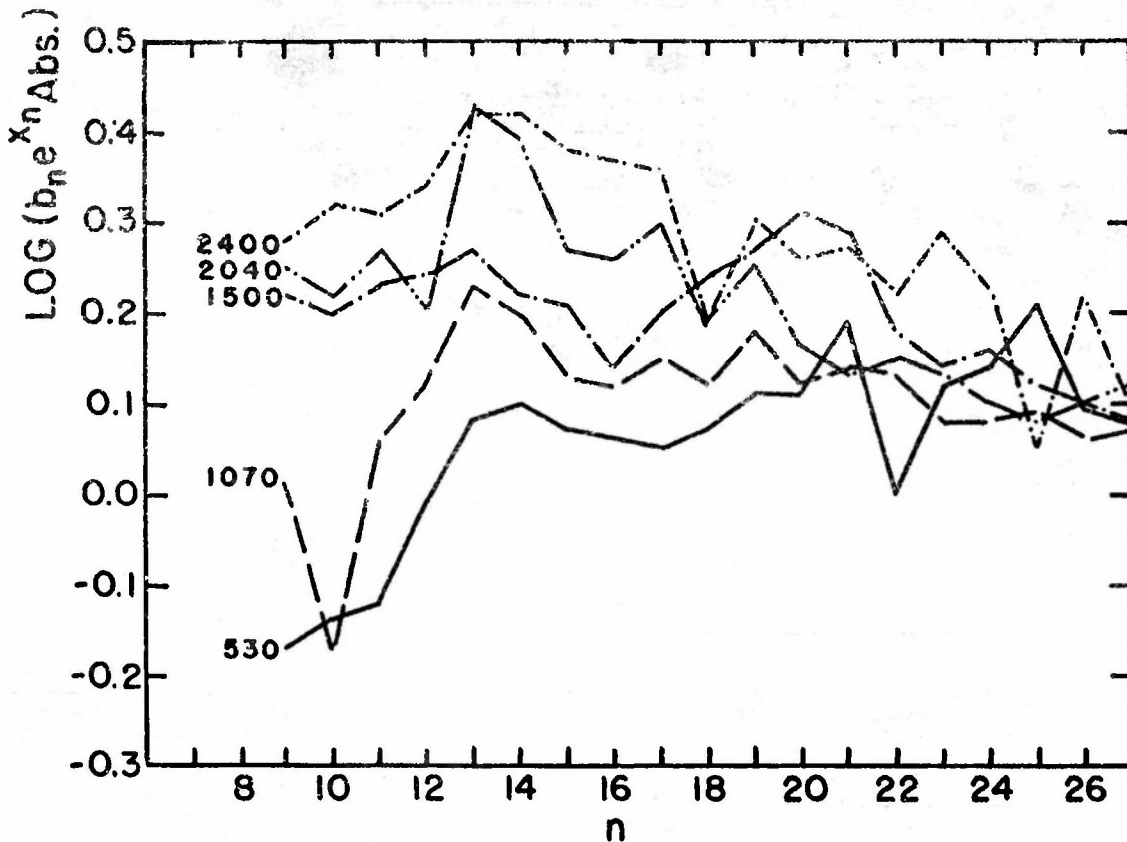


FIGURE VII     $\text{Log}(b_n \cdot e^{x_n} \cdot \text{Abs.})$  vs.  $n$     (a)



**FIGURE VIII      Log ( $b_n \cdot e^{X_n} \cdot \text{Abs.}$ ) vs.  $n$  (b)**

which was not shown in the results when we used the continuum as a reference point. We may interpret this discrepancy as due primarily to the inaccuracy of the measurements of  $E_{W_1}$  values for greater heights, where these lines are very much weakened. Since the smoothed values of the continuum are used in the former case, such discrepancies were corrected.

Except at the greatest heights, the only anomalies in  $R_n$  appear at  $h = 960$  km. Here  $R_n$  seems abnormally high, and the  $R_n$ -curve has a rather peculiar shape. In order to minimize such effects we constructed  $R_n$  diagrams by taking mean values of  $R_n$  at several succeeding heights, except for 960 km and heights higher than 1930 km, in the following way. We took the mean of the  $R_n$  at 530, 640, 750, and 850 km and plotted the value for the mean height,  $h = 685$  km. Similarly, we chose combinations of 1070, 1180, 1280, 1390 km and 1500, 1600, 1820 km to determine the mean values for  $h = 1230$  and 1640 km, respectively. Thus we obtained an  $R_n$  curve for three heights shown in Figure IX. The deviations of points for individual heights are smoothed by this averaging procedure, and all the points lie well within a clearly defined  $R_n$  curve. Further, the height at which the slope of the  $R_n$  curve changes sign for a given  $n$ , more clearly indicated

by Figure IX. The general characteristics of the effects of  $b_n$  and self-absorption, concluded from the systematic change of the  $R_n$  curves in Figure VII, may be explained more conclusively in Figure IX.

In the preceding discussions about  $R_n = \log e^{X_n} \cdot b_n \{ \text{Abs}_n \}$ , we implicitly ignored the term  $e^{X_n}$ , which depends on the temperature. If the chromosphere is assumed to be isothermal, the qualitative interpretations should not be altered at all. On the other hand, if there is a temperature gradient the  $e^{X_n}$  term may affect slightly the shape of the  $R_n$  curves. However,  $e^{X_n}$  has a very small value, even for low temperatures, and decrease exponentially with temperature. We shall come back to this question again in the next section, but in Table XIV, we show the values  $\log e^{X_n}$  computed for various  $T_e$  to compare the order of magnitude with  $R_n$  in Figures VII, VIII, and IX.

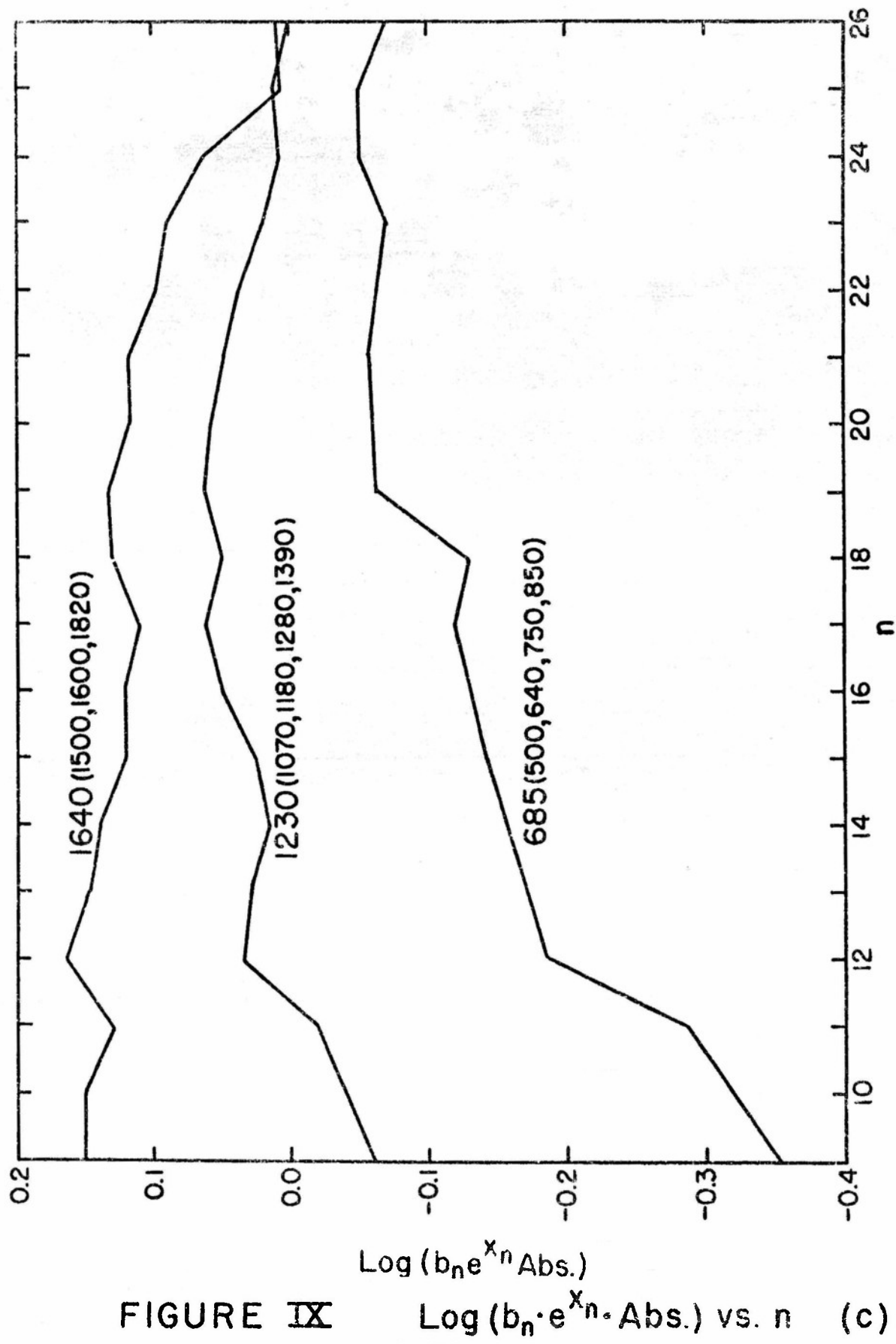
Table XIV.

$T_e$	n	$\log e^{X_n}$								
		10	11	12	13	15	17	20	25	30
5,000	0.14	0.11	0.09	0.08	0.06	0.05	0.03	0.02	0.02	0.02
10,000	.07	.06	.05	.04	.03	.02	.02	.01	.01	.01
20,000	.03	.03	.02	.02	.02	.01	.01	.01	.01	.01
30,000	0.02	.02	.02	.01	.01	.01	.01	.00	.00	.00

We see in the above table  $e^{X_n}$  is negligible for  $T_e$  higher than 20,000° and is appreciable only for lower order Balmer lines at lower temperatures. In the next section we will include this factor for an appropriate temperature to determine the observed value of  $b_n$ .

#### §4. Determination of the observed $b_n$ .

In the previous section we calculated the observed values of  $R_n$  that are shown in Figures VII, VIII, and IX. To eliminate  $e^{X_n}$  from  $R_n$ , we must know the temperature distribution in the chromosphere. But, the contribution of this term is very small and we can treat it as a secondary correction. If we once obtain  $b_n$  or  $\{ \text{Abs}_n \}$ , we may estimate the temperature distribution, after which we can eliminate  $e^{X_n}$  and repeat the process successively. A larger contribution to  $R_n$  comes from  $b_n \{ \text{Abs}_n \}$ . Either  $b_n$  or  $\{ \text{Abs}_n \}$  can be determined if we know the other. If we have a knowledge of the chromospheric temperature and electron density (the latter is much less sensitive to  $b_n$  than the former), we can calculate  $b_n$  theoretically, then determine  $\{ \text{Abs}_n \}$ ; or we can obtain  $N_2$  from  $b_2$ ,  $T_e$  and  $N_e$ , then compute the theoretical value of  $\{ \text{Abs}_n \}$  to compare with the observed  $\{ \text{Abs}_n \}$ . At present we have only a value for  $T_e$  derived from the



continuum. We wish, however, to get a model from the line intensity independent of the continuum. In section 2 we developed a method to get  $N_{2\zeta}$  observationally at each height. To derive  $N_2$  from this result, we have to know the temperature at each height, since  $\zeta$  in this case is a function of  $T_e$ . However,  $N_{2\zeta}$  was obtained by a purely empirical method and  $\{\text{Abs}_n\}$  is a function of  $N_{2\zeta}$ , so we can calculate  $\{\text{Abs}_n\}$  without assuming the temperature. Then we can obtain the observed values of  $b_n$ , choosing the parameter  $e^{X_n}$  to give a best fit with the theoretical  $b_n$  computed for various temperatures. Thus, we can determine the temperature empirically and repeat the procedure to reach a final consistent model of the chromosphere.

The values of  $N_{2\zeta n,0}$  tabulated in page 61 to page 62, were used to estimate  $\{\text{Abs}_n\}$  at each height. Then, by subtracting this from  $R_n$ , obtained from the line and continuum intensities, (cf. Figure VII), we obtained the values of  $\log e^{X_n} b_n$ , that are plotted against  $n$  in Figure X. The values corresponding to the blended lines,  $b_{14}$ ,  $b_{28}$ , and  $b_{30}$  were omitted. The different lines used to distinguish each height are the same as we used in Figure VII. For each height, we have included in our calculations only the lines for which  $\log N_{2\zeta n,0}$  was less than 1. (For example, for the lowest height,  $n < 15$  was not included). To estimate  $\log b_n$ , we subtracted  $\log e^{X_n}$  computed for the appropriate temperature. Since  $e^{X_n}$  is negligibly small for  $T_e > 20,000^\circ$  and  $n < 10$ , this diagram itself gives  $\log b_n$  directly if the chromospheric temperature is higher than  $20,000^\circ$ . At first glance, we see that  $b_n$  is practically the same for all heights except the highest. This implies that the chromosphere is isothermal at least in the region lower than 2000 km. We will discuss this point later.

If we assume that the chromospheric temperature is as low as  $5000^\circ$ , we must subtract  $\log e^{X_n}$  computed in Table XIV to estimate the observed  $\log b_n$  corresponding to  $5000^\circ$ . We see from Table XIV that the  $\log b_n$  lines will be lowered by a maximum amount of 0.14, at  $n = 10$ . If, however,  $T_e = 5000^\circ$ ,  $\log b_n$  should be equal to zero, since the radiation temperature of the chromosphere is nearly  $5000^\circ$ , giving a Boltzmann distribution, with  $b_n = 1$ . Thus we estimate the real temperature to be somewhat higher than the photospheric radiation temperature.

The apparent shapes of the  $\log b_n$  versus  $n$  curves seem to be nearly straight, with perhaps a slight rise towards the lower order  $n$ . Therefore, we take a mean of  $\log b_n$  obtained for four different heights, 530, 1070, 1500, and 2040 km to determine the value of  $\log b_n$  at each  $n$ . Then, an analytical expression of  $\log b_n$  as a function of  $n$  may be obtained by fitting these mean values with either of the following two forms:

$$\log b_n = -0.13 (\pm 0.022) + 6.7 (\pm 0.28) \cdot \frac{1}{n} \quad (4.1)$$

or

$$\log b_n = 0.73 (\pm 0.049) - 0.024 (\pm 0.0011) \cdot n. \quad (4.2)$$

The form (4.1) was used for fitting the theoretical computations for  $T_e = 35,000^\circ$  given in Chapter IV, and the linear form (4.2) was used for the

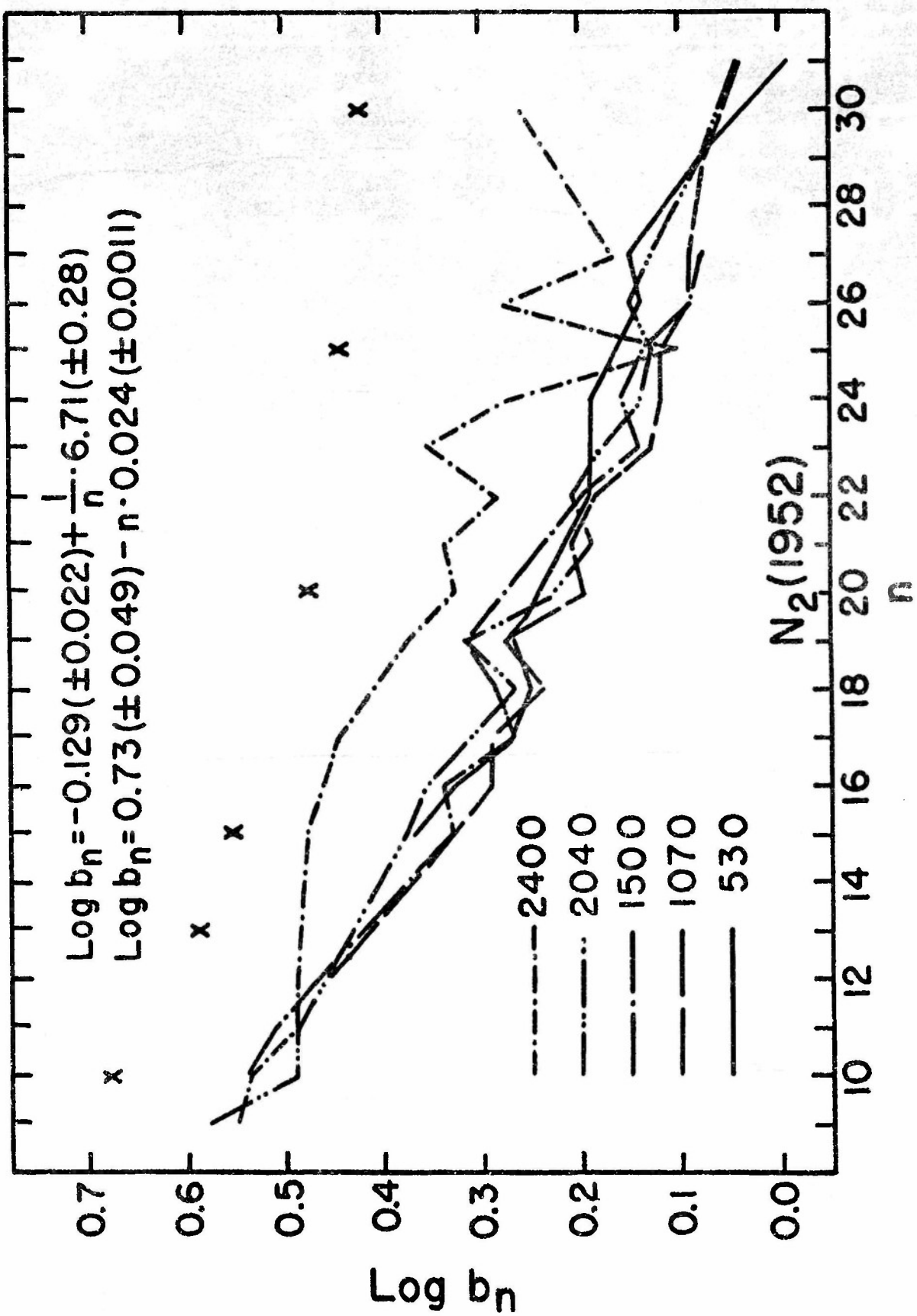


FIGURE X Log b<sub>n</sub> vs. n (a)

determination of  $N_{1\alpha}$  in section 2. From the probable errors shown, we see that  $\log b_n$  is well represented by (4.2). In section 2, we obtained a value of  $B$ , corresponding to the coefficient of  $n$  in (4.2), of 0.024 or 0.022. This remarkably good agreement may be regarded as a check on the consistency of both computations.

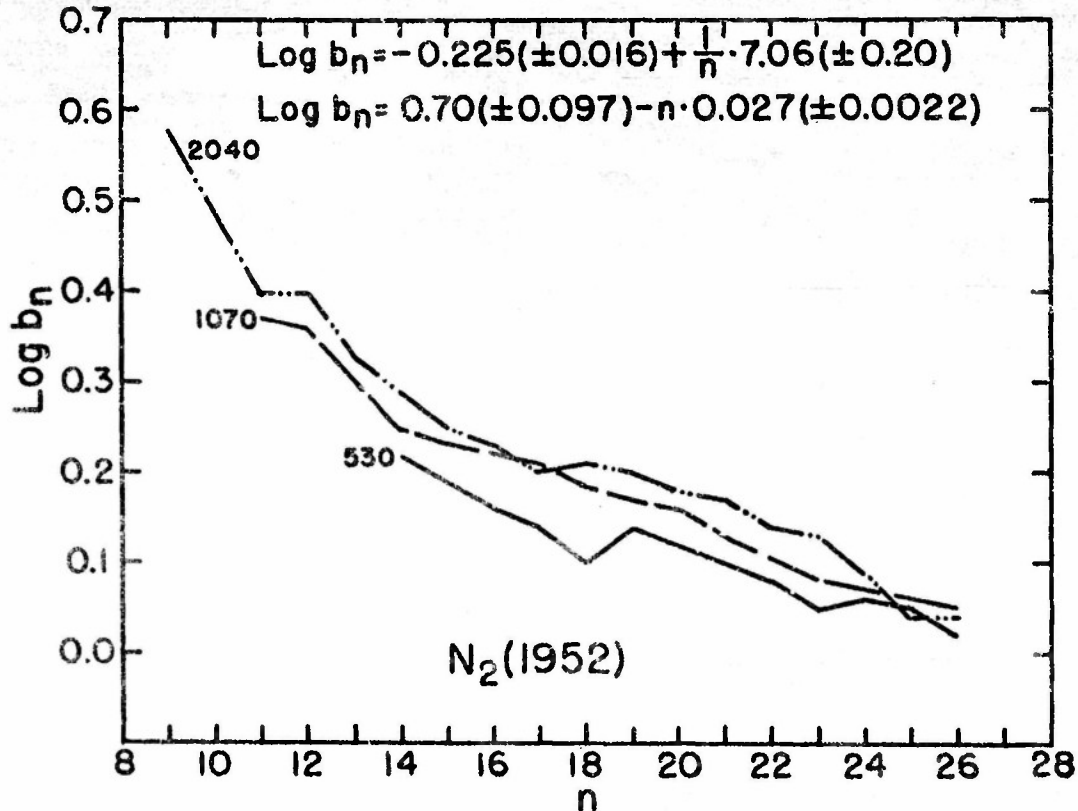


FIGURE XI Log  $b_n$  vs.  $n$  (b)

The approximate theoretical values of  $\log b_n$  for  $T_e = 35,000^\circ$  are indicated by  $\times$  in Figure X. This shows that the observed  $b_n$  indicate a chromospheric electron temperature somewhat lower than  $35,000^\circ$ . To get further information about the exact value of the temperature, we have to compute  $b_n$  for several ranges of  $T_e$  lower than  $35,000^\circ$ .

Figure XI is a similar diagram of  $\log b_n$  derived from Figure IX.  $R_n$  in this case was obtained by taking the intensity of Balmer lines relative to the higher lines instead of to the continuum. It was then averaged for four successive heights in the same way that we averaged the corresponding results for the continuum comparison. If our assumption of negligible  $\{\Delta s_n\}$  and  $b_n$  for the lines higher than  $n = 27$  as well as the continuum is true, then both Figure X and XI should be identical except for a slight difference of height represented on the diagrams. We obtained the following algebraic expressions for  $\log b_n$  in Figure XI:

$$\log b_n = -0.22 (\pm 0.016) + 7.1 (\pm 0.20) \cdot \frac{1}{n} \quad (4.3)$$

$$\log b_n = 0.70 (\pm 0.097) - 0.027 (\pm 0.0022) \cdot n. \quad (4.4)$$

The values represented by the above formulae are slightly smaller than those in (4.1) and (4.2).

Finally, we shall consider the following computations as a rough estimation of the contribution of self-absorption to the  $R_n$  curves. In Chapter IV, we obtained  $N_2$  from 1932 eclipse data from a different method. As we have discussed previously, various observed results indicate that the chromosphere in 1952 was in a considerably different condition. Therefore one may not, in a rigorous sense, apply the results of 1932 to 1952. However, it may be interesting to estimate  $\log b_n$  using  $N_2$  obtained from 1932, and compare the results to those discussed above. Figure XII shows the diagram corresponding to Figure X, thus obtained. The mean  $\log b_n$  curve in Figure XII approximately coincides with the mean curve in Figure X. This is a rather unexpected result if we take into account the considerable difference in  $N_2$  values between the two eclipses, as discussed in section 2. It may be partly due to the small contribution of self-absorption to  $R_n$  for higher order lines.

### §5. Comparison to the model obtained from the Balmer continuum, and the determination of $b_2$ .

In the preceding sections, it was pointed out that we can determine the values of  $T_e$  and  $n_e$  independently from the emission in the continuum. The analysis of the continuum data from the 1952 eclipse was carried out by Athay, Pecker, and Thomas (1954). From the intensity of the Balmer free-bound emission relative to the photospheric scattered light and emission from the negative hydrogen ion, at the Balmer series limit, they determined the values of  $T_e$  and  $n_e$  at each height. Table XV shows their results for the region lower than  $h = 3000$  km.

Table XV

Model of chromosphere obtained from the Balmer continuum\*

Height (km)	500	1000	1500	2000	2500	3000
$T_e$	5,500	6,000	6,500	7,100	7,800	8,600
$\log n_e$	11.65	11.44	11.21	11.02	10.82	10.61

\*From Table VI in the forthcoming paper by Athay, Pecker, and Thomas.

We see in the above table that the electron temperature is slightly higher than the photospheric radiation temperature and increases slowly upward. According to the method discussed in section 2, we can calculate from equation (2.6) the values of  $N_2(h)$  at each height corresponding to the

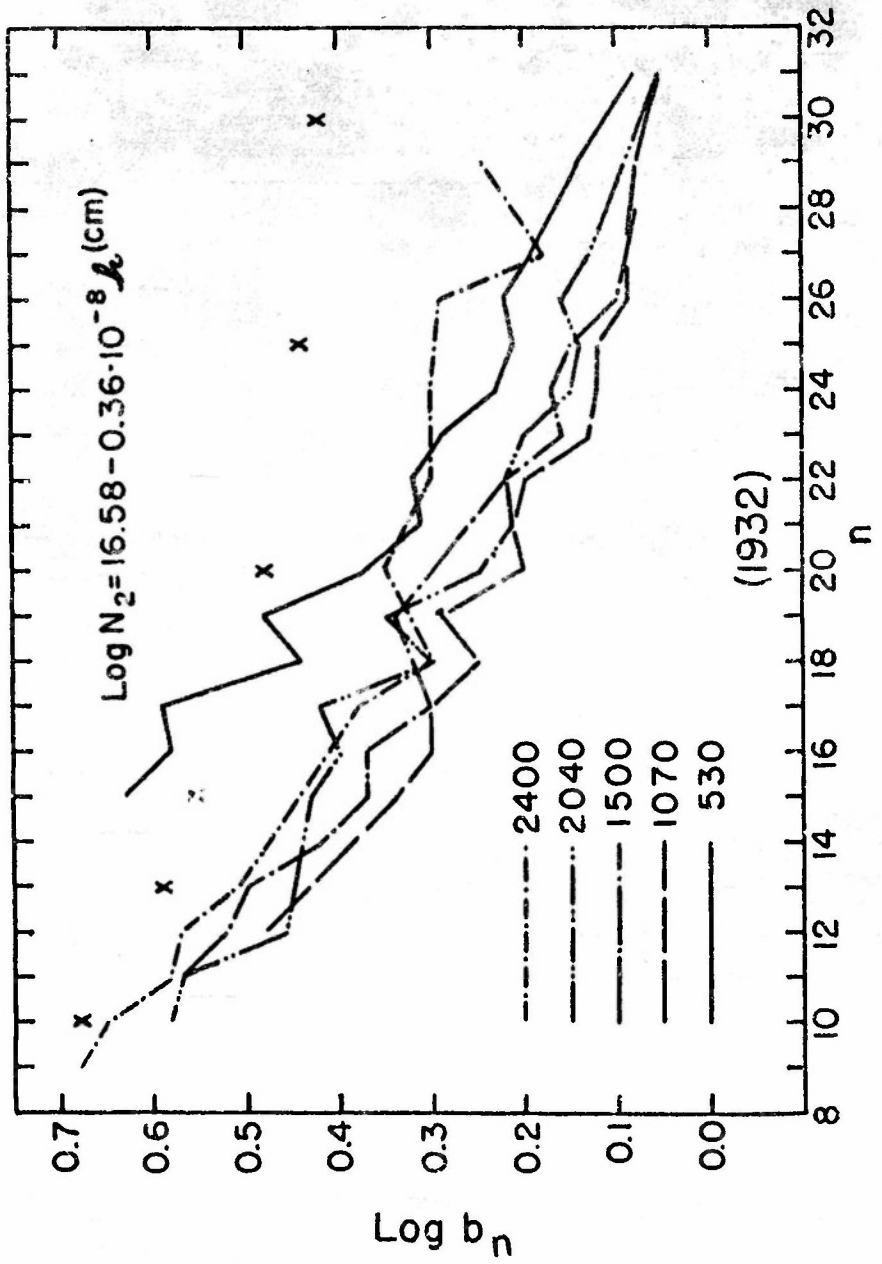


FIGURE XIII Log  $b_n$  vs.  $n$  (c)

temperature given in Table XV. The values of  $N_2(h)$  thus obtained are shown in Table XVI in comparison with the values corresponding to  $T_e = 6,500^\circ$ .

Table XVI

Values of  $N_2(h)$ 

Height (km)	500	1000	1500	2000	2500	3000
log $N_2(h)$ for $T_e$ in Table XV	16.10	15.84	15.56	15.29	15.02	14.75
log $N_2(h)$ for $T_e = 6,500^\circ$	16.14	15.86	15.56	15.27	14.98	14.69

The differences between  $N_2(h)$  for the two cases are very small. Hence the assumption of constant temperature does not necessarily lead to an appreciable error, at least for the determination of  $N_2(h)$ .

In the previous section, we calculated the observational values of  $b_n$ . These values lead to one determination of electron temperature and electron density. If we have the theoretical value of  $b_n$  for small intervals of  $T_e$  and  $N_e$ , we can obtain  $T_e$  and  $N_e$  from these results and compare with those in Table XV. At the present, we have concluded only that  $T_e$  estimated from the line intensity is lower than  $35,000^\circ$  and may be constant throughout the lower region of the chromosphere. The values of  $T_e$  in Table XV seem to agree with this conclusion.

We now proceed to calculate values of  $b_2$  from the  $T_e$ ,  $n_e$ , and  $N_2$  values in Tables XV and XVI. From equation (2.8) in Chapter III, the number of hydrogen atoms per cubic centimeter that are in the second level at chromospheric height  $h$  may be written

$$n_2(\tau) = \left( \frac{\pi^2}{2\pi mk} \right)^{3/2} \frac{\omega_2}{2} n_i(\tau) n_e(\tau) b_2(\tau) e^{X_2 T_e(\tau)} \quad (5.1)$$

In the present case, we may transform from  $n_2(h)$  to  $N_2(h)$ , the total number of hydrogen atoms in the second level within a column of unit cross-section along the line of sight by the following formula:

$$N_2(\tau) = \sqrt{\frac{2\pi r}{\beta_2}} n_2(\tau) = 5.73 \cdot 10^9 n_2(\tau) \quad (5.2)$$

in which we set  $\beta_2 = 1.33 \cdot 10^{-8} \text{ cm}^{-1}$  according to the result obtained in equation (2.4).

Hence, after substituting numerical values, we have from equations (5.1) and (5.2)

$$N_2(\tau) = 9.46 \cdot 10^6 \cdot n_e^2(\tau) \cdot b_2(\tau) e^{\frac{x_2}{kT_e} - \frac{3}{2}} \quad (5.3)$$

where we introduced the usual approximately,  $n_i = n_e$ , in the chromosphere. Taking the logarithms of equation (5.3), we may write  $b_2(h)$  in the following form:

$$\log b_2 = 5.02 + \log N_2(\tau) - 2 \log n_e(\tau) - \frac{1.715 \cdot 10^4}{T_e(\tau)} + \frac{3}{2} \log T_e(\tau). \quad (5.4)$$

By substituting the values  $N_2(h)$  given in Table XVI and  $n_e(h)$  and  $T_e(h)$  in Table XV, we can obtain the empirical value of  $\log b_2$  at each height. The results are shown in Table XVII. We see that  $\log b_2$  increases considerably with height. By comparing the values of  $\log b_2$  thus obtained

Table XVII

Observed values of  $\log b_2$

Height (km)	500	1000	1500	2000	2500	3000
Log $b_2$	0.32	0.79	1.24	1.63	2.03	2.45
$\frac{d \log b_2}{dh} \cdot 10^{-8} \text{ cm}^{-1}$	0.94	0.90	0.78	0.80	0.84	

with the theoretical values computed for small interval of  $T_e$  and  $n_e$ , we can examine the model derived from the continuum for internal consistency. For constant values of  $n_e$ ,  $b_n$  is larger for higher  $T_e$  than for lower  $T_e$ . Since  $b_n$  is a function of both  $T_e$  and  $n_e$ , however, we may not conclude immediately that the increase of  $b_n$  with height, shown in Table XVII, indicates the increase of  $T_e$  upwards. However, theoretical calculations by Thomas (1949a) have shown that  $b_n$  is not as sensitive to a change of  $N_e$  as it is to a change of  $T_e$ . The above table shows that  $b_n$  increases by a factor of 100 over a height range of 2,500 km. Hence, we may conclude that a temperature increasing upwards is implied.

We can prove the internal consistency of the results given in Table XVII in the following manner:

Taking logarithms of equation (3.1) Chapter V, and differentiating with respect to  $h$ , we have the height gradient of the Balmer free-bound emission at the series limit

$$\frac{d \ln E_\infty}{dh} = \frac{d \ln N_i N_e}{dh} - \frac{3}{2} \frac{d \ln T_e}{dh} \quad (5.5)$$

We have ignored the term  $-d \ln \beta / dh$  from the above equation, since we showed earlier that  $\beta$  is constant, at least for the region lower than 3,000 km in the chromosphere.

Similarly, from equation (5.1), we can write

$$\frac{d \ln N_2}{dh} = \frac{d \ln N_i N_e}{dh} + \frac{d \ln b_2}{dh} - \frac{\chi_2}{k T_e^2} \frac{dT_e}{dh} - \frac{3}{2} \frac{d \ln T_e}{dh} \quad (5.6)$$

in which we note that

$$\frac{d \ln n_2}{dh} = \frac{d \ln N_2}{dh}, \quad \frac{d \ln n_i n_e}{dh} = \frac{d \ln N_i N_e}{dh}$$

for  $d \ln \beta / dh = 0$ , as we mentioned above. Substituting equation (5.6) into (5.5), we have

$$\frac{d \ln E_\infty}{dh} = \frac{d \ln N_2}{dh} - \frac{d \ln b_2}{dh} + \frac{1.72 \cdot 10^4}{T_e^2} \frac{dT_e}{dh} \quad (5.7)$$

Hence, using the above equation, we can calculate the  $b_2$ -height gradient from the emission-height gradient in the continuum. Substituting the following values obtained from the 1952 data:

$$\frac{d \ln E_\infty}{dh} = 2.19 \cdot 10^{-8} \text{ cm}^{-1}, \quad \frac{d \ln N_2}{dh} = 1.33 \cdot 10^{-8} \text{ cm}^{-1}$$

and the values of  $T_e$  shown in Table XV, we obtain the  $b_2$ -height gradients. These values of  $d \log b_2 / dh$  are shown in Table XVIII. Comparing these results with those in Table XVII, we see that the agreement of  $b_2$ -height gradient is satisfactory. This may prove that the present determination of the values of  $N_2$  are consistent with the results obtained from the continuum.

Table XVIII

Height (km)	Value of $\frac{d \log b_2}{dh}$					
	500	1000	1500	2000	2500	3000
$\frac{d \log b_2}{dh} \cdot 10^{-8} \text{cm}^{-1}$	0.62	0.58	0.60	0.55	0.52	0.62

§6. Discussion of the comparison of the density-height gradient with the emission gradient.

In Chapter I it was mentioned that the emission-height gradient of the flash spectrum has been considered to be one of the anomalous features that can not be explained by a classical model of the chromosphere. All the earlier eclipse observations have shown that the emission-height gradient of the Balmer lines increase considerably towards the higher order lines. From the 1952 eclipse, Athay and others have found that the emission height gradient,  $a_n$ , increases monotonically from  $1.56 \times 10^{-8} \text{cm}^{-1}$  for  $H_{10}$  to the value of  $2.12 \times 10^{-8} \text{cm}^{-1}$  for  $H_{31}$ . The value of  $2.19 \times 10^{-8} \text{cm}^{-1}$  is obtained for the height gradient of the continuum at the Balmer series limit.

In the preceding sections, we have mentioned several pieces of evidence indicating that the assumptions of constant temperature and exponential decrease of hydrogen atoms are justifiable as a first approximation, in the lower region of the chromosphere. Under such assumptions, the integrated emission gradient determined from slitless flash spectra is equal to the height gradient of emission per unit volume. Therefore, if we ignore the effect of self-absorption as in the earlier analysis, the emission gradient of the line  $E_{n2}$  must be equal to the density gradient of the hydrogen atoms in the  $n$ th level. Further, if departures from thermodynamic equilibrium are ignored, the density gradients of all the energy states are the same. Thus, in such a classical model, the emission height gradients for all lines are identical also.

In section 5 of Chapter IV, the value of  $0.86 \times 10^{-8} \text{cm}^{-1}$  was obtained from the 1932 eclipse for  $\beta_2$ , the density gradient of hydrogen 2nd state. In section 2 of this chapter,  $\beta_2 = 1.33 \times 10^{-8} \text{cm}^{-1}$  was obtained from the 1952 data. These values are considerably lower than the emission-height gradient determined from the higher order lines. This disagreement is considered to be due to the effects of departures from thermodynamic equilibrium. As was discussed in Chapter II, departures from thermodynamic equilibrium decrease towards the higher members of the series and are negligible at the series limit. At the same time, the self-absorption for the highest line is negligibly small compared to that for lower lines. Hence, from the above considerations, the emission gradient,  $a_\infty = 2.19$ , at the series limit may be considered as the density gradient of hydrogen in the highest level. Therefore, we see that there is considerable difference in our present results between  $\beta_2$  and  $\beta_\infty$ .

In the present thesis, the density-height gradients were assumed to be the same for all levels. Since our results seem to show different values of  $\beta_n$  for different  $n$ , the assumption of a constant gradient is not strictly justified. We have to take the dependence of  $\beta_n$  upon  $n$  into account. From equation (2.7) in Chapter III, we see that the emission in the Balmer lines is a function of  $n_1$  and  $n_2$ . Hence, if we include the dependence of  $\beta_n$  on  $n$ , both  $\beta_1$  and  $\beta_2$  enter into the integration over the volume. Therefore, it is impossible to perform the integration analytically as was done in Chapter III, and it must be done numerically. Further, since  $\beta_n$  depends on both  $b_n$  and the self-absorption, it is difficult to derive its value for every line. It seems that the only way to carry out the numerical integration is by a trial and error method of successive approximation.

At the present, it is more difficult to estimate numerically the errors brought into the results by the assumption of  $\beta$  constant with  $n$ , than to estimate the errors due to the assumption regarding line profiles - namely, we assumed that the central intensity of each line is solely determined by the amount of Doppler broadening. In the expression for the self-absorption derived in Chapter III, self-absorption is a function of the atomic absorption coefficient at the line center. Hence, it might be necessary to consider Stark broadening, particularly since the electron temperature was found to be less than 30,000° in the lower region of the chromosphere. Further, in a rigorous calculation, one has to consider the optical depth at the line center as a transfer problem. Thus, the problem ultimately becomes much more difficult.

One should note, however, that the present analysis was based on the relative intensities of the lines, considering, in particular, the relative amount of self-absorption and  $b_n$ . Therefore, the aggregate effect of all the small errors may not be appreciable in the final results.

### §7. Concluding remarks.

Considerable differences between the Balmer line intensities observed at the 1932 and 1952 eclipses appeared. In the lower region of the chromosphere, the absolute values of line intensities of the 1952 spectra are about five times as large as those of 1932. The emission-height gradients of Balmer lines are also approximately 40% larger in 1952 than in 1932 data. The theoretical investigation treated in Chapter IV and Chapter V indicated that these differences are due mainly either to an essential variation of the physical conditions in the chromosphere from time to time or to inhomogeneity, i.e., absence of spherical symmetry in the chromosphere. We shall discuss these points by comparing the numerical results of this chapter with those of Chapter IV.

In Chapter IV, it was concluded that the departure from thermodynamic equilibrium was not a predominant effect in the 1932 eclipse observations, and the difficulties that appeared in using the classical theory to explain the low Balmer decrement could be solved by including the effects of self-

absorption only. On the other hand, for the 1952 data our analysis showed that the two effects are equally important and the values of  $b_n$  obtained are not at all negligible. The calculations in section 3 of Chapter IV for determining  $b_n$  and the amount of self-absorption simultaneously also agree with this conclusion. The successive computations based on the least square principle did not converge in the analysis of the 1932 data, whereas for the 1952 data it gave consistent solutions for  $b_n$  and self-absorption. Hence, the failure in applying the method to the 1932 observations may be the negligibly small values of  $b_n$ . As we have discussed in section 2, this difference is clearly seen in the characteristic curve of Balmer decrements shown in Figure III.

Considerable variations were also apparent in the values of the density-height gradient,  $\beta$ . The value of  $0.83 \times 10^{-8} \text{ cm}^{-1}$  was given for  $\beta_2$  (1932), whereas  $\beta_2$  (1952) was  $1.33 \times 10^{-8} \text{ cm}^{-1}$ . Since these values of  $\beta_2$  are independent of  $T_e$ , and all the other assumptions are the same for both analyses, the differences in  $\beta_2$  should be interpreted as an actual variation of chromospheric conditions. All the above measurements and comparisons were based on the assumption of a spherically symmetric distribution of physical parameters in the chromosphere.

As we discussed in Chapter I, Athay, Evans, and Roberts (1953) have found a locally intensified region in the 1952 spectra taken at the west limb of the sun. Their preliminary study shows that the hydrogen emission gradient in this active region is only one third as high as at the east limb, although there appears to be an exponential decrease of intensity with height. The Balmer decrements in this region are larger than in the east limb region; and the observed decrements from H<sub>9</sub> to H<sub>28</sub> exceed the thermodynamic equilibrium decrements at all heights. Similar over-intensification of the helium lines and coronal yellow line are noted in the same west limb region.

They suggest that these observations indicate a local increase of electron density and electron temperature so that severe departures from thermodynamic equilibrium have taken place. They report that two flares were observed at this region on the day of the eclipse, and that the observations suggest a moderate limb flare in some stage of its development. Furthermore, the west limb spectra show other irregularities. All the chromospheric lines are absent on one side of the region of intensified emission.

It seems that these observations indicate evidence of an irregular structure of the chromosphere due to surface activity of the sun. There may be finer irregularities, such as spicule configurations, which are not detectable within the limit of resolution of the spectra. Thus, the chromosphere might have to be considered as a mixture of disturbed regions, as has been suggested by Hagen, (1953).

Another possible cause of disagreement of the results from one eclipse to the other, may be some technical error in the measurements. Particularly, the height determination based on the moon's profile may admit

considerable errors.

It is interesting to note that in one quantity the data from the 1932 and 1952 eclipses agree quite well, compared to the large discrepancies between absolute values of emission-height gradients and  $\beta_2$ 's for the two eclipses. That quantity is the difference between continuum height gradient and  $\beta_2$ . It is an important quantity, since, as discussed in section 5, it gives a measure of the  $b_2$ -height gradient.

## REFERENCES

- Alfvén, H. 1947 M.N. 101, 281.  
               1950 Cosmical Electrodynamics (Oxford Clarendon Press).
- Allen, C. W. 1937 Ap. J. 85, 165.  
               1941 M.N. 107, 426.  
               1949 M.N. 109, 343.
- Athay, R. G., Billings,  
     D. E., Evans, J. W.  
     and Roberts, W. O. 1954 Ap. J. (in press).
- Athay, R. G., Evans,  
     J. W. and Roberts,  
     W. O. 1953 The Observatory, 73, 244.
- Athay, R. G., Pecker,  
     J.C. and Thomas,  
     R. N. 1954 Private communication.
- Baumbach, S. 1937 A.N. 263, 121.
- Bell, B. 1951 Special Report, No. 35, Harvard University.
- Biermann, L. 1948 Zs. f. Ap. 25, 161.
- Chamberlain, J. W. 1953 Ap. J. 117, 387.
- Cillié, G. G. and  
     Menzel, D. H. 1935 Harvard Circular 410.
- Davidson, C. R. and  
     Stratton, F.J.M. 1927 Mem. R. Astr. Soc. 64, Part 4.
- Edels, H. and  
     Craggs, J. D. 1951 Proc. Phys. Soc. A. LXIV, 562.
- Giovanelli, R. G. 1948a Australian J. Sci. Res., A. 1, 275.  
               1948b Ibid., p. 289.  
               1948c Ibid., p. 305.  
               1948d Ibid., p. 360.
- Goldberg, L. 1939 Ap. J. 89, 673.
- Hagen, J. P. 1951 Ap. J. 113, 547.  
               1953 Paper presented at A.A.S. Meeting, August 1953.

- Houtgast, J. 1952 Convegno Volta, p. 33.
- Hoyl, F. 1949 Some Recent Researches in Solar Physics,  
(Cambridge: At the University Press).
- Hulst, H. C. van de 1946 B.A.N. 10, 79  
1947 Ap. J. 105, 471.  
1953 The Sun, Chapter 5, The Chromosphere and  
the Corona (Chicago: The University  
of Chicago Press).
- Koelbloed, D. and 1951 Proc. K. Nederl. Akad. v. Wetensch. 54, 468.  
Veltman, W.
- Inglis, D. R. and 1939 Ap. J. 90, 439.  
Teller, E.
- Matsushima, S. 1948 Mem. Ap. 1, 27.  
1952 Ap. J. 115, 544.
- Matsushima, S. and 1947 Mem. Col. Sci. Kyoto Univ. 25, 63.  
Miyamoto, S.
- Menzel, D. H. 1931 Pub. Lick Obs. 17, Part 1.
- Menzel, D. H. and 1948 Tech. Report, No. 3, ONR Project M 720-5.  
Bell, B.
- Menzel, D. H. and 1937 Ap. J. 85, 88.  
Cillie, G. G.
- Menzel, D. H. and 1937-45 A series of papers in Ap. J. (All references  
others are given in last paper, Ap. J. 102, 239).
- Menzel, D. H. and 1935 M.N. 96, 77.  
Pekeris, C. L.
- Minnaert, M. 1953 The Sun, Chapter 3, The Photosphere.  
(Chicago: The University of Chicago  
Press).
- Miyamoto, S. 1947 Mem. Col. Sci. Kyoto Univ. 25, 31.  
1949a Publ. Astr. Soc. Japan, 1, 10.  
1949b Ibid., p. 14.  
1951a Ibid., 2, 102.  
1951b Ibid., p. 113.  
1951c Ibid., 3, 61.  
1951d Ibid., p. 67.  
1953 Zs. f. Ap. 31, 282.

- Miyamoto, S. and Kawaguchi, I. 1950 Publ. Astr. Soc. Japan, 2, 114.
- Pannekoek, A. and Minnaert, M. 1928 Verh. Akad. Wetensch. Amsterdam, 13, No. 5.
- Pecker, J. C. 1951 Ann. d'Ap. 14, 152.
- Pierce, K. and Goldberg, L. 1948a Tech. Report No. 1. ONR Project M 720-5.  
1948b Ibid. No. 2.
- Redmann, R. O. 1942a M.N. 102, 134.  
1942b Ibid., p. 140.  
1952 The Observatory, 72, 870.
- Roberts, W. O. 1945 Ap. J. 101, 136.
- Schwarzschild, M. 1948 Ap. J. 107, 1.
- Shane, C. D. 1941 Pub. A.S.P. 53, 200.
- Thomas, R. N. 1948a Ap. J. 108, 130.  
1948b Ibid., p. 142.  
1949a Ibid., 109, 480.  
1949b Ibid., 110, 12.  
1950a Ibid., 111, 165.  
1950b Ibid., 112, 337.  
1950c Ibid., p. 343  
1952 Ibid., 115, 550.
- Thomas, R. N., Krook, M., Menzel, D. H., and Bhatnagar, P. 1953 Harvard University Scientific Report No. 8 (AROC Contract AF 19(604)-146)
- Ueno, S. 1950 Publ. Astr. Soc. Japan, 2, 61.
- Unsöld, A. 1952 Convegno Volta, p. 22.
- Wildt, R. 1947 Ap. J. 105, 36.
- Woolley, R.v.d.R. and Allen, C. W. 1950 M.N. 110, 358.
- Woolley, R.v.d.R. and Stibbs, D.W.N. 1953 The Outer Layers of a Star, (Oxford: University Press).
- Woltjer, L. 1954 Private communication.

- |             |       |   |
|-------------|-------|---|
| Wurm, K.    | 1948a | Zs. f. Ap. <u>25</u> , 109.                               |
|             | 1948b | Mitt. Bergedorf, 21, Nos. 202 and 206.                    |
| Zanstra, H. | 1950a | Proc. K. Nederl. Akad. v. Wetensch., <u>53</u> ,<br>1289. |
|             | 1950b | M.N. <u>110</u> , 491.                                    |